Dissertation

submitted to the

Combined Faculties for the Natural Sciences and for Mathematics

of the Ruperto-Carola University of Heidelberg, Germany

For the degree of

Doctor of Natural Sciences

presented by

B.S. Nurlanbek Duishoev,

born in Batken, Kyrgyzstan

Oral Examination: 3rd February 2015

Characterization of the Role of RPGRIP1 in Microtubule Dynamics and Golgi Organization

Referees: Dr. Marko Kaksonen

                         Prof. Dr. Walter Nickel

Summary

The Golgi is a membranous organelle that forms a hub of the secretory pathway in eukaryotic cells. The materials synthesized in ER are transported to the Golgi where they processed further and sorted to their cellular destinations including endosomes, lysosomes and plasma membrane or secreted to the extracellular space. In lower eukaryotes the Golgi is found as disk-shaped cisternae, which can be combined to a ministack. In higher eukaryotes like mammalian cells the Golgi ministacks fuse with each other to form a single complex called the Golgi ribbon, which often localizes to the pericentrosomal area. The Golgi matrix proteins, the centrosome and the microtubule cytoskeleton have a critical role in the assembly and integrity of the Golgi ribbon and this pericentrosomal positioning. The ribbon organization and positioning of the Golgi are important in many cellular processes including cell migration, polarization and differentiation and subject to dynamic regulation. However, the molecular mechanism of dynamic regulation of the Golgi organization and positioning is not well understood.

In this study we performed an RNAi screen to find new candidates that would enable us to understand the regulation of Golgi organization and positioning. The screen targeted 680 genes that encode for peripheral proteins. Visual analysis of the Golgi phenotypes revealed 70 genes whose depletion affected Golgi morphology and positioning. Depletion of one of the screening hits, a centrosomal protein named RPGRIP1, lead to an elongated and uncondensed Golgi ribbon organization. Characterization of RPGRIP1 revealed that RPGRIP1 depletion leads to decreased centrosomal nucleation of microtubules and increased

microtubule stability, and we showed that Golgi reorganization is due to this increased microtubule stabilization. High-resolution imaging revealed that the Golgi ribbon is bound to stable microtubule protofilaments. Our experiments also show that ectopic microtubule stabilization leads to a loss of compact organization and pericentrosomal positioning of the Golgi.

In summary, we propose a new model in which Golgi ribbon organization and positioning is regulated by stable microtubules. We also show for the first time the role of RPGRIP1 in microtubule dynamics in addition to its scaffolding role in organizing the primary cilium.

Zusammenfassung

Der Golgi ist ein membranumgebenes, zelluläres Organell das einen Knotenpunkt im sekretorischen Transportweg von eukaryotischen Zellen einnimmt. Von dem ER aus, in welchem das Material synthetisiert wird, erfolgt anschließend der Transport zu dem Golgi Komplex. Dort wird das Material weiter bearbeitet und anschließend zu den zellulären Zielorten wie Endosomen, Lysosomen und die Plasmamembrane transportiert oder in den extrazellulären Raum sekretiert. In niederen Eukaryoten existiert der Golgi als einzelne Membran–Zisternen, oder als Ministack aus mehereren Zisternen die übereinander gelagert sind. In Säugetieren dagegen verschmelzen die Golgi Ministacks miteinander, um einen einzigen Komplex, denGolgi-Apparat, auszubilden, deroft im perizentrosomalen Bereich der Zelle lokalisiert ist. Die Golgi Matrix Proteine, das Zentrosom und das Mikrotubuli-Zytoskelett haben entscheidende Rollen bei der Montage und der Integrität des Golgi-Apparats und dessen perizentrosomalen Positionierung. Die dynamische Regelung der Organisation und Positionierung des Golgi ist in vielen zellulären Prozessen, einschließlich der Zellmigration, der Polarisierung und der Differenzierung wichtig. Allerdings ist der molekulare Mechanismus der dynamischen Regelung der Golgi-Organisation und -Positionierung noch unklar.

In dieser Arbeit wurde ein RNAi-Screen durchgeführt, um neue Kandidaten zu finden, die die Regulierung der Golgi-Organisation und – Positionierung beeinflussen, um diese besser zu verstehen.. Es wurden 680 Gene, die für periphäre Membranporteine kodieren, nach deren „knock-down" auf einen Effekt auf die Golgi-Organisation getestet.Nach visueller Analyse der Golgi- Phänotypen wurden 70 Kandidatengene identifiziert deren Depletion die Golgi- Morphologie und Positionierung

stark veränderten. Die Depletion von einem der Kandidaten, einem zentrosomalen Protein namens RPGRIP1, führte zu einer länglichen und nicht kondensierten Ausbreitung des Golgi in der Zelle Die weitere funktionale Charakterisierung von RPGRIP1 ergab, daß RPGRIP1-Depletion zu einer verminderten zentrosomalen Nukleation und erhöhten Stabilität von Mikrotubuli führt. Außerdem konnte gezeigt werden, daß die beobachtete Golgi Re-Organisation aufgrund der erhöhten Stabilisierung von Mikrotubuli zu Stande kommt. Weitere Experimente zeigten,, daß der Golgi-Apparat an stabile Mikrotubuli-Protofilamenten gebunden ist und daß auch eine ektopische Stabilisierung von Mikrotubuli zum Verlust der kompakten Organisation und perizentrosomalen Positionierung des Golgi führen kann. eEs wird somit ein neues Modell der Regulation der Golgi-Organisation und –Positionierung vorgeschlagen, das hauptsächlich durch stabile Mikrotubuli bestimmt wird. Zudem wird in dieser Arbeitzum ersten Mal die Rolle des Proteins RPGRIP1 in der Regulation der Mikrotubuli-Dynamik und der Golgi-Organisation beschrieben.

Acknowledgements

During my PhD, I learned a lot about scientific approach and scientific thinking. Thus I would like to thank Rainer Pepperkok and Martin Lowe for giving me the opportunity to pursue my PhD thesis in their groups. Their critical suggestions in our meetings were essential part of my scientific training. I would like to thank my thesis advisory committee members: Walter Nickel, Marko Kaksonen Anne-Claude Gavin for guiding with constructive suggestions throughout my project. I would like to express my gratitude to Marko Kaksonen and Walter Nickel for generously giving their time to be referee of my thesis.

Throughout last 4 year I got great support from many people, especially I would like to thank ALMF staff for technical support. I also had a great collaboration with Anna Steyer, a PhD student in Schwab team and I wish to acknowledge her help to set up and perform correlative light electron microscopy.

EMBL provides rich and lively environment for scientific growth by organizing various activities and events. Its highly international atmosphere provided me great opportunity to meet different people who helped me not only get acquinted with different cultures but also widen my scientific horizon. Within the group, I was lucky enough to have a supervisor like Christian Schuberth who helped me throughout my project with valuable advices and discussions. I learned a lot from his talent to put small bits into perspective and ability to communicate complicated ideas. I also want to highlight willingness and openness of my Italian colleague Paolo Ronchi who with his critical discussions kept me earthly and focused. Lastly, but not least, I would like to thank Fatima Verissimo and all other members of the Pepperkok group for friendly atmosphere.

Table of Contents

1   Introduction

1.1 The Golgi apparatus is the central organelle of secretory pathway

1.1.1 The role of the Golgi apparatus in the secretory pathway

The Golgi apparatus is an evolutionary conserved, membrane-bound organelle that plays a key role in the secretory pathway of all eukaryotic cells (Figure 1). Newly synthesized proteins that have to be secreted or localized along the secretory pathway are first synthesized and translocated into the endoplasmic reticulum (ER). The primary role of the ER lumen is to provide an environment that facilitates protein folding and this is achieved by post-translational modifications and abundant chaperones. Once folded, nascent proteins are packaged into COPII coated vesicles at specialized ER domains called ER exit sites (ERES) to be delivered to the Golgi complex (Barlowe, 1994). As the secretory cargo proteins pass through the Golgi, most proteins are subjected to post-translational modifications such as glycosylation, phosphorylation and sulfation, as well as proteolytic cleavage (Mellman & Simons, 1992). These modifications are essential for protein folding, sorting and functioning of the protein. Detailed mechanism of intra-Golgi transport of cargo is not well understood and two main models have been proposed: cisternal maturation and vesicular transport. Cisternal maturation model proposes that the Golgi cisternae are transient compartments and move from *cis* to

trans whereas the second model proposes that cisternae are stable compartments and the cargo move via vesicles (Balch et al., 1984; Glick & Malhotra, 1998; Orci et al., 1986; Pelham, 1998; Rothman & Wieland, 1996). The proteins transiting the Golgi are destined to different destinations and an important function of the Golgi is to sort proteins in order to deliver them to their final destinations including endosomes, lysosomes and plasma membrane. Unlike the ER, where different domains fuse to form one continuous compartment, the Golgi is composed of multiple, physically separated sub-compartments (Dunphy & Rothman, 1985). This membrane-bounded sub-compartmentalization has been conserved during evolution and this structural organization appears to be critical for its function (Mollenhauer & Morré, 1991).
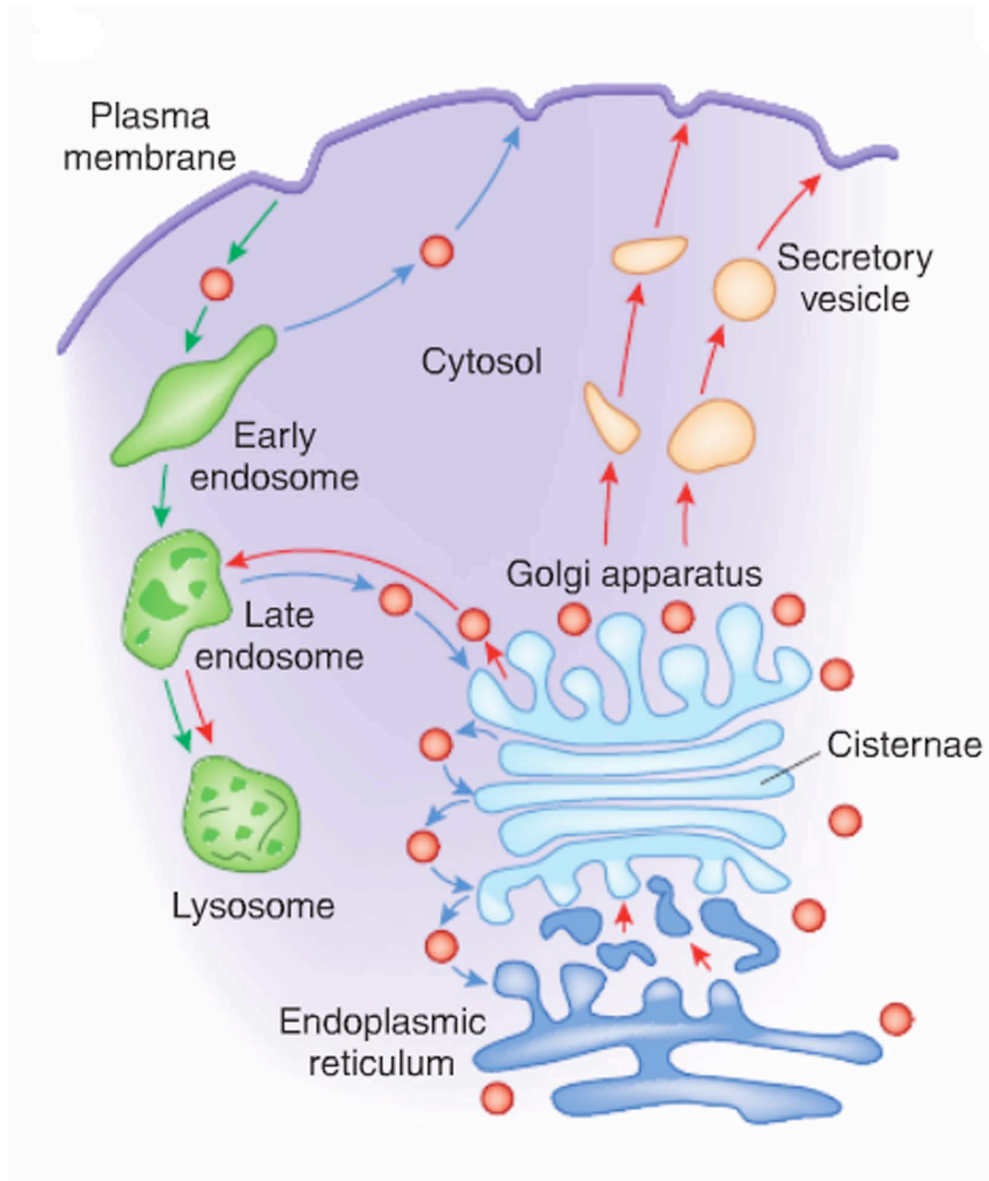
Figure 1: Scheme of secretory pathway in mammalian cells

Proteins are synthesized in the endoplasmic reticulum and are transported to the Golgi apparatus. In Golgi apparatus they are post-translationally modified in a successive manner and sorted further to different destinations including plasma membrane, endosomes and lysosomes. Figure adapted from *(Xu & Esko, 2009)*.

1.1.2 Organization and Evolution of the Golgi Architecture

The structural unit of the Golgi complex (GC) is a disc-like membrane-bounded structure called Golgi cisterna. Golgi cisternae in lower eukaryotes are often dispersed throughout the cytoplasm and function independently (Preuss et al., 1992). In higher eukaryotes, however, they are arranged in ordered stacks of 4-8 cisternae to form a Golgi stack (Figure 2) (Ladinsky et al., 1999; Rambourg et al., 1996). The Golgi stack is polarized with a *cis*-side which is primarily exchanging proteins and lipids with the endoplasmic reticulum (ER), whereas the *trans*-side is interfacing with the plasma membrane and compartments of the endocytic pathway (Dunphy & Rothman, 1985; Farquhar, 1985). Different Golgi resident enzymes that function in post-translational modification of the cargo protein display preferential localization to particular sub-compartment of the Golgi stack (*cis*, *medial* or *trans*) and this is essential for sequential step-wise modification of the cargo proteins (Bard & Malhotra, 2006; De Matteis & Luini, 2008). In flies, plants and fungi the stacks are dispersed throughout the cytoplasm. In vertebrates, in contrast, the Golgi stacks are connected laterally by tubules to form a ribbon-like structure, which has a juxta-nuclear localization (Ladinsky et al., 1999; Rambourg & Clermont, 1990).

Joining the Golgi cisternae into single connected ribbon, introduces another level of complexity in regulation: its overall architecture and localization. The Golgi matrix, a detergent insoluble network of proteins, is thought to form the skeleton of the Golgi complex (Slusarewicz et al., 1994). A number of components of the Golgi matrix proteins have been identified and localized to the *cis*-, *medial*-, and *trans*-cisternae of the Golgi ribbon (Figure 2). The core Golgi matrix proteins are represented by golgin and GRASP family proteins and are thought to regulate final function and architecture of the GC which include: vesicle tethering in anterograde and

retrograde trafficking in the ER-Golgi system, stacking of Golgi cisternae, interactions with the cytoskeleton, maintenance of structure and connectivity of the Golgi ribbon (Dippold et al., 2009; Gillingham & Munro, 2003; Ramirez & Lowe, 2009; Short et al., 2002).
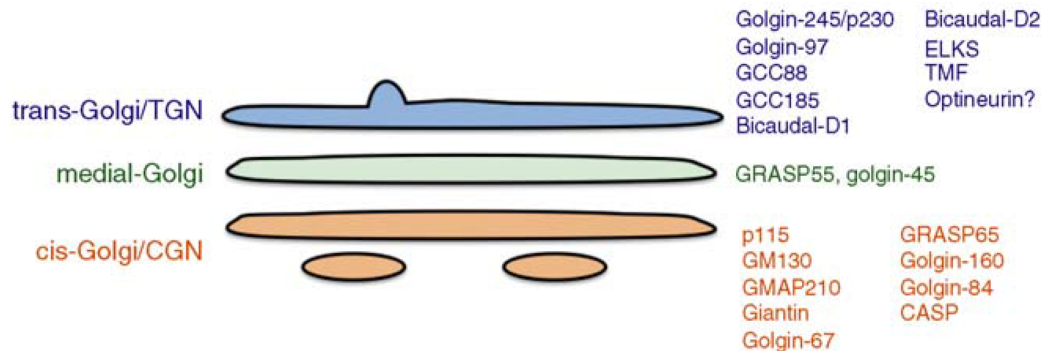
Figure 2: The Golgi ministack and preferential localization of different Golgins

The Golgi ministack is composed of stacked Golgi cisternae that are polarized into *cis*-Golgi, *medial*-Golgi and *trans*-Golgi. Many golgins and GRASP protein have been identified at the Golgi and they show preferential localization to *cis*-, *medial*- or *trans*-region. Figure adapted from *(Goud & Gleeson, 2010)*.

Golgins are long coiled-coil proteins that form homo-dimers and attach to the Golgi membranes via the carboxy-terminus (Munro, 2011). Coiled-coil domains form long rod-like structures that can protrude to distally located compartments (Hayes et al., 2009; Sinka et al., 2008). Golgin proteins are found on the *cis*-face of the Golgi, around the rims of the stack and on the *trans*-face of the Golgi. Canonical *cis*-Golgi golgins include GM130, GMAP210 and Golgin-160. As the *cis*-Golgi is at the interface with the ER, *cis*-Golgi golgins are implicated in tethering of ER-

derived transport vesicles to the Golgi (Cao et al., 1998; Nakamuraet al., 1997; Rios et al., 1994; Satoh & Warren, 2008; Striegl et al., 2010) as well as in attaching the Golgi membranes to microtubules and the centrosome (Infante et al., 1999). Three golgins, namely Giantin, Golgin-84 and CASP, were reported to have a trans-membrane domain. They are localized on the rims of the Golgi stack and on COPI coated vesicles (Bascom et al., 1999; Gillingham et al., 2002; Renna et al., 2005). Lastly, GRIP domain golgins (golgin-97, RanBP2α, lmh1p, andp230/golgin-245) are found predominantly on the *trans*-Golgi. RNAi studies revealed that down-regulation of these proteins leads to Golgi fragmentation and inhibition of retrograde transport from endosomes to Golgi suggesting a structural and a trafficking role at the *trans*-Golgi (Barr, 1999; Kjer-Nielsen et al., 1999; S Munro & Nichols, 1999) .

Other proteins that have important function at the Golgi are GRASP55 and GRASP65 (Golgi reassembly stacking proteins). GRASPs are membrane inserted proteins and were shown to homodimerize via the GRASP domain (Barr et al.,1997). This finding lead to the suggestion that GRASPs might be involved in stacking of the Golgi cisternae and lateral linking of the Golgi stacks. GRASP65 (predominantly found on the *cis*-side) localization to Golgi depends on a myristoylation domain and its ability to bind the *cis*-Golgin GM130 (Dippold et al., 2009; Gillingham & Munro, 2003; Ramirez & Lowe, 2009; Short et al., 2005; Shorter & Warren, 2002). GRASP55 (predominantly on the *medial-* to *trans*-side) localization also depends on the myristoylation domain and its ability to bind to *med/trans* Golgi proteins, including golgin-45 (Short et al., 2001) .

On the ultra-structural level, the precise role of the individual Golgi matrix components remain unclear, however, functional studies hint to the redundant roles of individual golgin proteins. In *Drosophila*, knockdown of dGRASP partially unlinks the Golgi whereas co-depletion of dGRASP and

dGM130 results in a complete loss of Golgi stacking (Kondylis et al.,, 2005). Redundant roles of Golgi matrix proteins, namely GM130, Golgin45, GRASP65 and GRASP55, were also reported when assessing the relative contribution of golgins and GRASPs in cisternal adhesion in mammalian cells (Lee et al., 2014). Even though the Golgi matrix proteins are thought to form the 'skeleton' of the GC, they are not sufficient to maintain the Golgi ribbon organization and highly depend on the microtubule cytoskeleton. As both depolymerization and stabilization of the microtubule cytoskeleton result in loss of the Golgi ribbon organization, the dynamic nature of the microtubule cytoskeleton apparently holds the major key for the regulation of Golgi organization (Pavelka & Ellinger, 1983; Rogalski & Singer, 1984; Thyberg & Moskalewski, 1985; Turner & Tartakoff, 1989)

1.2 Microtubules form a dynamic cytoskeleton

Microtubules are dynamic cytoskeletal structures composed of 13 protofilaments that form the wall of the hollow tube of the microtubule. α/β-tubulin heterodimers are the structural unit of the microtubules and by polymerization form protofilaments of the microtubules (Nogales et al., 1998; Nogales et al., 2006). When bound to GDP, the tubulin dimer is in a bent conformation, which fits poorly into the straight wall of the microtubule. Exchanging GDP by GTP into its active site straightens the dimer and facilitates incorporation into the microtubule thus promoting polymerization (Figure 3) (Buey et al., 2006; Wang & Nogales, 2005). Dimer addition triggers the hydrolysis of GTP to GDP and enables the dimer to revert to a bent conformation, which highly favors the dissociation of GDP-tubulin and drives microtubule depolymerization (Dogterom et al., 2005).
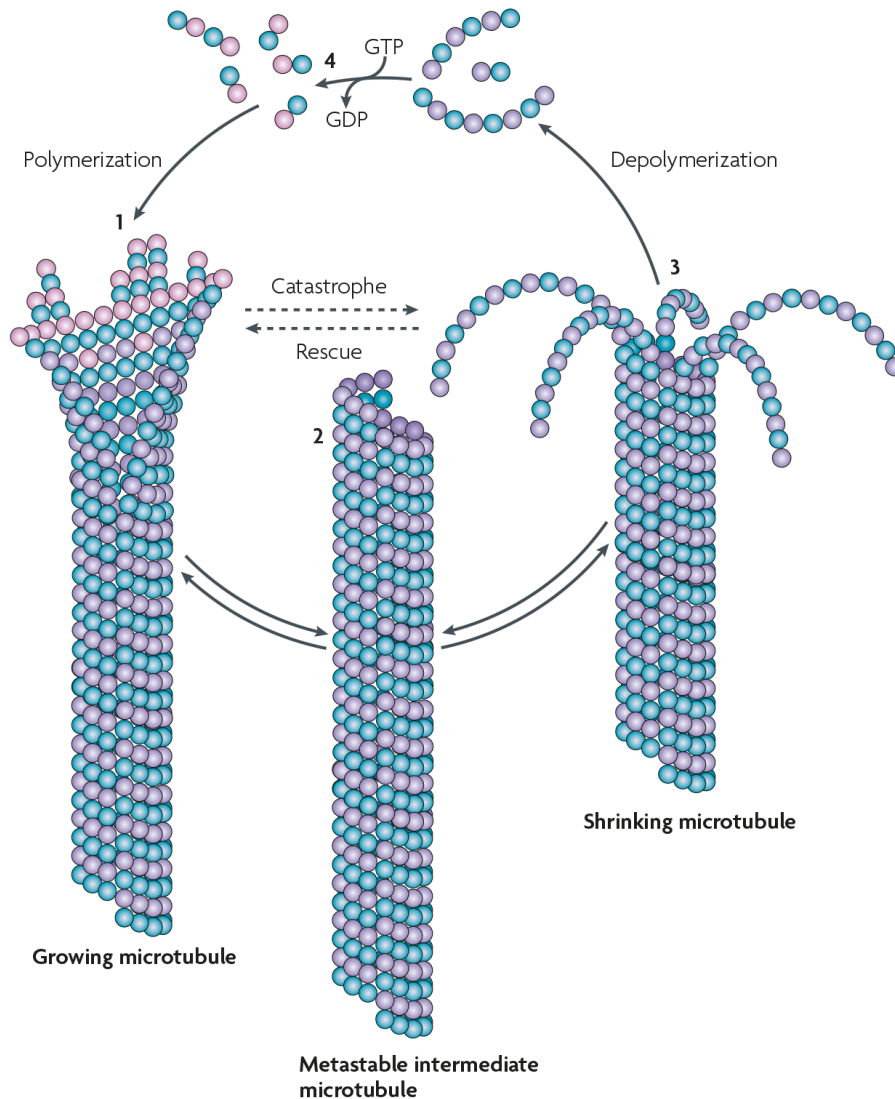
Figure 3: Dynamic instability of microtubules

Three states of microtubule protofilaments are shown: growing, intermediate and shrinking state. Tubulin dimers bound to GTP drive polymerization of the microtubules. GTP is hydrolyzed to GDP when the dimer is incorporated into the protofilament. GDP hydrolysis changes the conformation of the dimer and this favors depolymerization of the protofilament forcing the microtubule to alternate between growing and shrinking phases. Figure adapted from *(Akhmanova & Steinmetz, 2008)*.

In vitro, microtubules alternate between growth and shrinking phases, a behavior referred to as dynamic instability (Mitchison et al., 1984)(Mitchison 1984). However, *in vivo* the dynamics of the microtubule cytoskeleton is under tight regulation. Microtubules nucleate from different microtubule organizing centers (MTOCs), the centrosome being the major one mammalian cells, and often minus-end of the microtubule protofilament remain anchored to the MTOC. Spatial and temporal coordination of microtubule-associated proteins (MAPs) and microtubule-interacting proteins further regulate microtubule stabilization and spatial organization of microtubules thus generating different pools of microtubules. Early comparative studies on biochemical properties of dynamic and long-lived, stable pools of microtubules revealed distinct post-translational modifications (PTMs). Stable microtubules preferentially accumulate PTMs including acetylation (at lysine-40 residue of alpha-tubulin), de-tyrosination (removal of C-terminal tyrosine) and polyglutamylation (at gulatamate residue near the C-terminus) and confer novel functions to microtubules (Bulinski et al., 1991; Schulze et al., 1987; Webster et al., 1989). Indeed, differential regulation of microtubules and subsequent changes in physical and biochemical properties are found to be critical for fundamental processes including mitosis, cell division and differentiation, intracellular transport, cell motility and polarization (Westermann et al., 2003).

1.2.1 Different mechanisms of microtubule dynamics regulation

MAPs modulate microtubule dynamics in diverse ways including stabilization and destabilization of the microtubule lattice, sequestering of free tubulin and stabilization or destabilization of the ends of microtubules (Akhmanova et al., 2008). The roles of microtubule lattice stabilizing MAPs

are evident and commonly studied in neuronal cells. Malfunctioning of MAPs in neurons have been linked to many neurodegenerative disorders including Parkinson's disease, Huntington's disease and Alzheimer's disease. Tau proteins, often mutated in neurodegenerative diseases, reduce microtubule dynamics by stabilizing the microtubule lattice (Drubin et al., 1986). Overexpression of tau proteins induce microtubule bundling, indicating that they can also cross-link parallel microtubules (Kanai et al., 1989). Similar stabilizing roles have been attributed to other MAPs such as MAP2 and MAP4, which are generally expressed in neuronal and non-neuronal tissues, respectively (Dehmelt et al., 2004).

Microtubule severing factors employ various mechanisms to destabilize microtubules. Katanin is a microtubule severing protein that localizes to the centrosome (Gee et al., 1997). It has been demonstrated that katanin is responsible for the majority of M-phase severing activity in Xenopus eggs (McNally et al., 1996), and that it is essential for releasing microtubules from the neuronal centrosome. On the other hand, MT destabilizing factors, such as stathmins induce microtubule catastrophe events by sequestering tubulin heterodimers (Howell et al., 1999).

Microtubules can grow and shrink via their minus- or plus-ends *in vitro*. However, *in vivo* minus-ends of microtubules are often anchored and stabilized. Therefore, the plus-end of the microtubule is the important site that determines the fate of the microtubule in cells. Plus-end tracking proteins (+TIP) are specialized MAPs that are conserved in all eukaryotes and specifically accumulate at growing microtubule plus ends (Schuyler et al., 2001).

1.2.2 Regulation of microtubule dynamics by +TIP network

MT plus-end-tracking proteins (+TIPs) constitute a structurally diverse group of MAPs (Figure 4). By binding to the MT ends, +TIPs can modulate the MT's structure and accessibility for interaction with other proteins and thus can transmit antagonistic effects on microtubule dynamics (Akhmanova et al., 2008). The main mammalian +TIPs can be grouped into three subgroups according to their plus-end targeting domains.
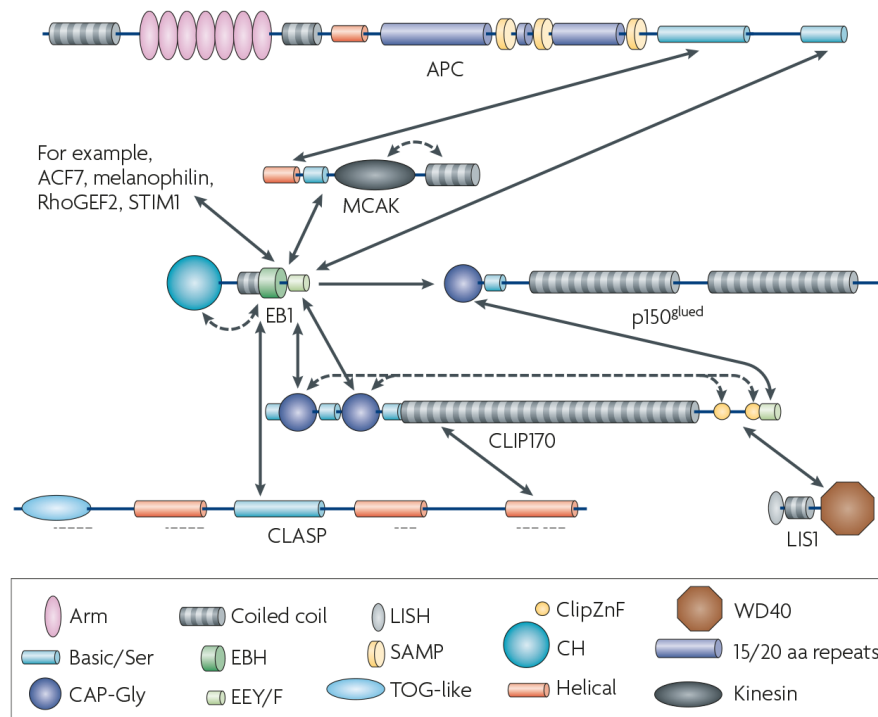
Figure 4: Microtubule +TIP network.

Dynamic interactions between main components of microtubule +TIP network are schematically shown. Solid and dashed lines represent inter-molecular and intra-molecular interactions, respectively. EB1 directly interacts many proteins of the network and plays a key role in regulation of the microtubule dynamics. Figure adapted from *(Akhmanova et al., 2008)*.

End-binding (EB) proteins are characterized by a conserved N-terminal microtubule targeting domain and a C-terminal oligomerization domain (Lansbergen et al., 2006). End-binding protein 1 (EB1) stabilizes microtubules by localizing to the plus-tip and facilitating cortical capture of the microtubules. EB1, together with adenomatous polyposis coli (APC), at the cell cortex binds to mDia1, a downstream component of the Rho signaling, and suppresses microtubule catastrophe events and leads to microtubule stabilization (Lansbergen et al., 2006; Wen et al., 2004). Indeed, depletion or over-expression of EB1 leads to loss or increase of the stable pool of microtubules, respectively (Wen et al., 2004).

The members of the *CLIP family* act as rescue factors that help to convert shrinking microtubules into growing ones (Komarova et al.,2002). CLIP170 supports microtubule stabilization by forming a tripartite complex with Rac1 and IQGAP1 in response to Cdc42 signaling. IQGAP1 localizes to cell-to-cell contact sites and at the leading edge and by interacting with CLIP170 retains microtubule growing-ends at the cell cortex (Galjart, 2005). There are also evidences that CLIP family members can interact with the dynein-dynactin complex at the cell cortex and contribute to microtubule stabilization (Lansbergen et al., 2004).

Other important +TIP network components including above mentioned APC, microtubule-actin cross-linking family 7 (MACF) and CLIP-associating proteins (CLASPs) contain *extensive stretches of basic and Serin residues*. Similar to CLIPs, this group of proteins also retain microtubule plus ends in the peripheral cortical region, where microtubules are pausing or alternate between short polymerization/depolymerization phases (Drabek et al., 2006; Lansbergen et al., 2006; Mimori-Kiyosue et al., 2005; Wu et al., 2008). Overexpression of CLASP1 and CLASP2 lead to accumulation of EB1 along the MTs (Mimori-Kiyosue et al., 2005) suggesting a downstream pathway that involves EB1 mediated

stabilization. CLASPs are also involved in maintenance of perinuclear microtubule stabilization by anchoring MTs at the Golgi (Efimov et al., 2007).

These comprehensive networks of MAPs at the microtubule lattice and plus-ends in addition to dynamic instability of microtubules enable fast and fine modulation of microtubule dynamics. The microtubule cytoskeleton adapts quickly to various extracellular and intracellular stimuli and it has an essential role in the organization and positioning of the Golgi In the following, different existing models will be discussed on how microtubules regulate Golgi organization.

1.3 Existing models of Golgi ribbon positioning

The Golgi ribbon organization and localization is dynamically regulated despite its complex organization. In certain processes the Golgi is subject to dramatic changes and acquires various morphologies. In cell division the Golgi goes through extensive fragmentation and – depending on the proposed model - (at least some of) the Golgi localized proteins are recycled to the ER. However, upon mitotic exit with the resumption of secretion from the ER, the Golgi vesicles assemble into ministacks throughout the cell and subsequently fuse to form the Golgi ribbon (Bevis et al., 2002; Miles et al., 2001; Pelletier et al., 2002; Ward et al., 2001; Zaal et al., 1999). Furthermore, the canonical Golgi ribbon organization is also lost during muscle cell differentiation where one subset of Golgi membranes relocates to the nuclear envelope and the other subset lose perinuclear localization (Lu et al., 2001). This organization was shown to be important to organize the microtubule network as the Golgi acts as a MTOC (Oddoux et al., 2013). In addition, the Golgi ribbon fragments and

reassembles during its dynamic polarization in cell migration and inhibition of fragmentation was reported to interfere with polarization (Bisel et al., 2008). During neuronal differentiation, one of the neurite outgrowth branches becomes an axon and the Golgi is preferentially found at the base of axons in neurons. The Golgi relocation to neurite outgrowth site was reported to precede and define axon formation (de Anda et al., 2005; Zmuda et al., 1998). These observations highlight the dynamic nature of the GC, which exists despite its complex architecture and is apparently controlled by tight regulatory elements controlling both the short-term and long-term GC organization.

The Golgi targeted vesicles are formed throughout the cell including the ER, at endosomes and lysosomes and even at areas close to the plasma membrane. Centripetal movement of Golgi targeted vesicles is well characterized and is thought to be a dynein mediated process (Harada et al., 1998; Roghi & Allan, 1999; Vaisberg et al., 1996). In agreement, inhibition of dynein (the major microtubule minus-end targeted motor protein) by RNAi or by overexpression of the p50 subunit, or treatment of cells with various microtubule network disrupting drugs lead to extensive fragmentation of the Golgi apparatus (Echeverri et al., 1996; Presley et al., 1997). Besides being implicated in Golgi ribbon maintenance, the golgin proteins are also accepted to contribute to Golgi positioning. GMAP210 and Golgin-160 are *cis*-Golgi protein and each is required for minus-end movement (Ríos et al., 2004; Yadav et al., 2009). However, once Golgi membranes accumulate in the pericentrosomal area, it's not clear how the Golgi maintains its pericentrosomal localization. The positioning of the Golgi apparatus has been largely attributed to cell cytoskeleton and motor proteins. Depending on the cellular model, either microtubules or actin filaments have the greater influence, whereas the impact of intermediate

filaments is very limited (Gao & Sztul, 2001; Gao et al., 2002; Toivola et al., 2005).

1.3.1 Regulation of Golgi positioning by the actin cytoskeleton

The actin cytoskeleton has an established role in organization and regulation of the secretory pathway (Lanzetti, 2007). In addition, perturbations of the actin cytoskeleton were reported to give rise to alterations in Golgi architecture. Interference of actin cytoskeleton dynamics using depolymerizing actin toxins (cytochalasin D, latrunculin B, mycalolide B) or stabilizing drug (jasplakinolide) invariably leads to compaction of the Golgi complex at the centrosomal area (Babiá et al., 1999; Valderrama et al., 1998, 2001). These observations later lead to studies that revealed a whole machinery of actin cytoskeleton regulators at the Golgi membranes. The mammalian Golgi hosts dozens of actin filaments components, effectors and regulators which are in turn involved in vesicle transport (beta/gamma-actin, short actin filaments, Syne 1B, Tropomyosin isoform Tm5NM-2, Drebrin, Syndapins, Dynamin2, mAbp1, Cdc42, Coronin 7, TC10), cell polarity (Scar2, Arp2/3, Cdc42/Par6/alphaPKC, LIMK1) and the maintenance and positioning of the Golgi (Ankyrins, Spectrin beta III, ARP1, WHAMM, MACF1b, Scar2/Arp2/3, AKAP350, conventional and unconventional myosin (Egea et al., 2006; Ikonen et al., 1997; Montes de Oca et al., 1997). Interestingly, depletion or constitutive activation of actin nucleators like the formin family member mDia (mammalian Diaphanus) or the formin-like 1/FMNL1 and INF2 results in Golgi ribbon fragmentation, indicating an important role actin of dynamics in regulation of Golgi ribbon positioning (Colón-Franco et al., 2011; Zilberman et al., 2011). Another important component of the actin machinery at the Golgi are spectrins, which commonly assemble into

planar cytoskeletal sheets composed of spectrin molecules cross-linked by short actin filaments and were originally found to provide flat shape in erythrocytes (Beck, 2005; Bennett & Chen, 2001). Later, certain variants of spectrin, spectrin beta III, and Syne-1 were shown to localize to the Golgi and to form a skeleton stabilized by actin filaments that binds to the Golgi surface via peripheral proteins, ankyrins, thus forming stable cytoskeletal structure (Gough et al., 2003; Holleran et al., 2001, Stankewich et al., 2001). The spectrin-ankyrin based skeleton was implicated in flat organization of the Golgi cisternae. These observations indicate that ribbon deformations of the Golgi most probably are consequences of ultrastructural defects. Consistently, electron microscopy analysis of the Golgi phenotypes upon treatment with actin toxins revealed deformation in cisternal stacking (Egea et al., 2006). However, the active role of the actin cytoskeleton in dynamic ribbon organization of the Golgi and positioning needs to be investigated further.

1.3.2 Regulation of Golgi positioning by the centrosome

The partnership between the Golgi apparatus and the centrosome, a major microtubule organizing center (MTOC) in cells, is very well studied. In interphase cells, the Golgi and the centrosome are often found in close spatial proximity and this relationship is important for cell polarization, as well as a prerequisite for cell migration (Sütterlin & Colanzi, 2010). Interestingly, certain proteins were shown to localize to both the centrosome and the Golgi apparatus. These proteins with dual localization then lead to speculations about existence of direct linkers between the two organelles. AKAP450 is a large coiled-coil domain containing protein that can localize to both the centrosome and the Golgi via two distinct domains (Shanks et al., 2002; Larocca, et al., 2002). As the centrosome targeting

(C-terminus) and the Golgi targeting domains (N-terminus) of AKAP450 were found on two different termini of the coiled-coil domain, it was suggested that AKAP450 might play an anchoring role for Golgi membranes to the centrosome. Indeed, the expression of the Golgi targeting domain alone resulted in loss of pericentrosomal localization of the GC (Hurtado et al., 2011).

A similar bridging function was attributed to GMAP210, a golgin protein localized preferentially on the *cis*-Golgi. GMAP210 was shown to bind to the Golgi via its N-terminus while its C-terminus can bind to the minus-ends of the microtubules, which are often anchored to the centrosome (Infante et al., 1999). Additionally, GMAP210 can also bind to gamma-tubulin, which interacts with pericentriolar material (Ríos et al., 2004). Active involvement of GMAP210 in maintenance of the GA pericentrosomal localization was proven by ectopically targeting GMAP210 to mitochondria that lead to clustering of mitochondria around the centrosome (Rios et al., 2004). The discovery of several other proteins, such as TBCCD1 and Hook3, that exhibit dual localization and whose depletion showed detachment of the Golgi from the centrosome, indicated that these linker proteins function in redundant pathways. Yet the contribution of each proteins is nevertheless required for GC pericentrosomal positioning (Gonçalves et al., 2010; Walenta et al., 2001).

1.3.3 Regulation of Golgi positioning by the concerted effort of centrosomal and Golgi derived microtubules

In a recent study it was suggested that the Golgi complex depends on the centrosome only during early Golgi biogenesis: laser ablation of the centrosome did not have any effect on maintenance and function of the already-assembled Golgi complex, MT array organization, cell polarization

and motility (Vinogradova et al., 2012). However, when the Golgi is assembled in the absence of the centrosome the cell is incapable of polarized cell migration (Vinogradova et al., 2012). Additionally, the Golgi was shown to nucleate a subset of microtubules in a CLASP-dependent manner and are also required for proper Golgi ribbon assembly and continuity (Miller et al., 2009). The absence of Golgi-derived MTs lead to the formation of a circular Golgi ribbon whereas in their presence the Golgi displayed a rather tangential oval Golgi organization (Miller et al., 2009). These results lead to a two stage model of Golgi ribbon assembly where in the first stage (also called g-stage), the Golgi membranes self-assemble peripherally via Golgi derived CLASP dependent microtubules and in a second stage (also called c-stage) the assembled Golgi membranes move to the center via centrosomal microtubules. It is thought that the main role of Golgi derived microtubules is to pre-merge Golgi ministacks that are captured more easily by centrosomal microtubules. Thus, Golgi nucleated microtubules cluster the Golgi stacks and contribute to the ribbon integrity whereas centrosomal microtubules provide spatial cues only early during biogenesis. Once the Golgi ribbon is formed, the function of centrosome for Golgi ribbon maintenance and polarization is dispensable (Miller et al., 2009).

1.3.4 Regulation of Golgi positioning by stable microtubules

Even though the Golgi positioning is maintained upon centrosome ablation, microtubule depolymerization by treatment with nocodazole leads to extensive Golgi fragmentation (Sandoval et al., 1984). This indicates that the major function of the centrosome for Golgi biogenesis would be to provide spatial cues for Golgi ribbon formation by generating a radial array of microtubules. Upon nocodazole washout, peripheral Golgi fragments

move along the radial of microtubules towards the center and display high colocalization with the stable pool of microtubules (Kreis, 1987; Marsh et al., 2004; Skoufias et al., 1990; Thyberg & Moskalewski, 1989). Interestingly, the pericentrosomal accumulation of the Golgi membranes precedes microtubule de-tyrosination, suggesting that the Golgi might induce MT stabilization upon fragment centralization (Skoufias et al., 1990; Kreis, 1987). Golgi nucleated microtubules go through early stabilization and are γ-tubulin dependent (Chabin-Brion et al., 2001). In several studies it was reported that stable microtubules might be important for the maintenance of the Golgi structure and its localization (Cao et al., 1998; Nakamura et al., 1997; Rios et al., 1994; Satoh & Warren, 2008; Striegl et al., 2010). Indeed it was found that the loss of the stable pool of microtubules resulted in fragmentation and loss of pericentrosomal localization of the Golgi apparatus (Koegler et al., 2010; Ryan et al., 2012). CLASP and GMAP210 were shown to have a dual binding role between Golgi and MTs and could function as linker between these two compartments. Functional studies using RNAi correlated the loss of stable microtubules and concomitant fragmentation of the Golgi apparatus. CAP350, like AKAP450, possesses dual binding ability to both pericentrosomal microtubules and the GA. Depletion of CAP350 leads to loss of stable microtubules and thus leads to Golgi fragmentation (Hoppeler-Lebel et al., 2007). It was suggested that CAP350 accumulates at microtubule minus ends and maintains a pericentrosomal stable subset of microtubules (Hoppeler-Lebel et al., 2007). This pool was found to play a role in maintenance and integrity of the Golgi (Hoppeler-Lebel et al., 2007). Dystonin-a2 isoform, a nuclear membrane protein, mediates perinuclear MT stability by interacting with MAP1B. Loss of MT stability and acetylation lead to a fragmentation of the Golgi. Rescue of the MT acetylation by Trichostatin A (TSA), a drug that inhibits a major microtubule

deacetylase Histone deacetylase 6, or by overexpression of MAP1B rescued the Golgi ribbon organization as well (Ryan et al., 2012). These high associations suggest that stable microtubules could enforce ribbon formation by providing stable tracks for Golgi membranes and facilitate efficient merging of ministacks. Additionally, as stable microtubules locations in the cell dynamically change in response to various processes, such as cell polarization, it could provide a consistent mechanism for regulation of Golgi localization. Indeed, stabilization of the microtubules by Taxol, leads to relocation of the Golgi membranes to the periphery (Rios et al., 2004).

2 Aim of Study

Given the increasing number of factors implicated in organization of the Golgi, it is still unclear how its organization and pericentrosomal positioning are regulated. The questions that need to be addressed include whether pericentrosomal localization of the Golgi membranes is maintained by anchoring to the centrosome or by continuous accumulation of Golgi material that is achieved by the growing and shrinking of microtubules? Then how do the changes in microtubule dynamics affect the Golgi organization? Is it due to subsequent accumulation of PTMs on the microtubules and the resulting change in biochemical properties? As the Golgi membranes do not just accumulate in pericentrosomal area, but rather assemble into one unified and polarized structure, it's also important to elucidate the composition and the nature of the Golgi ribbon 'skeleton'.

In order to identify new regulators of Golgi ribbon organization and answer the posed questions, the specific objectives of this thesis were:

i. Identify new genes by siRNA-mediated screening which influence Golgi organization and positioning in mammalian cells
ii. Characterize the molecular function of the obtained candidate(s)
iii. Integrate the findings with the known components (cytoskeleton, centrosome) regulating Golgi organization

3 Results

3.1 RNAi screen to identify novel regulators of the Golgi complex

To identify novel regulators of the Golgi organization and positioning, siRNA screen was performed. The RNAi library was designed in the Pepperkok Group (by Vibor Laketa) and targeted 680 peripheral membrane proteins that possess PH, PX, C1, C2, FYVE, ENTH, ANTH, BAR, FERM or PDZ domains (Staehelin et al., 2008). Images of Hela cells stably expressing a GFP-tagged Golgi marker (GalNAc-T2 or GalT) after RNAi transfection had also been already acquired (Christian Schuberth; see Methods for details of the screening).

Manual quantification of these images acquired after 72h of RNAi transfection revealed various Golgi phenotypes (Figure 5). In total 4 images, resulting from 2 siRNA treatments, were analyzed per gene and each image was scored as following: 0 – if <10%; 0.5 – if 10%-30%; and 1 – if >30% of the cells possessed Golgi with abnormal phenotypes. An overall gene score was calculated by summing up the scores of the individual images and genes with 3 or higher score were classified as candidate hits. The quantification revealed 70 genes (*Supplementary Table 1*) as potential Golgi regulators, most of which were previously implicated in the context of membrane trafficking, lipid signaling and cell-to-cell and/or cell-to-matrix interactions before (*Supplementary Table 1*).

3.2 RPGRIP1 depletion leads to Golgi ribbon reorganization

Among the 70 candidate hits, we found a centrosomal protein RPGRIP1 that upon siRNA-mediated depletion leads to an uncondensed

and extended Golgi organization (32% increased in Golgi area) (Figure 6A, C) as compared to control treatment at the light microscopy level with no significant effect on Golgi fragmentation (Figure 6B). Immunostaining for Golgi matrix components, GM130, Giantin and Golgin84 upon RPGRIP1 depletion showed co-localization of these markers along the extended stretches of the ribbon, indicating that morphological changes are due to the ribbon reorganization and were not a GalNAc-T2 or GalT specific re-localization (Figure 6A). Consistently, an ultra-structural analysis of the Golgi organization by correlative light-electron microscopy (CLEM) revealed Golgi stacks in extended arms of the Golgi with no significant stacking defect (Figure 7).

In earlier studies, RPGRIP1 was attributed a scaffolding role in centrosome and in primary cilium organization of ciliated cells (Roepman et al., 2005). In a recent report, increased microtubule acetylation was observed in retina of Rpgrip1 deficient mice (Patil et al., 2012). Mass-spec analysis with RPGRIP1 showed interaction with IQGAP1, a potent microtubule stabilizing protein at the cell cortex, and many tubulin isoforms (Coene et al., 2011). In fractionation studies, RPGRIP1 was found predominantly in the cytoskeletal fraction of wild-type mice (Patil et al., 2012). These accumulating observations about RPGRIP1 suggest that it might also have a function in regulation of microtubule dynamics in addition to a scaffolding role in the centrosome. In this study, in RNAi screen we found that RPGRIP1 depletion leads to loss of compact, pericentrosomal Golgi positioning and shape of the Golgi ribbon acquires elongated, uncondensed architecture (Figure 6A). To our knowledge, RPGRIP1 had previously never been linked to the secretory pathway. So far mainly the centrosome and the microtubule cytoskeleton have been implicated in the Golgi positioning. As RPGRIP1 is a centrosomal protein with possible function in microtubule dynamics with effects on the Golgi

positioning and architecture, it was a good candidate to investigate in detail. To elucidate how RPGRIP1 depletion is leading to an elongated Golgi ribbon we set out to characterize the cellular function of the protein. As earlier studies focusing on the role of RPGRIP1 in cultured cells were carried in RPE1 cells and RPGRIP1 depletion also shows Golgi reorganization upon RPGRIP1 depletion in RPE1 cells, we decided to use both Hela and RPE1 cell lines for our further experiments.

3.3 Isoform specific expression of RPGRIP1

3.3.1 Organization and Localization of RPGRIP1 isoforms

The RPGRIP1 locus contains 25 exons and transcripts undergo extensive alternative splicing. The NCBI gene database lists 7 predicted isoforms and 9 isoforms submitted from different studies for the RPGRIP1 locus [http://www.ncbi.nlm.nih.gov/gene/57096]. The most studied longest isoform has N-terminal coiled-coil, tandem C2 domains in the middle and C-terminal RPGR interacting domain (Figure 8A). C2 domains, encoded by exons 14-16, were shown to be important for its scaffolding function (Roepman et al., 2005) however some isoforms do not possess this domain (Figure 8B, 8C). In addition, RPGRIP1 isoforms display species specific and tissue specific expression however no isoform specific function has been reported (Schu et al., 2005, Lu et al., 2005, Koenekoop et al., 2005).

Table 1: Grouping of RPGRIP1 isoforms

Group name	Isoforms
RPGRIP1-FL	NM_020366.3 AJ417067

RPGRIP1-E10	XM_006720208.1
	XM_005267879.1
	XM_005267879.1
	AF260257
RPGRIP1-E12	XM_005267881.1
	AF227257
RPGRIP1-E14	AF265666
	AF265667
	BX571740
RPGRIP1-NoC2	XM_006720209.1
	AK301780
	BC039089
RPGRIP1-E15	
	XM_006720210.1

To check for isoform specific localization that can provide a hint for isoform specific functions, we first grouped isoforms into 6 groups according to similarity of their exon organization and gave simplified names as indicated in Table 1. Then we cloned one construct from each group into GFP vector and expressed RPE1 cells. Except for the longest isoform, RPGRIP1-FL, all other isoforms displayed cytoplasmic, nuclear or both localizations (Figure 9). RPGRIP1-FL isoform showed cytoplasmic and punctuate localization throughout the cell. As we couldn't observe the previously reported centrosomal localization, we tagged the RPGRIP1-FL isoform with smaller epitope tags than GFP, i.e. myc and flag and observed mild accumulation in the centrosomal area (Figure 10). However, this was not observed in all transfected cells. As RPGRIP1 localization was claimed to be cell type dependent (Lu et al.,2005), we expressed the RPGRIP1-FL in ARPE19 cells and observed clear centrosomal staining

(Figure 11). From this we concluded that the RPGRIP1-FL does localize to the centrosome however its enrichment at the centrosome is cell type dependent and sensitive to protein tags. The localizations of other isoforms need to be tested again in ARPE19 cells and preferentially with smaller tags to be conclusive.

3.3.2 70kDa RPGRIP1 isoform is expressed in RPE1

To find which isoform(s) is/(are) expressed in RPE1 and Hela cells, we treated cells with anti-RPGRIP1 siRNAs and performed western blot with rabbit polyclonal anti-RPGRIP1 antibody (abRPGRIP1, see Methods for details) raised against 'BC039089.1' isoform which has 70kDa size. All 3 siRNAs against RPGRIP1 depleted the 70kDa band in RPE1 cells with strongest depletion using siRPGRIP1_5, which was then used in our further experiments (Figure 12). There are several other isoforms, both predicted (XM_006720209) and reported (AF265666, AF265667, AK301780) with an approximate size of 70kDa. A similar sized band was observed with abRPGRIP1 antibody in Hela and ARPE19 cells, where RPGRIP1 was claimed to be expressed in other studies (Shu et al, 2005). However, no depletion was detected with 3 different siRNAs against RPGRIP1 (Figure 13A). It's possible that isoforms in Hela and APRE19 cells are not recognized by abRPGRIP1 antibody. So we generated anoather polyclonal antibody against RPGRIP1 (gs-abRPGRIP1) and this antibody recognized several bands. However, none of the bands displayed significant decrease in response to 3 different siRNAs against RPGRIP1 in Hela and ARPE19, suggesting that this antibody was not specific (Figure 13B). So we conclude that 70kDa is expressed in RPE1 cells however in Hela and ARPE19 cells it still needs to be investigated to identify which

isoforms are expressed. We also currently don't know which of the 70kDa isoforms is expressed in RPE1 and where it localizes. As the overexpression of RPGRIP1 constructs often lead to cell death, we decided to concentrate in the following work on characterizing the loss of RPGRIP1 function.

3.4 RPGRIP1 depletion leads to increased microtubule stabilization

3.4.1 RPGRIP1 depletion reduces microtubule nucleation and amount of polymerized tubulin

As mentioned in the Introduction (Section 1.3.2) some centrosomal proteins are implicated in pericentrosomal localization of the Golgi membranes by interacting with the Golgi matrix proteins. To find out how RPGRIP1 depletion is leading to the loss of compact pericentrosomal positioning of the Golgi, we hypothesized that RPGRIP1 might bind to Golgi membranes peripherally via its C2 domain. A structural modeling study of the RPGRIP1 C2 domain suggested that it would function in a calcium independent manner (Roepman et al., 2005). To test whether the RPGRIP1 C2 domain would bind to Golgi membranes, we cloned it into a mammalian RFP expression vector and expressed it in Hela cells. The sequence of the RPGRIP1 C2 domain was taken from another study (Roepman et al., 2005). However, the RPGRIP1 C2 domains displayed cytoplasmic and nuclear localization with no particular enrichment to any membranous compartment (Figure 14A, 14B). RPGRIP1 paralog RPGRIP1L that shows 29% amino acid identity in sequence also has C2 domains where sequence similarity is highest (52% identity) (Arts et al., 2007). Expression of RPGRIP1L C2 domain also displayed cytoplasmic

and nuclear localization similar to RPGRIP1 C2 domain (Figure 14C). The sequence of the RPGRIP1L C2 domain was taken from another study (Roepman et al., 2005). As the full-length construct also did not show Golgi localization, we concluded that RPGRIP1 probably does not have centrosome bridging function in Golgi positioning.

Next we hypothesized that the Golgi uncondensation upon RPGRIP1 depletion might be due to defects in centrosome organization and/or function. However, we could not detect any difference in organization of the centrosome both in Hela and RPE1 cells as seen by immunostaining and quantification of protein amount (as inferred from intensity) for two centrosome components after RPGRIP1 depletion: pericentrin and gamma-Tubulin and by number of centrosomal foci per cell, suggesting a rather minor role of RPGRIP1 in centrosome organization (Figure 15).

As the centrosome functions as a major microtubule-organizing center (MTOC) in mammalian cells, we asked whether microtubule nucleation was affected. To address this we treated Hela cells with siRNAs against RPGRIP1 for 72h and cooled the cells on ice for 1h to depolymerize microtubules. Then cells were warmed to 37°C and fixed after 0, 45 or 90 seconds. After immunostaining for tubulin and EB1, we classified cells into one of three classes depending on the nucleation stage: 'No Growth', 'Moderate Growth' and 'Extensive Growth' (Figure 16A). Depletion of CLASP lead to increased fraction of cells with 'Extensive Growth' after 45 and 90 seconds in consistent with reports where CLASP depletion lead fast microtubule growth (Mimori-Kiyosue et al., 2005) (Figure 16B). In contrary, depletion of RPGRIP1 lead to increased fraction of cells with 'No Growth' after 45 and 90 seconds suggesting that microtubule nucleation from centrosome is delayed upon RPGRIP1 depletion (Figure 16B). Then we asked if delayed microtubule

nucleation from the centrosome affects the amount of polymerized tubulin. Hela cells were treated with control and anti-RPGRIP1 siRNA and immunostained for polymerized tubulin after methanol fixation. Quantification of the polymerized tubulin upon RGPRIP1 depletion also revealed decreased amount of polymerized microtubules, however no major alterations in overall organization of microtubules were observed (Figure 17). Thus, we conclude that RPGRIP1 might regulate the microtubule nucleation capacity of the centrosome and could be involved in regulation of the microtubule cytoskeleton.

3.4.2 RPGRIP1 depletion leads to increased microtubule acetylation

As microtubule cytoskeleton acts as a substrate for various motor proteins, amount of polymerized tubulin is critical in many cellular processes including membrane trafficking, mitosis and cell migration. Many factors have been implicated in regulation of the microtubule dynamics that ultimately lead to stabilization or destabilization of the microtubule protofilament (Section 1.2.1). As we observed decreased amount of polymerized microtubules, we decided to measure how stability of these decreased pool of microtubules has changed upon RPGRIP1 depletion. Many reports have shown positive correlation between microtubule stability and its acetylation level (Piperno et al., 1987). Thus we also first measured microtubule acetylation level to infer about microtubule stabilization change. To test for microtubule acetylation change upon RPGRIP1 depletion, Hela and RPE1 cells were treated with anti-RPGRIP1 siRNA for 72h and analyzed both by immunofluorescence and western blot against acetylated tubulin. Our quantification of western blot results revealed 1.86 and 1.77 times increase in acetylated microtubules in Hela and RPE1 cells

respectively (Figure 18). This is consistent with a recent report where increased microtubule acetylation in the cell body was observed in retinal tissues of mice with Rpgrip1 -/- genotype (Patil et al., 2012). RPGRIP1 and RPGRIP1L have overlapping functions in primary cilium maintenance (Coene et al., 2011), however we didn't see any change in microtubule acetylation upon RPGRIP1L depletion (Figure 19).

Besides increased microtubule stabilization, increased activity of microtubule acetyltransferases, enzymes that acetylate microtubules, or decreased activity of microtubule deacetylases could also lead to increased microtubule acetylation (Akella et al., 2010; Hubbert et al., 2002). To rule out the possibility of increased activity of microtubule acetyltransferases we decided to measure kinetics of microtubule acetylation upon RPGRIP1 depletion. To measure microtubule acetylation, we treated cells with siRNAs for 72h and monitored the amount of acetylated microtubules at various time points after adding the drug Trichostatin A (TSA). TSA blocks the activity of the major microtubule deacetylase HDAC6 and rules out microtubule deacetylation reaction thus our measurements will directly show the kinetics of microtubule acetylation (Hubbert et al., 2002). We tested several TSA concentrations and different time points and found that 1µM TSA concentration is sufficient to completely block HDAC6 activity (Figure 20A) and fastest microtubule acetylation occurs within 5h of TSA administrations (Figure 20B). Quantification of acetylated microtubules by western blot at various time points revealed no significant change in kinetics of microtubule acetylation upon RPGRIP1 depletion but it was strongly reduced upon ATAT1 depletion, a major microtubule acetyltransferase (Figure 20C) (Akella et al., 2010). Next to rule out possibility of decreased microtubule deacetylation reaction upon RPGRIP1 depletion, we treated cells with anti-RPGRIP1 siRNA for 72h and TSA for 24h. Treatment of cells with TSA for

24h blocks the activity of HDAC6 and cells become saturated with acetylated microtubules. Then we washed away TSA and measured amount of acetylated microtubules at various time points by western blot. Our quantification of acetylated tubulin revealed fast deacetylation reaction (almost instant) in control and siRPGRIP1 treated cells but it was dramatically reduced upon HDAC6 depletion control (Figure 20D). Thus, we concluded that increased microtubule acetylation upon RPGRIP1 depletion is not due to change in activity of enzymes responsible for microtubule deacetylation or acetylation and most probably increased acetylation of microtubules is due increased microtubule stabilization.

3.4.3 RPGRIP1 depletion leads to increased microtubule stabilization

The acetylation level of microtubules correlates with the stable nature of the microtubules; however, it does not *per se* confer stability (Zilberman et al., 2009). Thus, to test if increased acetylated microtubules represent increased microtubule stabilization directly, RPGRIP1 depleted cells were treated with the microtubule depolymerizing drug nocodazole, and fixed after 0, 8, 20 minutes. Cells were stained for tubulin and the amount of polymerized tubulin after drug treatment was measured (See Methods for details of quantification). Consistent with the acetylation marker, microtubules in RPGRIP1 depleted cells were more resistant to nocodazole (Figure 21) and lead to increased microtubule stabilization. On the contrary, CLASP was shown to stabilize microtubules and its depletion removed the nocodazole resistant pool of microtubules, consistent with previously reported data (Figure 21) (Mimori-Kiyosue et al., 2005). This indicates that RPGRIP1 might have a more general function in the regulation of microtubule dynamics.

3.4.4 RPGRIP1 depletion leads to inefficient plus tip complex formation

Microtubule plus end tip dynamics have an important role in microtubule turnover and their organization is another distinguishing feature of stable versus dynamic microtubules. Fast-growing microtubules display longer plus-end tip 'comets' than slow growing microtubules, as one can observe when staining for EB1 (Bieling et al., 2007). As a consequence, overexpression of proteins that stabilize microtubules and decrease their polymerization speed (e.g. CLASP and CAP350), leading to the formation of short and rounded plus-end comets (Mimori-Kiyosue et al., 2005; Hoppeler-Lebel et al., 2007). In contrast, their depletion leads to faster microtubule growth speed and therefore longer plus-end comet size (Mimori-Kiyosue, 2005). Using this data as a basis, we tested whether EB1 comet shape is affected upon RPGRIP1 depletion in RPE1 cells. Cells were treated with anti-RPGRIP1 siRNA and immunostained for EB1 and tubulin. Major axis and minor axis of EB1 comets were measured as described in Methods and comets were classified into 3 groups according to ratio of comet major axis length to minor axis length as following: 'Non-growing' if ratio < 1.5, 'Intermediate' if ratio 1.5 < ratios < 4.5 and 'Growing' if ratio > 4.5. Quantification of distribution of different classes of EB1 commet revealed increased fraction of 'Non-growing' EB1 comets upon RPGRIP1 depletion (Figure 22).

In pull-down and mass-spectrometry experiments a well-known microtubule stabilizing protein, IQGAP1, was detected as novel interacting partner for RPGRIP1 (Coene et al., 2011). IQGAP1 localizes to cell-cell contact sites and to the leading edge and captures microtubule plus-ends at the cell cortex by interacting with CLIP170. So we hypothesized that RPGRIP1 depletion causes increased IQGAP1 accumulation at the

plasma membrane and thus leads to increased microtubule stabilization. However, immunostaining experiments did not reveal any association in microtubule stabilization and IQGAP1 accumulation. So the mechanism of RPGRIP1 depletion mediated microtubule stabilization still remains to be further investigated. Nevertheless, as microtubule dynamics have a critical role in positioning of the Golgi, the increased microtubule acetylation and/or increased stabilization caused by RPGRIP1 depletion is likely to be the cause of the loss of pericentrosomal positioning of the Golgi in these cells.

3.4.5 Effect of RPGRIP1 isoforms on microtubule stabilization

Up to now, functional studies on RPGRIP1 focused on characterization and importance of the C2 domain (Roepman et al, 2005; Fernandez-Martinez et al., 2011; Coene et al., 2011; Schu et al., 2005), however some isoforms (i.e. isoforms within the RPGRIP1-NoC2 group) do not possess this domain. This motivated us to test if role of RPGRIP1 in microtubule dynamics is specific to a particular isoform. As we didn't have RPGRIP1 isoform specific siRNAs, we measured microtubule acetylation by overexpressing different RPGRIP1 isoforms. Immunostaining and quantification of acetylated tubulin in transfected cells did not show a significant change as compared to GFP transfected cells (Figure 23). This result suggests that there is no gain of function upon overexpression of RPGRIP1. Next we tested whether overexpression of these constructs can complement increase of microtubule acetylation, as it would be very interesting to dissect the function of the different RPGRIP1 isoforms. However both the depletion of RPGRIP1 and overexpression of RPGRIP1

isoforms lead to increased cell death, so we were so far unable to attribute function of RPGRIP1 in microtubule dynamics to any particular isoform.

3.5 Golgi reorganization upon RPGRIP1 depletion is due to increased microtubule stabilization

The importance of microtubule acetylation in pericentrosomal localization of the Golgi was reported in several other studies, but the molecular mechanism is unknown. Increase of microtubule acetylation after treatment of cells with HDAC6 inhibitors such as Trichostatin A (TSA) or Tubacin leads to compaction of the Golgi ribbon around the centrosome (Ryan et al., 2012). On the other hand, kinesins are plus-end directed motors and transport vesicles away from the pericentrosomal area and they were reported to have increased affinity towards the acetylated pool of microtubules (Reed et al., 2006). Additionally, treatment of cells with Taxol, a potent microtubule-stabilizing drug, leads to increased microtubule stabilization and acetylation and to subsequent fragmentation and peripheral relocation of the Golgi vesicles (Rios et al., 2004). These observations indicate that, even though microtubule acetylation and stabilization are highly associated with each other, they might exert different and independent effects on the positioning of Golgi. Since RPGRIP1 depletion leads to both increase in acetylation and stabilization, we set out to identify which of these changes were responsible for the loss of compact organization and pericentrosomal positioning of the Golgi ribbon.

3.5.1 The Golgi reorganization is due to increased microtubule stabilization

To address whether the Golgi reorganization upon RPGRIP1 depletion is due to increased microtubule acetylation or stabilization, we decided to generate following three conditions: (1) increased stabilization + increased acetylation; (2) increased stabilization + decreased acetylation; (3) decreased stabilization + decreased acetylation and analyze Golgi organization. RPGRIP1 depletion was enough to generate condition (1) as described in previous experiments. To generate condition (2) we depleted ATAT1, a major alpha-tubulin acetyltransferase in mammalian cells (Akella 2010). Depletion of ATAT1 was shown to result in loss of microtubule acetylation and increased microtubule stabilization (Kalebic et al., 2013). Finally we depleted CLASP, a microtubule stabilizing protein, to generate condition (3) (Mimori-Kiyosue et al., 2005). Immunostaining revealed the decreased microtubule acetylation upon depletion of both CLASP and ATAT1 and increased acetylation upon RPGRIP1 depletion (Figure 24A, 24B, 24C). However, ATAT1 and CLASP depletions had opposing effects on the Golgi morphology, where increased Golgi uncondensation occurred upon ATAT1 similar to RPGRIP1 depletion but not upon CLASP depletions (Figure 24A, 24B, 24C). The Golgi reorganization was not observed upon co-depletion of RPGRIP1 with CLASP however it was pronounced upon co-depletion of RPGRIP1 with ATAT1. Additionally, overexpression of ATAT1 lead to an increased amount of acetylated microtubules but did not result in a significant change in Golgi organization and compaction (Figure 25). This result suggests that, the loss of compact organization of the Golgi upon RPGRIP1 depletion is due to increased microtubule stabilization rather than the increased acetylation.

3.5.2 The Golgi ribbon tracks align with stable microtubule tracks

In the previous section we described that increased microtubule stabilization caused increased Golgi uncondensation. Careful analysis of the images showed high association of the Golgi ribbon and stable microtubules. To confirm the Golgi and stable microtubule association, we performed high-resolution imaging in control and RPGRIP1 depleted cells immunostained against acetylated tubulin and Golgin84. RPGRIP1 depletion was used because this treatment provides well-resolved Golgi and acetylated microtubule tracks at the cell periphery. This revealed extensive colocalization of stable microtubule tracks with the Golgi ribbon arms in both control and RPGRIP1 depleted cells (Figure 26). Colocalization was more obvious in RPGRIP1 depleted cells where peripheral individual tracks of the acetylated microtubules and the Golgi ribbon are more resolved by the microscope. Spread of the Golgi following increased microtubule stabilization and high colocalization of the Golgi with stable microtubules suggest that stable microtubules might act as the skeleton of the Golgi ribbon. Role of GM130 and GRASP65 is very well established in maintenance of the Golgi ribbon organization. Depletion of GM130 (Puthenveedu et al., 2006) and GRASP65 (Barr, 1997; Wang et al., 2005) lead to inefficient merging of the ministacks and ultimately lead to fragmentation of the Golgi ribbon. So then we tested whether fragmentation of the Golgi upon depletion of GM130 or GRASP65 can be rescued by increased microtubule stabilization. Depletion of GRASP65 and GM130 alone resulted in fragmentation of the Golgi in consistent with previous reports (Figure 27A, 27C). Interestingly, co-depletion of RPGRIP1 with GRASP65 or GM130 increased the microtubule acetylation and concomitantly lead to decreased Golgi fragmentation and bigger Golgi elements indicating increased merging of the ministacks (Figure 27). This

result suggests that function of GM130 and GRASP65 to link the Golgi stacks together in assembly of the Golgi ribbon might be dispensable when an increased amount of stable microtubules is available. Taken together, our results suggest that the stable microtubules act as anchoring site and facilitate the assembly of the Golgi ministacks into ribbon organization.

3.5.3 The Golgi positioning is dictated by stable microtubules positioning

During cell migration both the Golgi complex (Bisel et al., 2008) and stable microtubules (Wittmann et al., 2003) are preferentially found on the leading edge. It's likely that stable microtubules not only are important for maintenance of pericentrosomal localization of the Golgi but also might be responsible for the dynamic positioning of the Golgi in response to various external stimuli. To test this hypothesis we asked whether ectopic microtubule stabilization could reposition the Golgi complex. To generate ectopic microtubule stabilization we treated cells with Taxol and, consistent with other reports, we observed an accumulation of microtubule bundles at the cell periphery. Live-imaging of the Golgi upon taxol treatment showed that the Golgi repositioned away from the perinuclear area and co-localized with microtubule bundles close to the periphery (Figure 28). The ability of stable microtubules to reposition the Golgi suggests that cells can regulate the Golgi positioning during processes such as polarization and migration by regulating the microtubule cytoskeleton. As mentioned in the introduction (Section 1.2.2), microtubules +TIPs facilitate capture of microtubules at the leading edge thus stabilizing the microtubule. This polarization of the microtubules might then result in polarization of the Golgi complex.

Examples of observed Golgi phenotypes

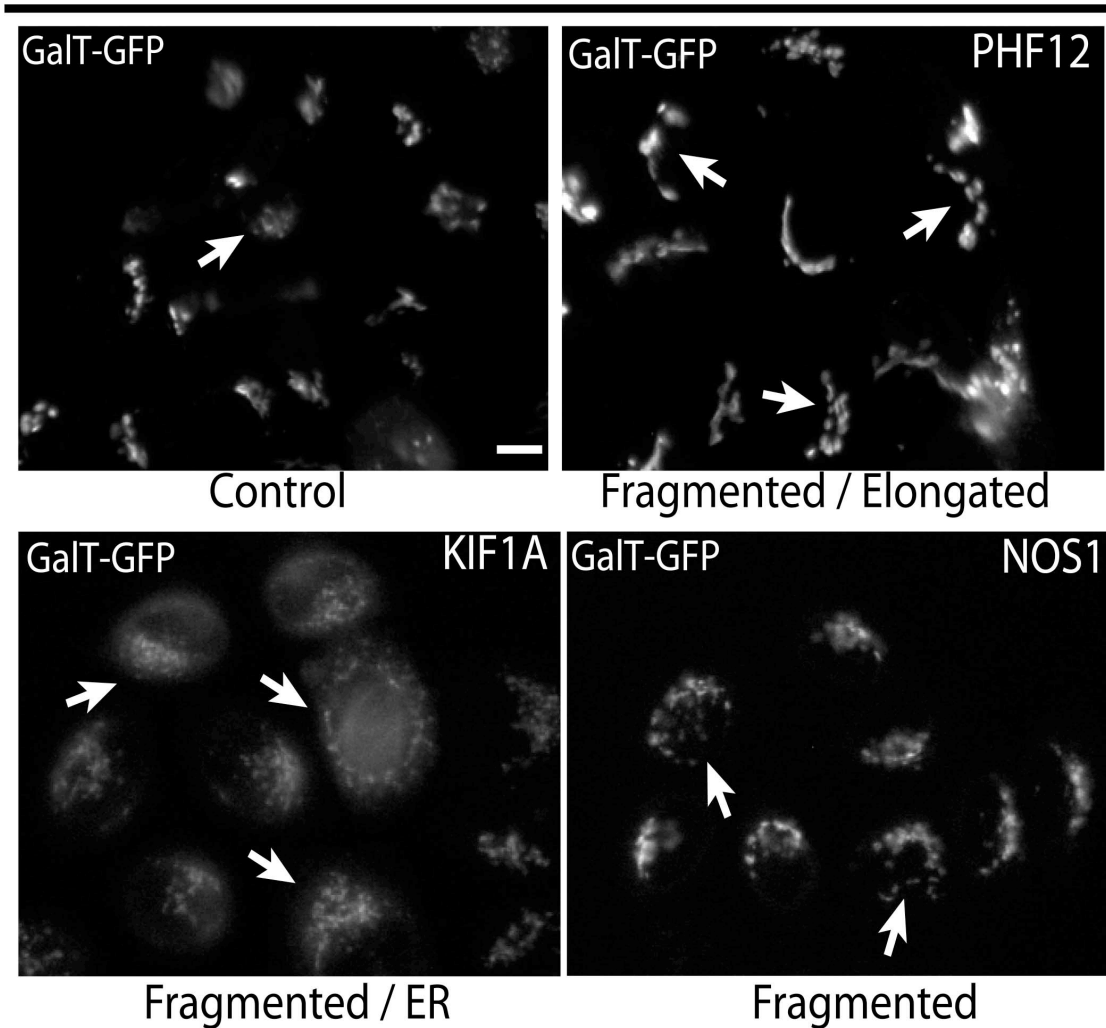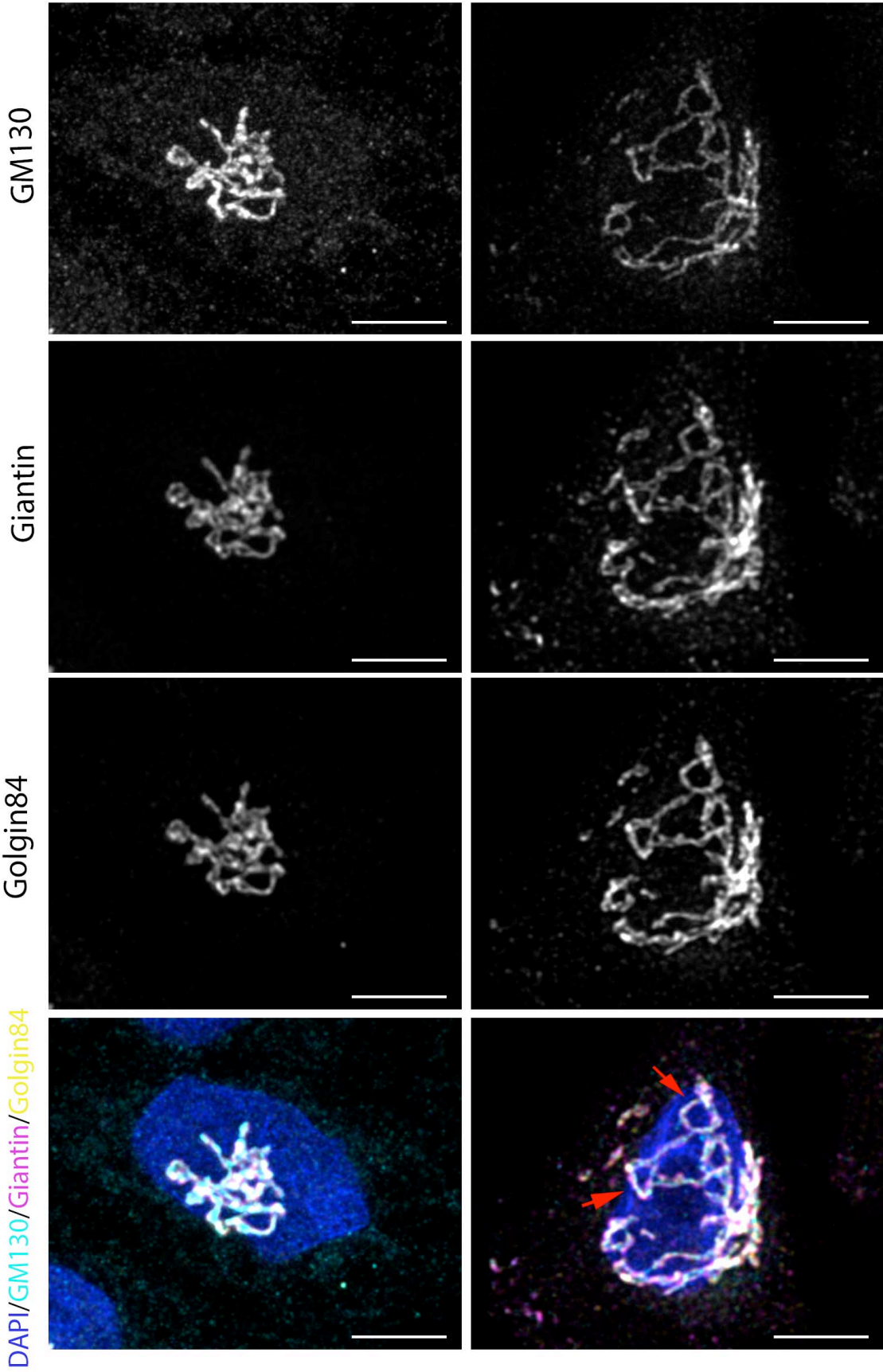**Figure 5: Different Golgi phenotypes observed in RNAi screen.**

The Golgi morphology upon siRNA mediated knock down of three candidate genes: PHF12, KIF1A and NOS1 is shown. Arrows indicate typical Golgi morphologies for different treatments. Scale bar - 5µm.

A

	siNEG9	siRPGRIP1
GM130		
Giantin		
Golgin84		
DAPI/GM130/Giantin/Golgin84		

B

C
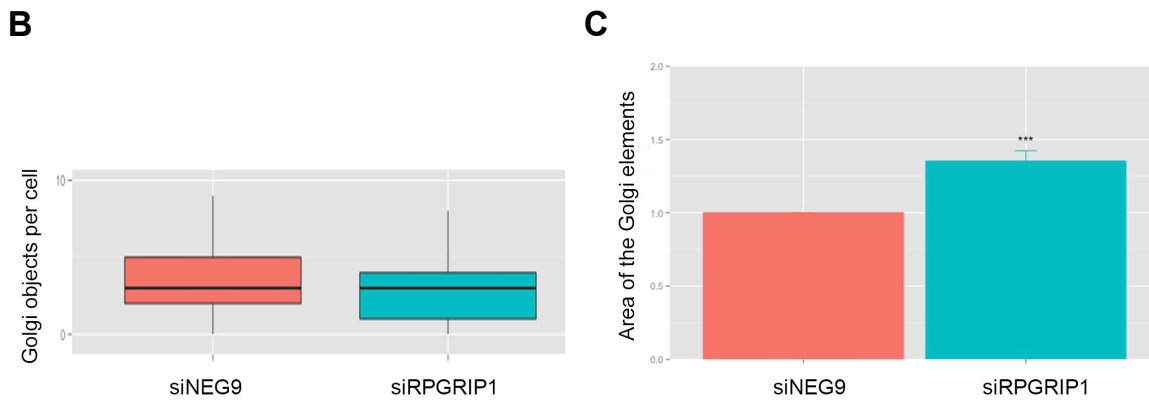
Figure 6: Effect of RPRGRIP1 depletion on Golgi organization.

A. Hela cells treated with control (siNEG9) and anti-RPGRIP1 (siRPGRIP1) siRNAs are immunostained against 3 different Golgi complex markers: GM130, Giantin and Golgin84. Colocalization of all Golgi markers in elongated arms of uncondensed Golgi (arrows) indicates uncondensation of the ribbon and not a reorganization of specific marker. Scale bar - 5µm. **B.** Quantification of Golgi fragmentation upon control and anti-RPGRIP1 siRNA treatment is shown. Number of Golgi fragments per cell was counted and pooled together from 4 different experiments and distributions are plotted with boxplot. Comparison of the medians did not shown significant difference between control and siRPGRIP1 treated cells. **C.** Quantification of Golgi area upon control and anti-RPGRIP1 siRNA treatment is shown. Golgi areas are quantified as described in Methods (check 'BigGolgiBlob') and normalized to control means. Comparison of the distributions shows increase (32%) in Golgi areas upon RPGRIP1 depletion (n=4, t-test, p-value < 0.01). Error bars represent standard error of the mean, '***' indicates 99% significance level.
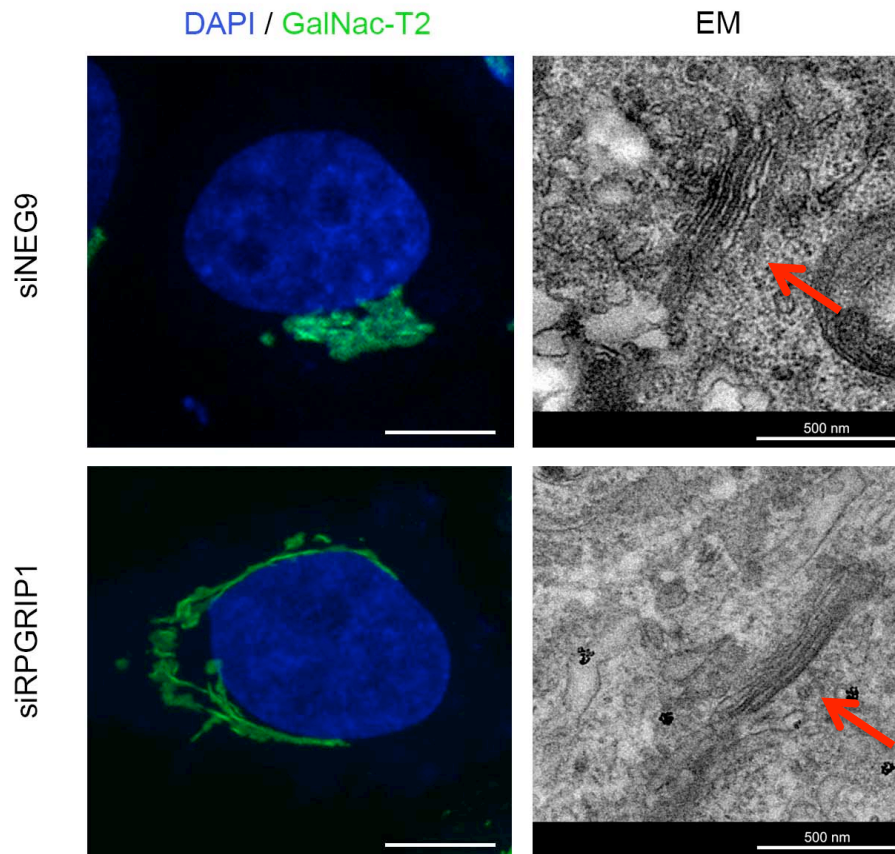
Figure 7: Effect of RPRGRIP1 depletion on Golgi stacking.

Fluorescence images of the control and siRPGRIP1 treated cells selected for CLEM (left panel). Scale bar – 5µm. Gridded MatTek dishes with coordinates were used to find back cells imaged with light microscopy in EM imaging. Electron tomograph sections of the cells corresponding to the stretched part of the Golgi apparatus are shown and canonical stacked organization of the Golgi cisternae is preserved (arrows, right panel).
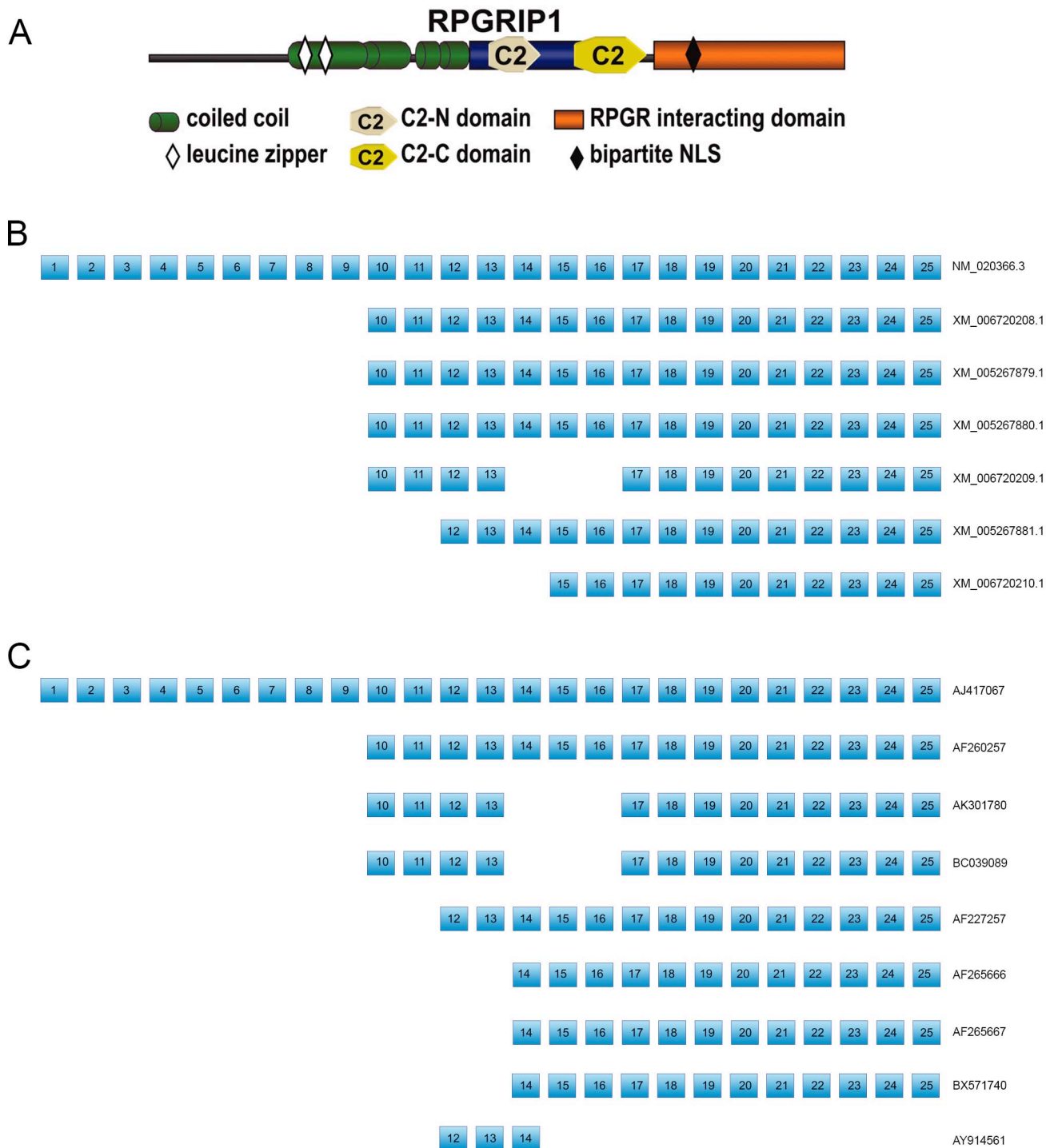
Figure 8: Organization of RPGRIP1 isoforms.

A. Domain organization of longest RPGRIP1 isoform (NM_020366.3). Adapted from (Roepman et al., 2005). **B.** Exon organization of predicted isoforms of RPGRIP1 is shown. C2 domains are encoded by exons 14-16. **C.** Exon organization of RPGRIP1 isoforms detected in previous studies.

GFP DAPI Merged

RPGRIP1-FL

RPGRIP1-E10

RPGRIP1-E12

RPGRIP1-E14

RPGRIP1-NoC2

RPGRIP1-E15
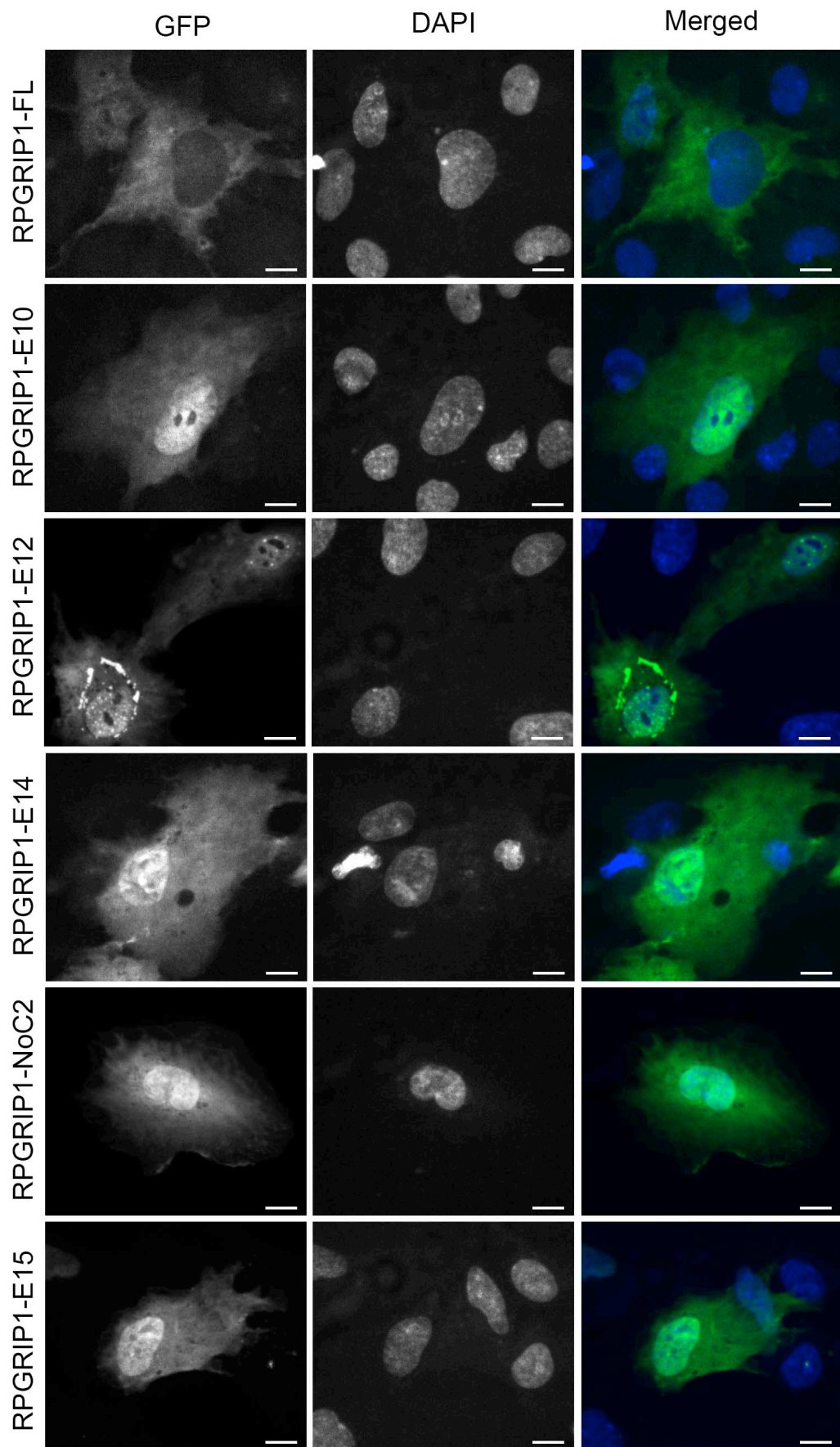
Figure 9: Localization of RPGRIP1 isoforms.

Predicted and submitted isoforms of RPGRIP1 were grouped into 6 groups according to their similarity in exon organization. One from each group is tagged N-terminally with GFP and expressed in RPE1 cells. RPGRIP1-FL isoform mainly localized to cytoplasm. All other isoforms displayed both nuclear and cytoplasmic localization. RPGRIP1-E12 isoform displayed dotty structures in nucleus in addition to perinuclear aggregates (Scale bar - 5μm).
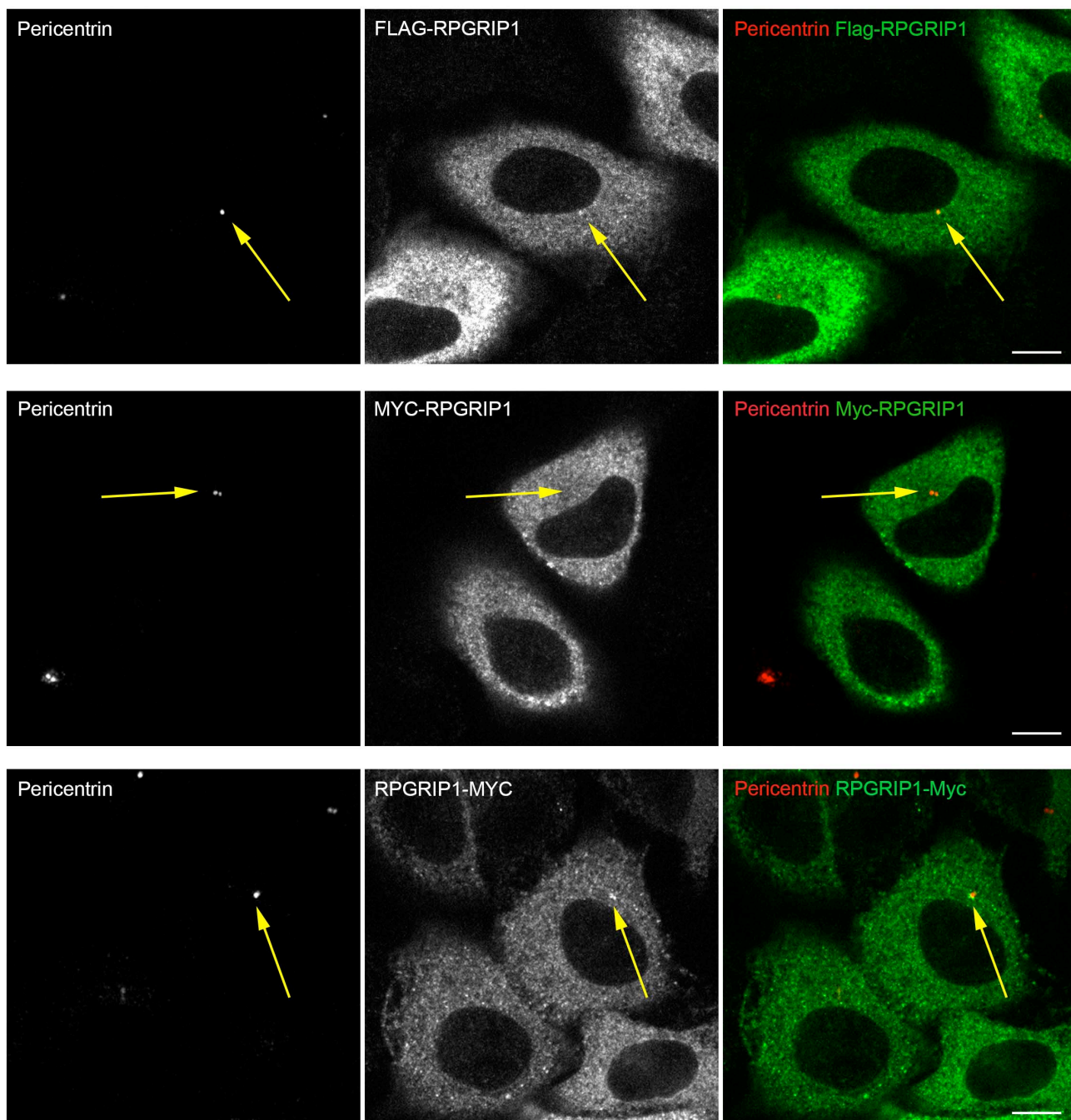
Figure 10: Localization of Myc and Flag tagged RPGRIP1.

Confocal slices of overexpressed Myc and Flag tagged RPGRIP1-FL isoform in Hela cells with anti-Pericentrin immunostaining is shown. No centrosomal staining is visible by MYC-RPGRIP1. Mild or clear centrosomal staining was observed in some cells but not all using FLAG-RPGRIP1 and RPGRIP1-MYC constructs. Scale bar - 5μm.
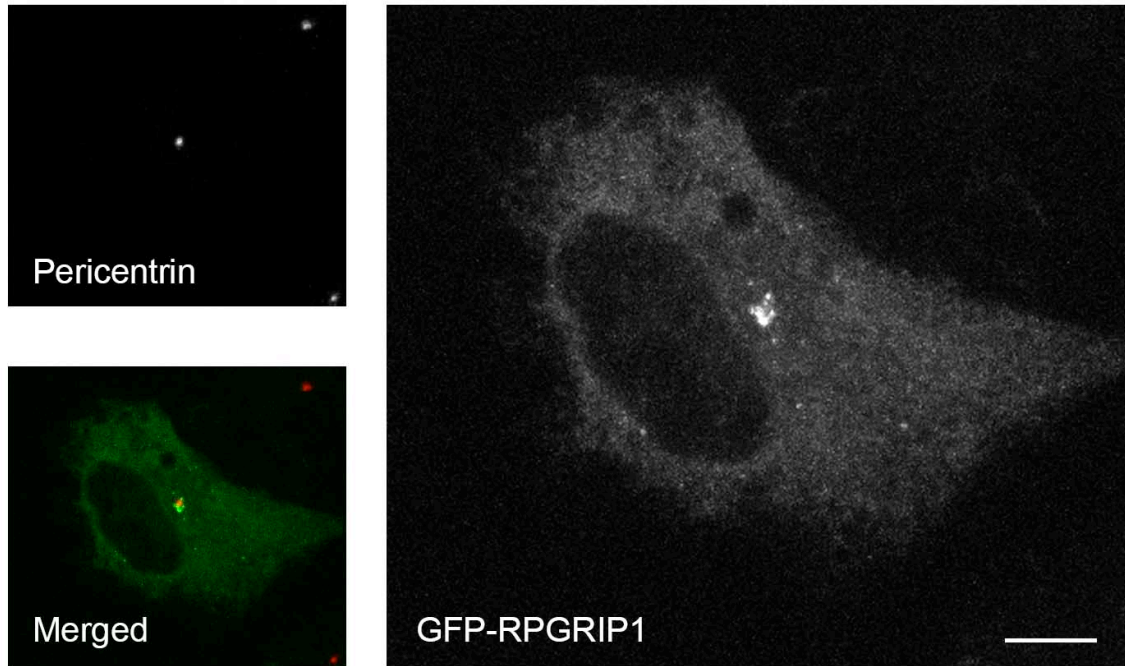
Figure 11: Localizaiton of RPGRIP1-FL in ARPE19 cells.

Maximum projection images of N-terminal GFP tagged RPGRIP1-FL expressed in ARPE19 cells with anti-pericentrin immunostaining is shown. Clear centrosomal localization was observed. Scale bar - 5µm.
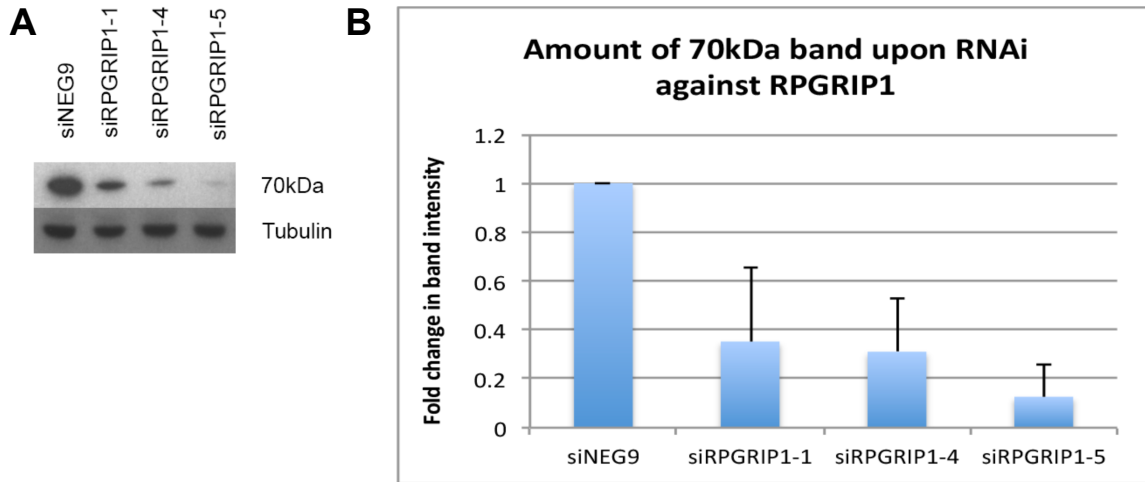
Figure 12: Isoform specific expression of RPGRIP1 in RPE1.

A. Western blot analysis of RPE1 cells using abRPGRIP1 antibody upon three different siRNAs against RPGRIP1. **B.** 70kDa band was depleted up to 90% with siRPGRIP1-5. Bar heights represent means of the three different experiments (n = 3, Error bar, +SD).

A

B
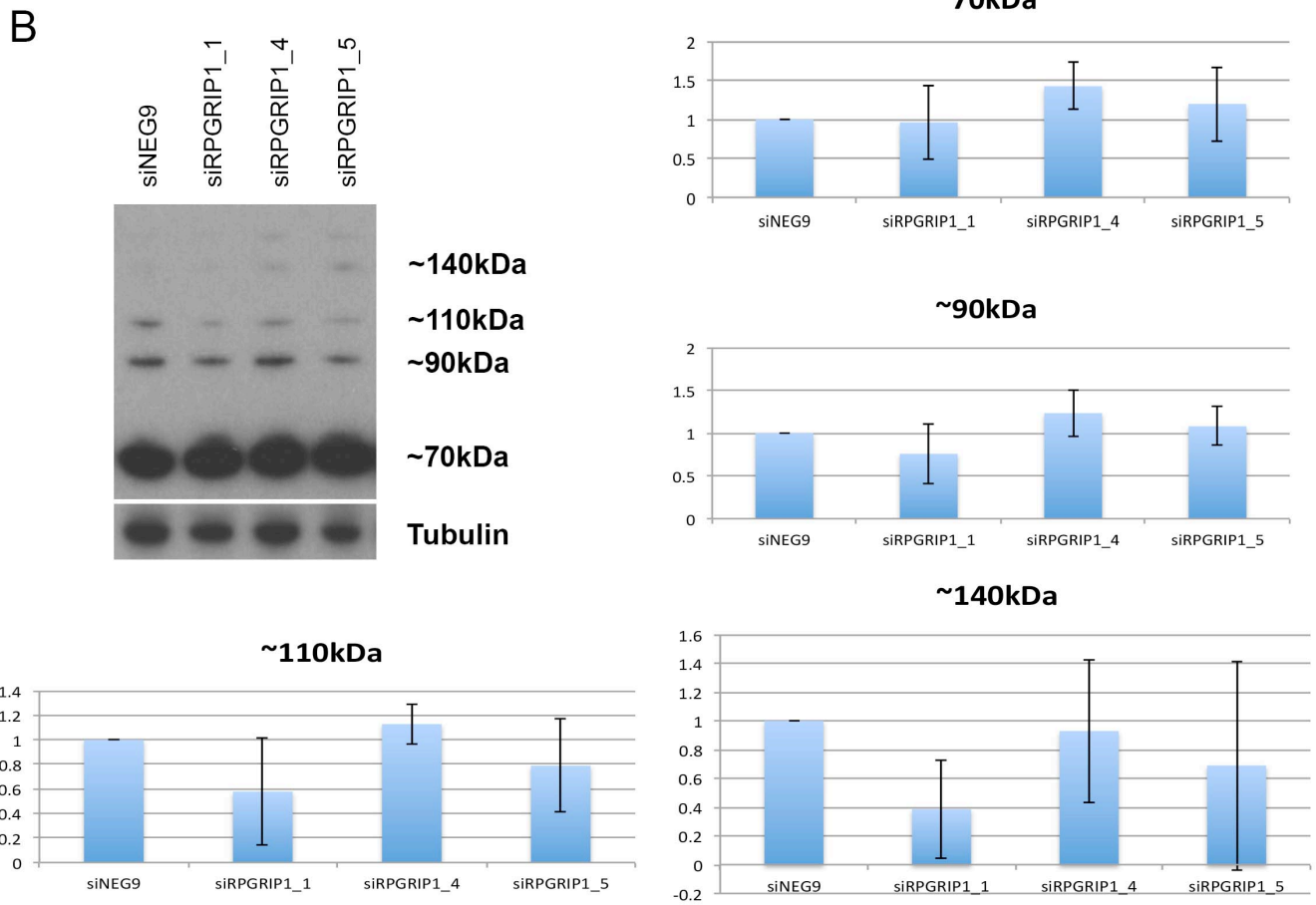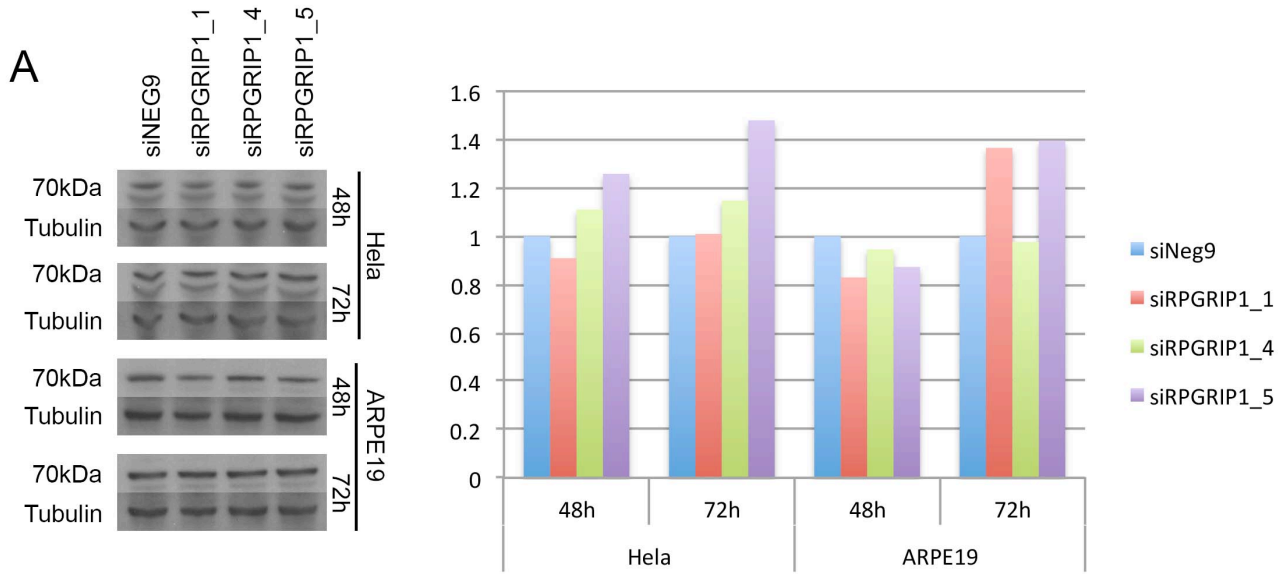
Figure 13: RPGRIP1 expression analysis in Hela and ARPE19 cells.

A. Western blot analysis of Hela cells treated with three different siRNAs against RPGRIP1 using gs-abRPGRIP1 antibody. Antibody recognizes several bands and quantifications of intensities are shown in bar chart with corresponding band size labeled in title. None of the bands display specific depletion with three different siRNAs (Error bar, +/- SD). **B.** Western blot analysis of Hela and ARPE19 cell lysates treated with three different siRNAs using abRPGRIP1 antibody (WB staining for only Hela cell lysate is shown). 70kDa band is visible when stained with abRPGRIP1 antibody. Quantification of the band intensities does not show any depletion upon anti-RPGRIP1 siRNA treatment.

A   RFP-RPGRIP1-C2

B

RPGRIP1-C2-RFP

C   RFP-RPGRIP1L-C2
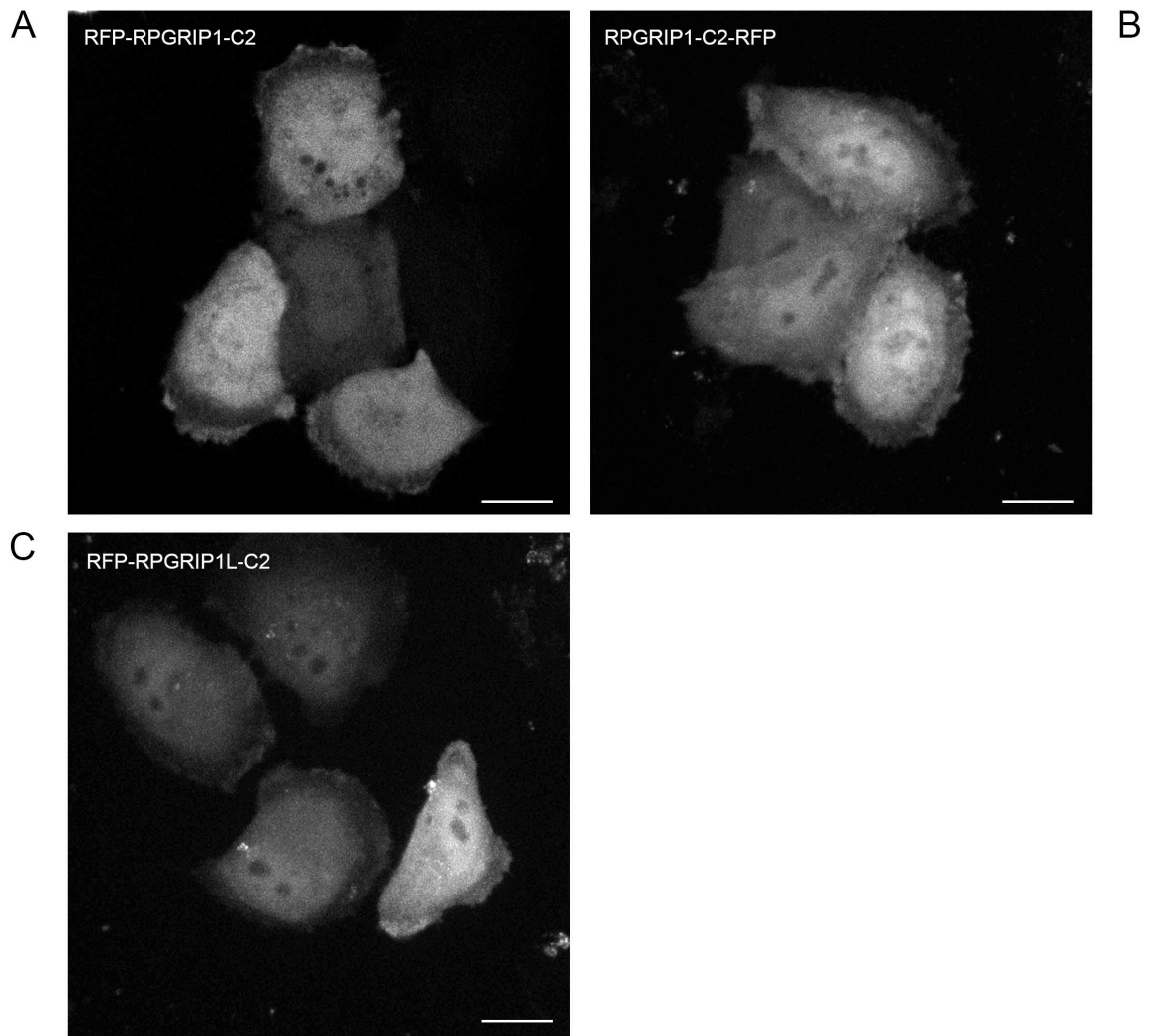
Figure 14: Localization of C2 domains of RPGRIP1 and RPGRIP1L.

N-terminal (**A**) and C-terminal (**B**) RFP tagged C2 domains of RPGRIP1 and N-terminal C2 domain of RPGRIP1L (**C**) expressed in Hela cells are shown. Subcloning of C2 domains was done as described in (Roepman et al., 2005). All constructs display cytoplasmic localization. Scale bar - 10µm.

A

	Hela	RPE1

DAPI/Pericentrin

DAPI/Gamma Tubulin

siNEG9

DAPI/Pericentrin

DAPI/Gamma Tubulin

siRPGRIP1

B
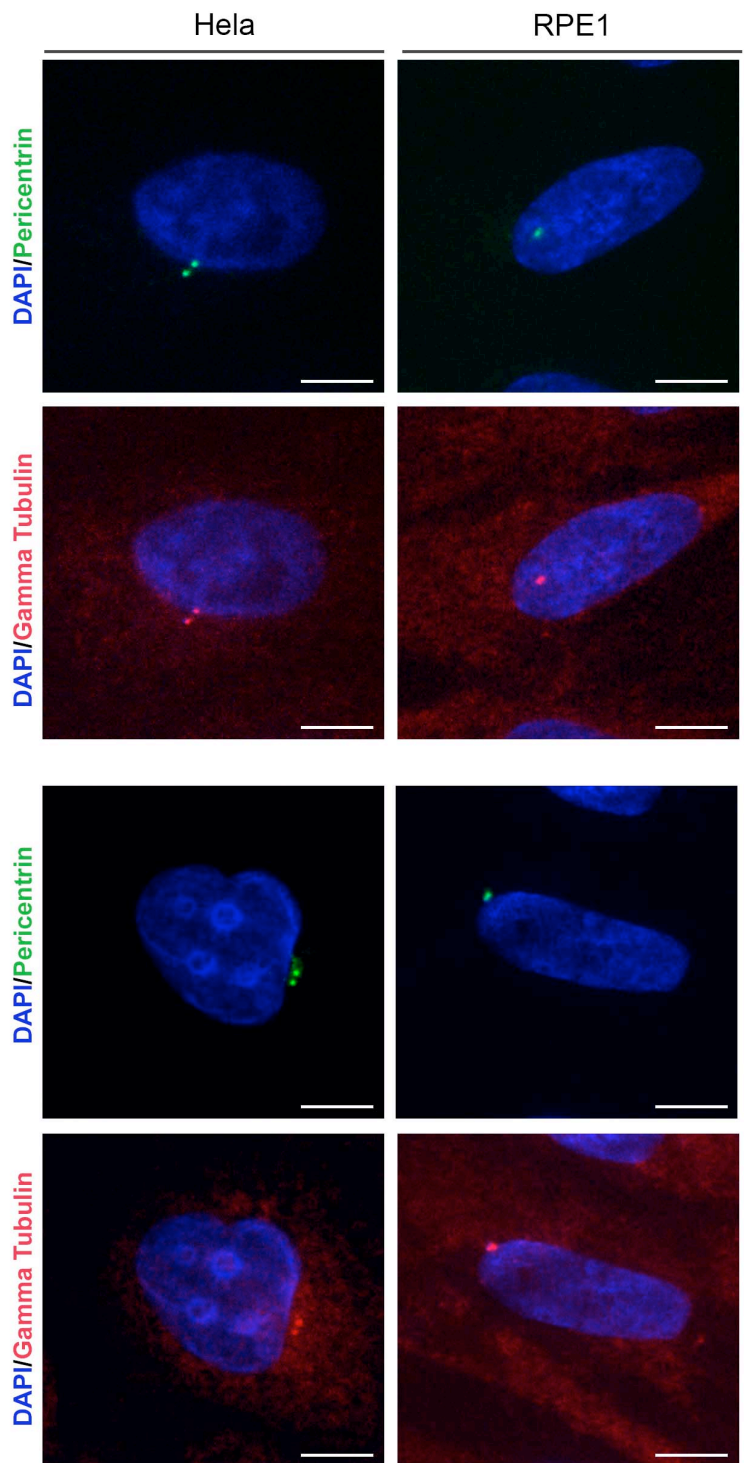
Effect of RPGRIP1 depletion on number of centrosomal foci

Number of centrosome foci

> 2
2
1

siNEG9   siRPGRIP1   siNEG9   siRPGRIP1

Hela   RPE1

C
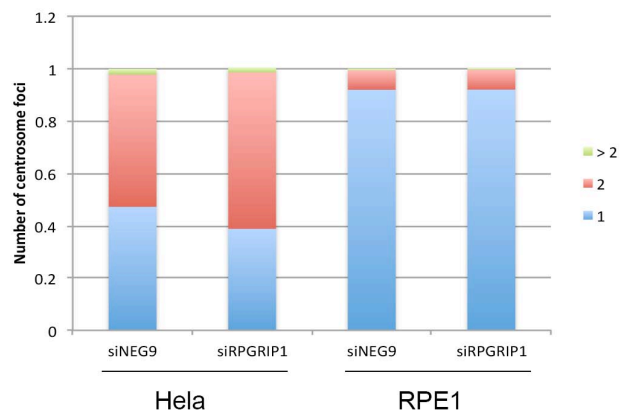
Effect of RPGRIP1 depletion on pericentrin amount at centrosome

Integrated intensity of pericentrin at centrosome

Hela   RPE1

siNEG9
siRPGRIP1

D
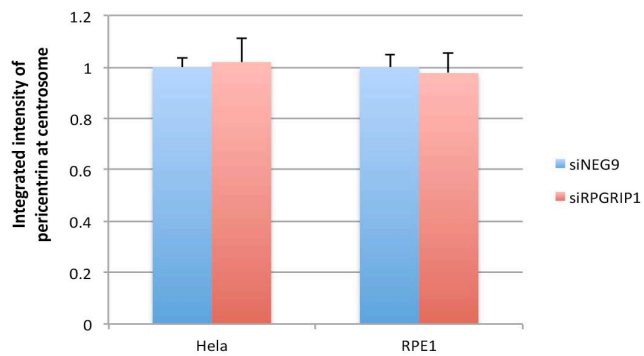
Effect of RPGRIP1 depletion on gamma tubulin amount at centrosome

Integrated Intensity of gamma tubulin at centrosome

Hela   RPE1

siNEG9
siRPGRIP1
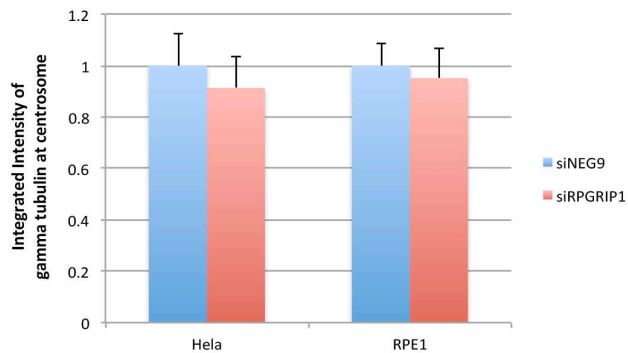
Figure 15: Effect of RPGRIP1 depletion on centrosome organization.

A. Hela and RPE1 cells were treated with control and anti-RPGRIP1 siRNA and immunostained against pericentrin and gamma-tubulin. Scale bar - 5µm. **B.** Counting of number of centrosomal foci per cell revealed no difference between control and siRPGRIP1 treated cells. Cells were pooled from two different experiments and 500-600 cells were counted in total. Quantification of gamma-tubulin (**C**) and pericentrin (**D**) intensities also revealed no significant differences between control and siRPGRIP1 treated cells in Hela and RPE1 cells (Bar heights: relative mean integrated intensities at the centrosome; Error bars, + SEM).

A

No Growth　　　Moderate Growth　　　Extensive Growth

DAPI / EB1 / Tubulin

B

Effect of RPGRIP1 depletion on microtubule nucleation

Fraction of cells at different stages of microtubule nucleation

siNEG9　　　siCLASP　　　siRPGRIP1

- Extensive Growth
- Moderate Growth
- No Growth
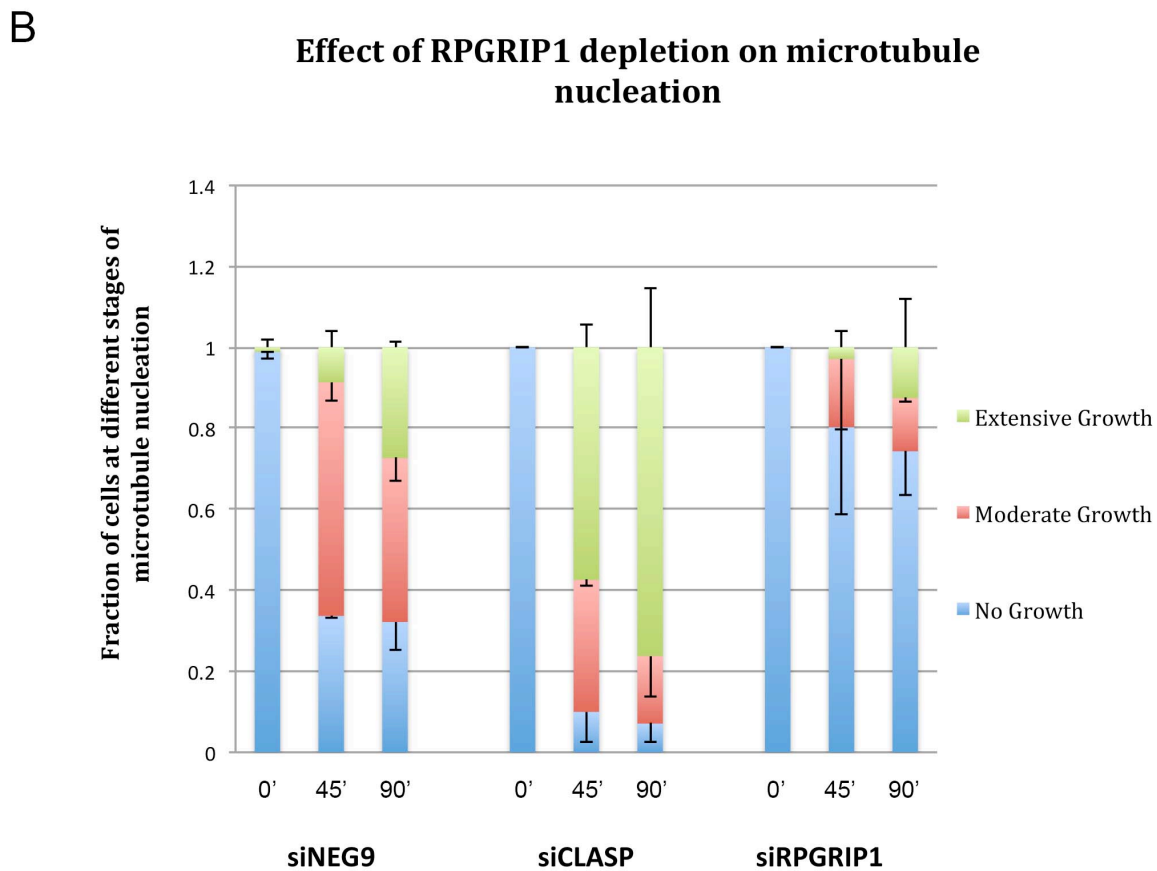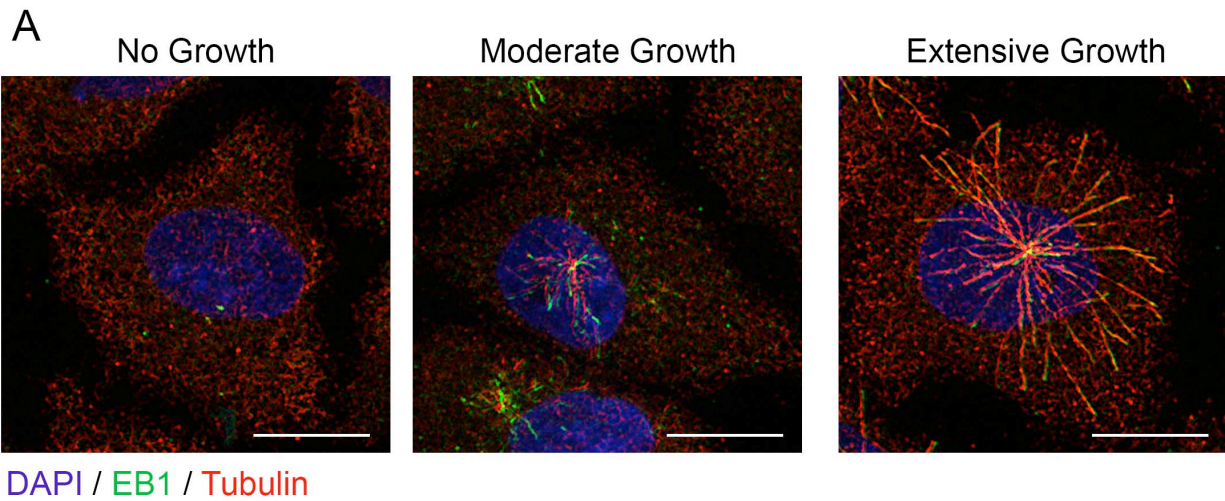
Figure 16: Effect of RPGRIP1 depletion on microtubule nucleation.

A. Hela cells were treated with control, siRPGRIP1 and siCLASP siRNAs for 72h. Cells were then cooled on ice for 1h to depolymerize microtubules and warmed up again to 37°C to initiate microtubule nucleation. Cells were fixed at 0, 45 and

90 seconds after warm up and stained with DAPI, EB1 and Tubulin antibodies. Cells were then classified into three different groups according to the microtubule nucleation stage. Scale bar - 10µm. **B.** Quantification of fraction of cells at different stages of microtubule nucleation is shown. RPGRIP1 depletion leads to delayed microtubule nucleation whereas CLASP depletion extensive microtubule growth as compared to control (Bar heights correspond to fraction means. Error bar, +SD or –SD).
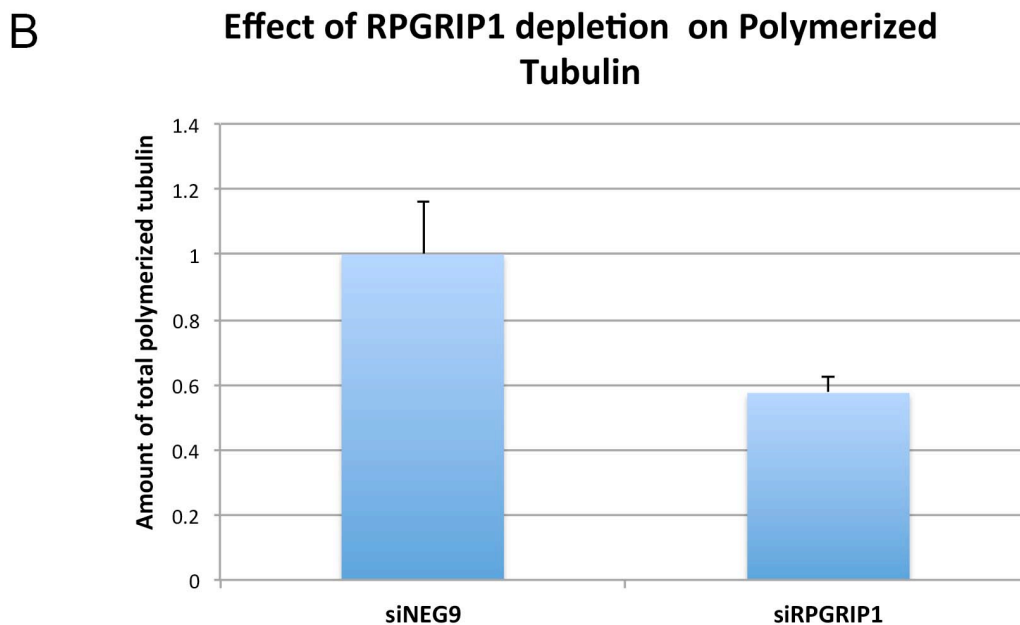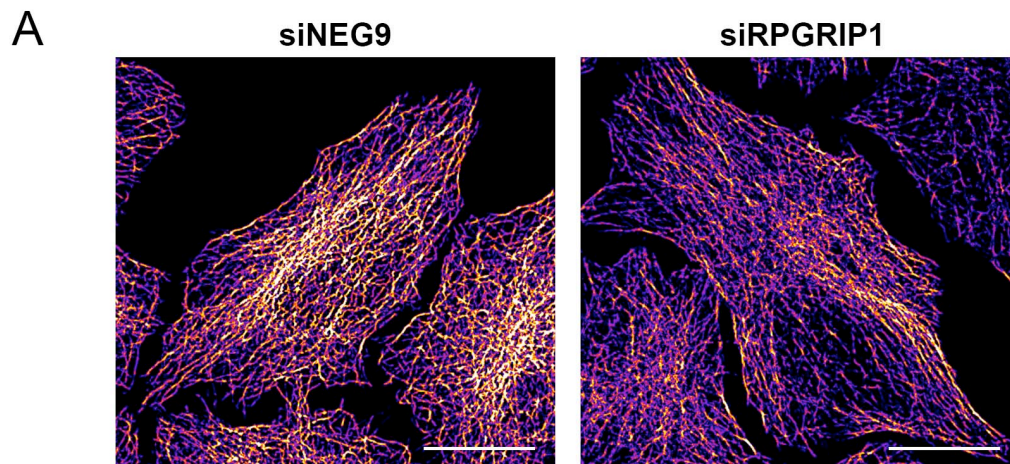
Figure 17: Effect of RPGRIP1 depletion on polymerized tubulin amount.

A. Control and siRPGRIP1 treated cells were methanol fixed and immunostained against tubulin. Cells were then imaged with confocal microscopy. Images of confocal slices are processed with ImageJ tubeness plugin to further increase intensities of tubular structures. Later processed images were thresholded and sum projected. Sum projected image of example cells are shown with intensity dependent 'Fire' lookup table of ImageJ. Scale bar - 10µm **B.** Integrated intensities of tubulin staining per cell in sum-projected images are quantified. Mean of median of 3 different experiments is shown and siRPGRIP1 treated cells show about 40% decrease in polymerized tubulin amount (Error bar, +SD).

70
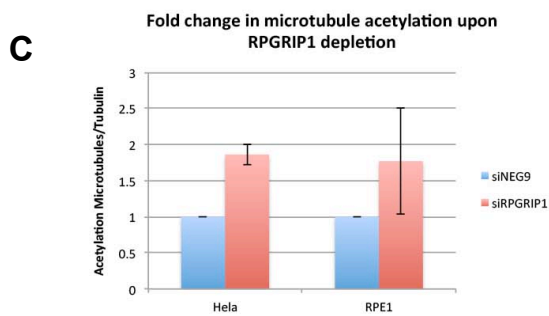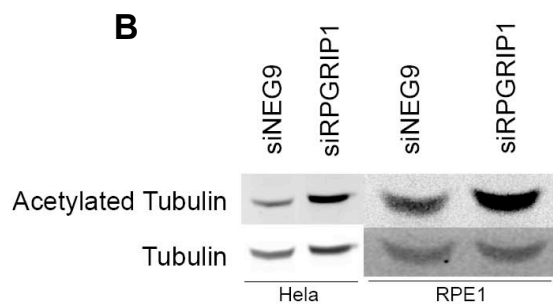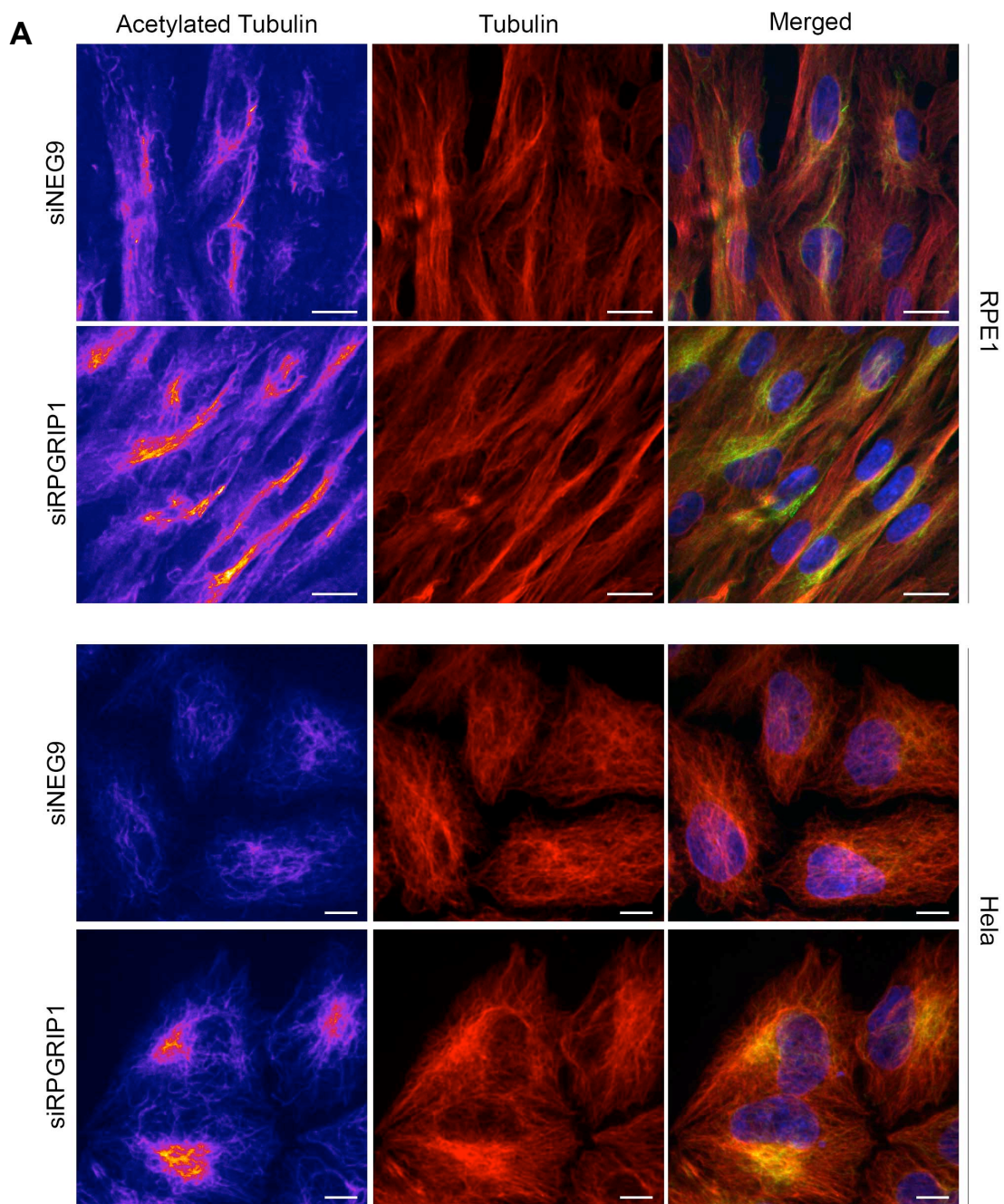
Figure 18: Effect of RPGRIP1 depletion on microtubule acetylation.

A. Control and siRPGRIP1 treated RPE1 (top panel) and Hela (bottom panel) cells are stained for acetylated tubulin (left column) and total tubulin (middle column). Scale bar: 10µm for RPE1 cells, 5µm for Hela cells. **B.** Western blot analysis of microtubule acetylation in Hela and RPE1 cells. For Hela cells siNEG9 and siRPGRIP1 lanes are cropped from the same membrane and stitched together. **C.** Quantification of western blot upon RPGRIP1 depletion shows 1.86 and 1.77 times increase acetylated microtubules in Hela and RPE1 cells respectively (Error bar, +/- SD).

A

RPGRIP1L-GFP   Pericentrin   RPGRIP1L-GFP/Pericentrin

B

Acetylated Tubulin

Tubulin

siNEG9
siRPGRIP1L_3
siRPGRIP1L_4

C
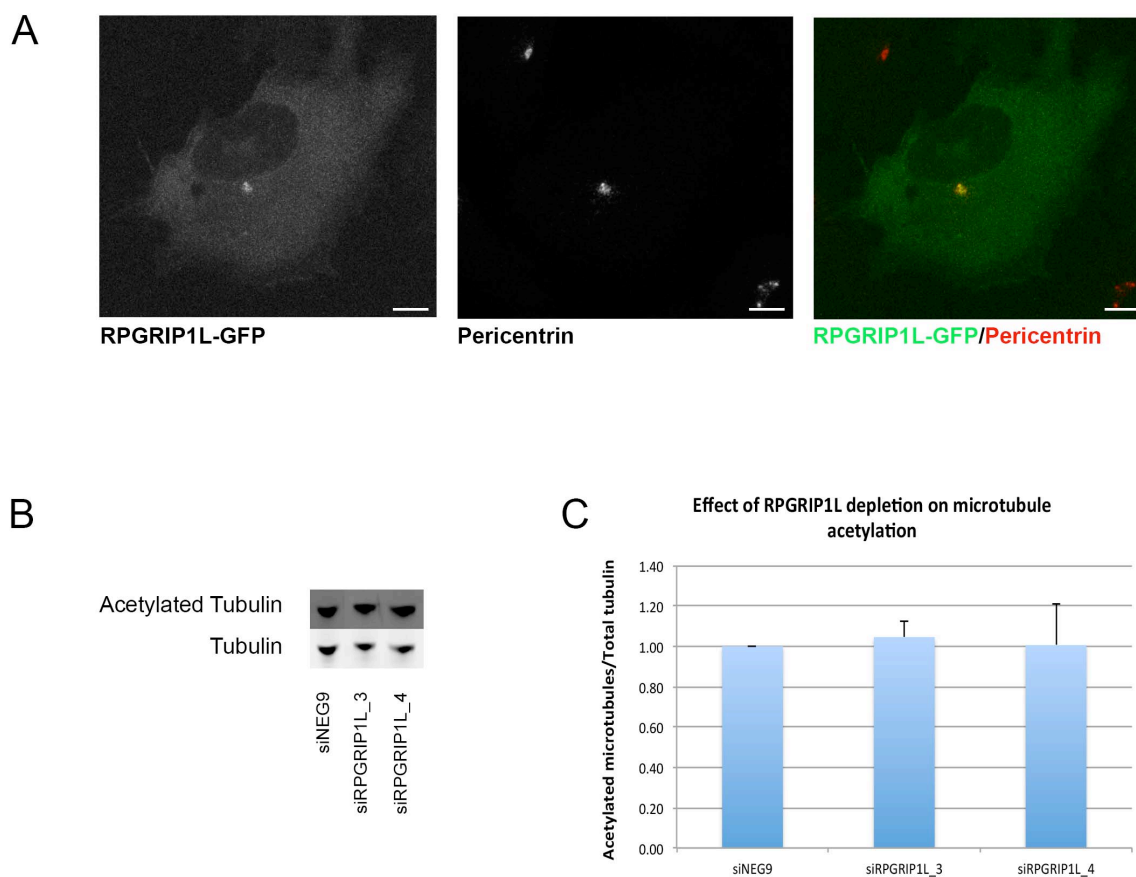
Figure 19: Effect of RPGRIP1L depletion on microtubule acetylation.

A. GFP tagged RPGRIP1L construct is expressed in Hela cells and immunostained against pericentrin. Clear colocalization was observed. Scale bar - 5µm. **B.** Hela cells treated with control and 2 anti-RPGRIP1L siRNAs are analyzed by western blot for acetylated tubulin. **C.** Quantification of acetylated tubulin by western blot revealed no significant difference in control and siRPGRIP1L treated cells (Error bar, +SD).

A. Microtubule acetylation response to TSA

B. Increase in acetylated tubulin upon TSA treatment

C. Effect of RPGRIP1 depletion on microtubule acetylation

D. Effect of RPGRIP1 depletion on microtubule deacetylation
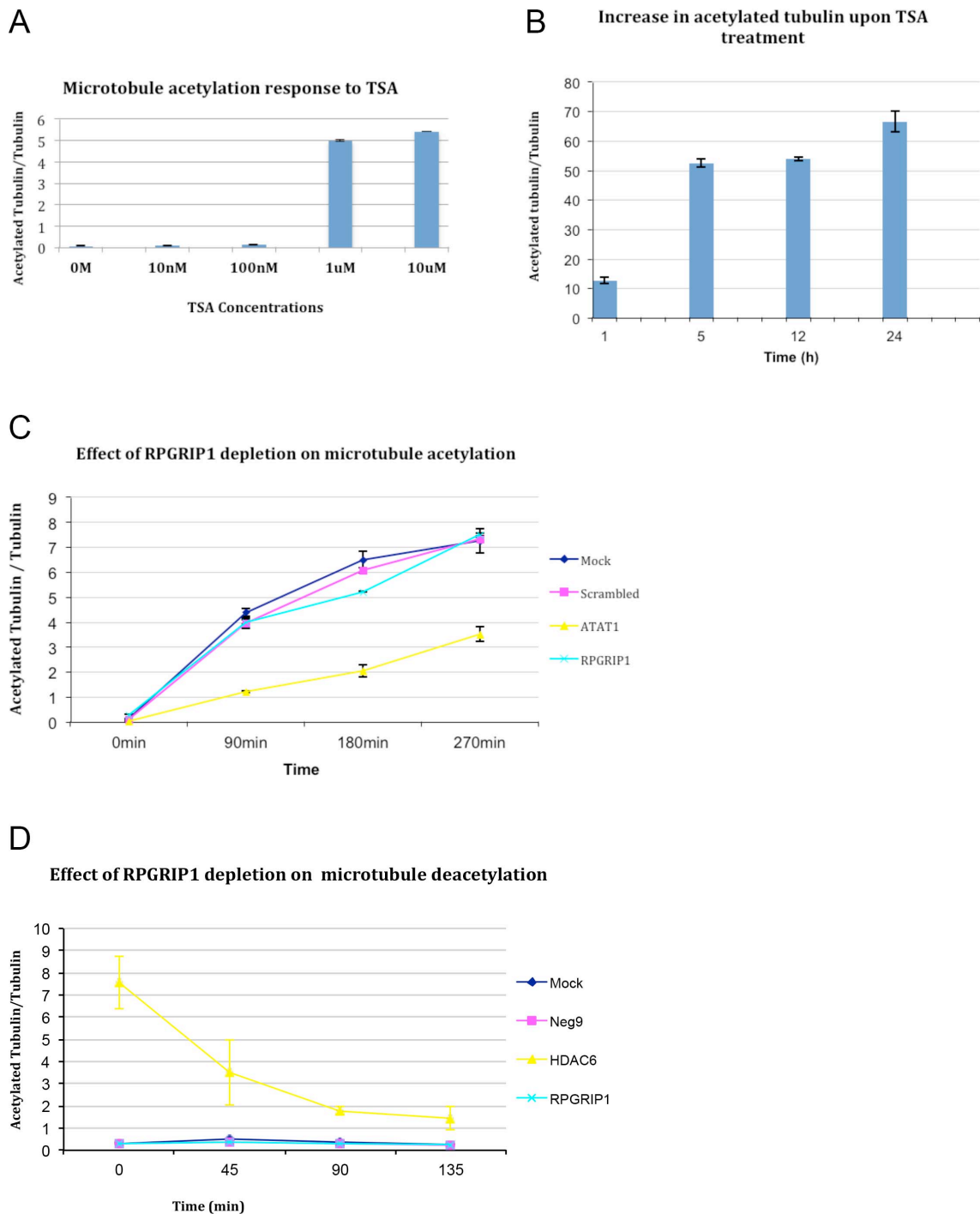
Figure 20: Effect of RPGRIP1 depletion on activity of microtubule acetyltransferases and deacetylases.

A. RPE1 cells were treated with various concentrations of TSA for 24h and analyzed by western blot with acetylated tubulin staining to find minimal concentration that completely blocks HDAC6 activity. 1µM concentration was

selected. **B.** RPE1 cells were treated with 1μM TSA for various time points and analyzed by western blot with acetylated tubulin staining to find a time points where change is the fastest. The fastest change was observed within 5h. **C.** RPE1 cells pretreated with control, siRPGRIP1 and siATAT1 are treated with 1μM TSA and analyzed by western blot every 90min for 270min. No delay upon RPGRIP1 depletion was observed however ATAT1 depletion significantly slowed down rate of microtubule acetylation (Error bar, +/- SD). **D.** RPE1 cells pretreated with control, siRPGRIP1 and siHDAC6 for 48h are treated with 1μM of TSA for 24h and then TSA was washed away again. Cells were analyzed by western blot every 45min after washout. Quantification of acetylated tubulin revealed no difference in speed of microtubule deacetylation however it was significantly delayed upon HDAC6 depletion (Error bar, +/- SD).

A

| No Nocodazole | 8min Nocodazole | 20min Nocodazole |

siNEG9

siCLASP

siRPGRIP1

B
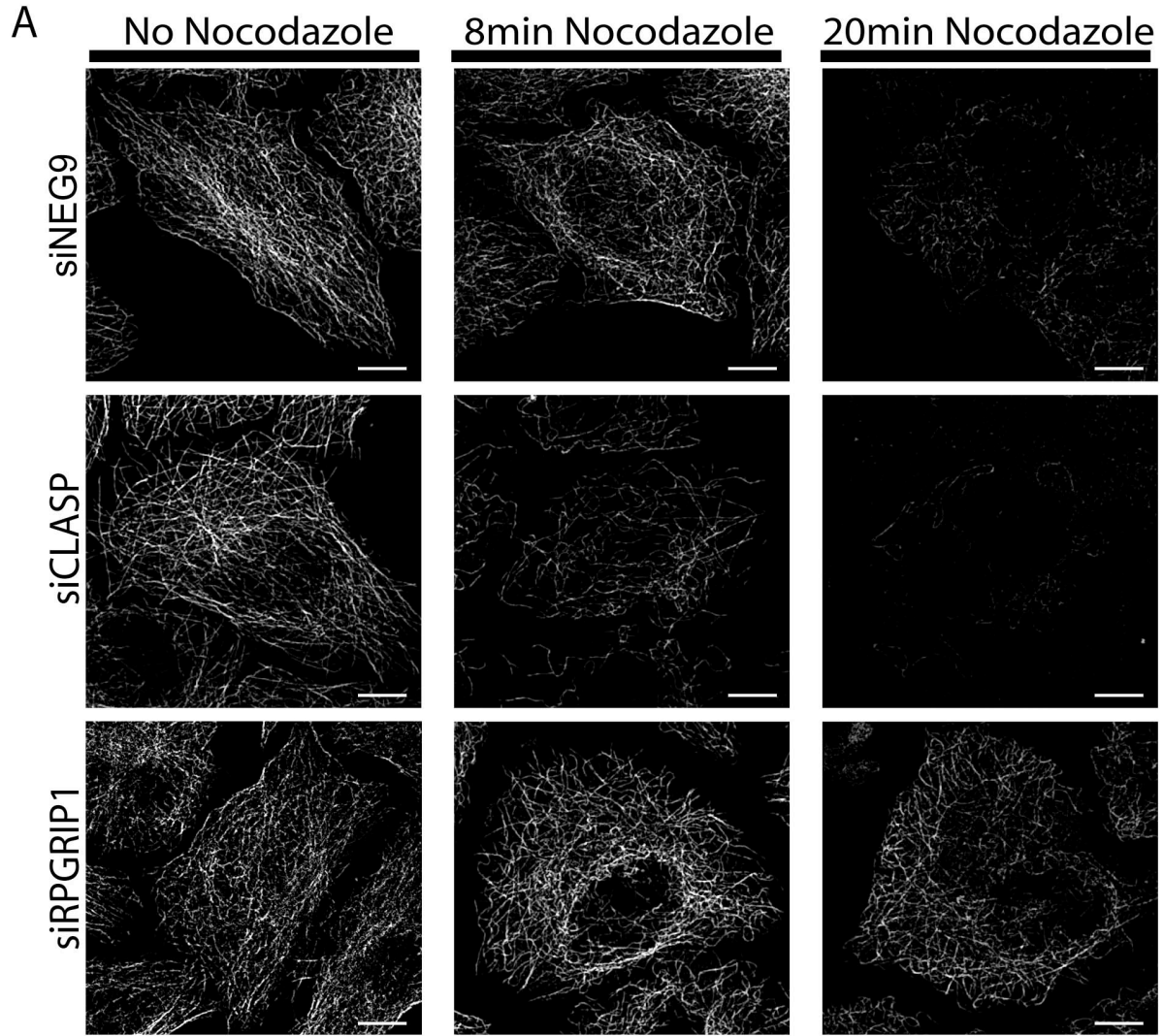
Effect of RPGRIP1 depletion on microtubule stability
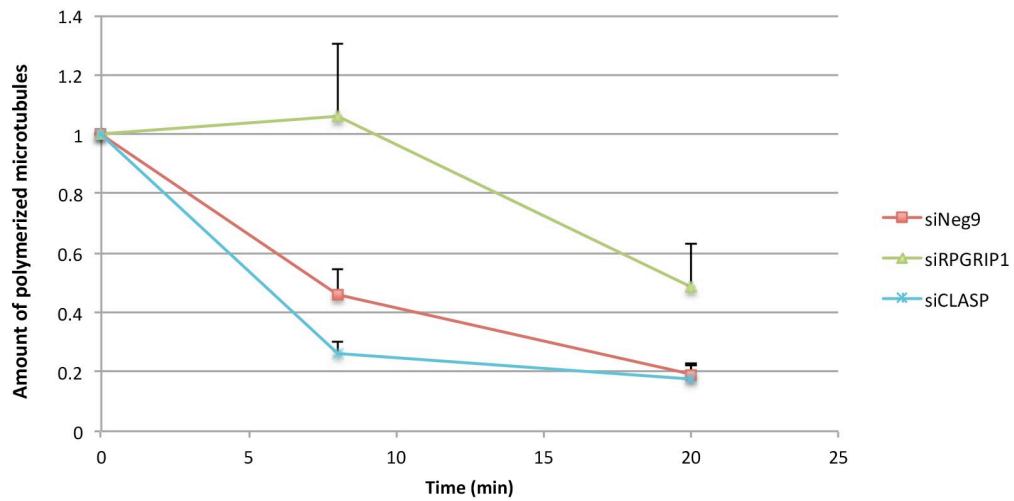
Figure 21: Effect of RPGRIP1 depletion on microtubule stability.

A. Hela cells are treated with nocodazole for 0min, 8min or 20min upon RNAi with control siRNA, siRPGRIP1 or siCLASP. Cells were fixed and immunostained against tubulin. Scale bar - 5µm. **B.** For each cell, integrated density of polymerized tubulin was quantified and plotted. CLASP depletion was used as a negative control for microtubule stabilization and its depletion subsequently lead to loss of stable pool of microtubules. In contrary, RPGRIP1 depletion resulted in increased pool of nocodazole resistant microtubules (Data points, mean of 3 replicates. Error bar, +SEM).
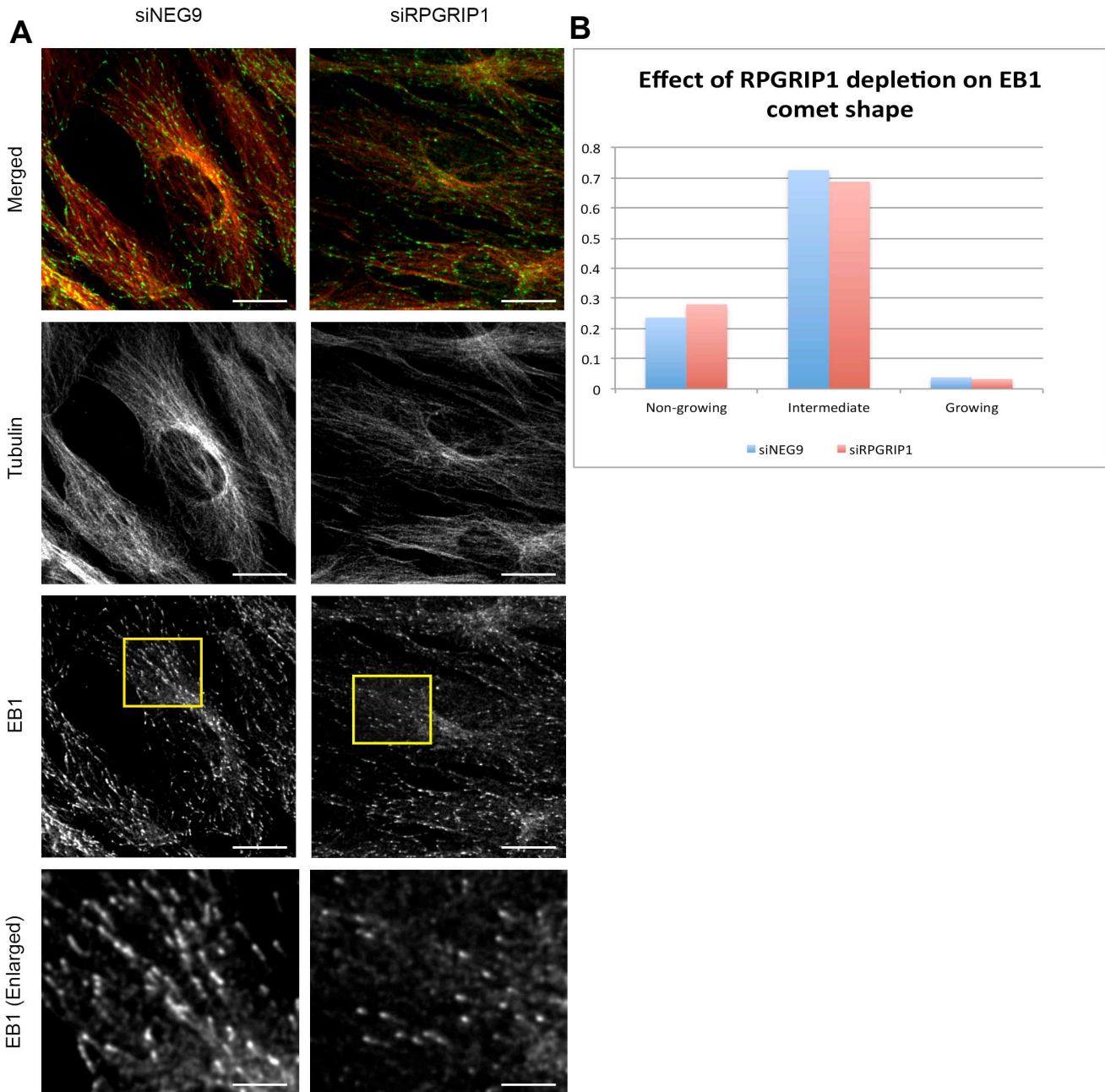
Figure 22: Effect of RPGRIP1 depletion on EB1 comet shape.

A. RPE1 cells are stained for EB1 and tubulin upon RPGRIP1 depletion. Part of image in EB1 image marked by yellow rectangles is enlarged in the bottom panel. Scale bar - 10µm - top 3 panels, 3µm – lowest panel. **B.** Quantification of effect of RPGRIP1 on EB1 comet shape distribution. EB1 comets were classified into three groups according to ratio of comet major axis to its minor axis as following: 'Non-growing' if ratio < 1.5, 'Intermediate' if 1.5 < ratio < 4.5 and 'Growing' if ratio < 4.5. Test of Equal Proportions with count data revealed 5% increase (p-value < 0.05) in 'Non-growing' fraction of EB1 comets.

Effect of RPGRIP1 isoforms on microtubule acetylation
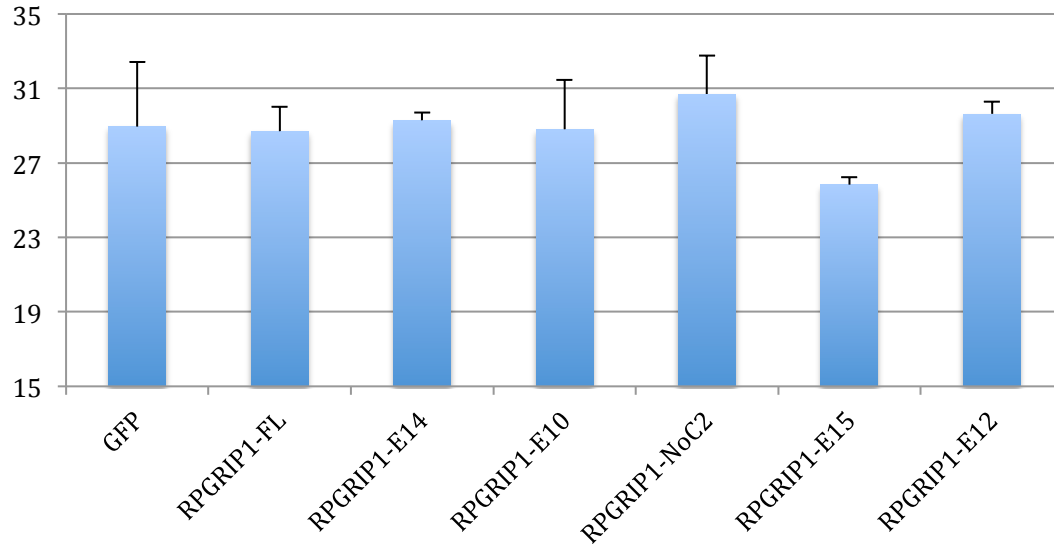
Figure 23: Effect of overexpression of RPGRIP1 isoforms on microtubule acetylation.

Cellular integrated intensity of acetylated microtubules in RPE1 cells expressing different RPGRIP1 isoforms is measured and plotted. No significant change microtubule acetylation was observed with any of the isoform overexpression (Bar heights: Error bar, +SEM).

A

	Acetylated Tubulin	Golgin84	Merged
siNEG9			
siRPGRIP1			
siATAT1			
siRPGRIP1 + siATAT1			
siCLASP			
siRPGRIP1 + siCLASP			
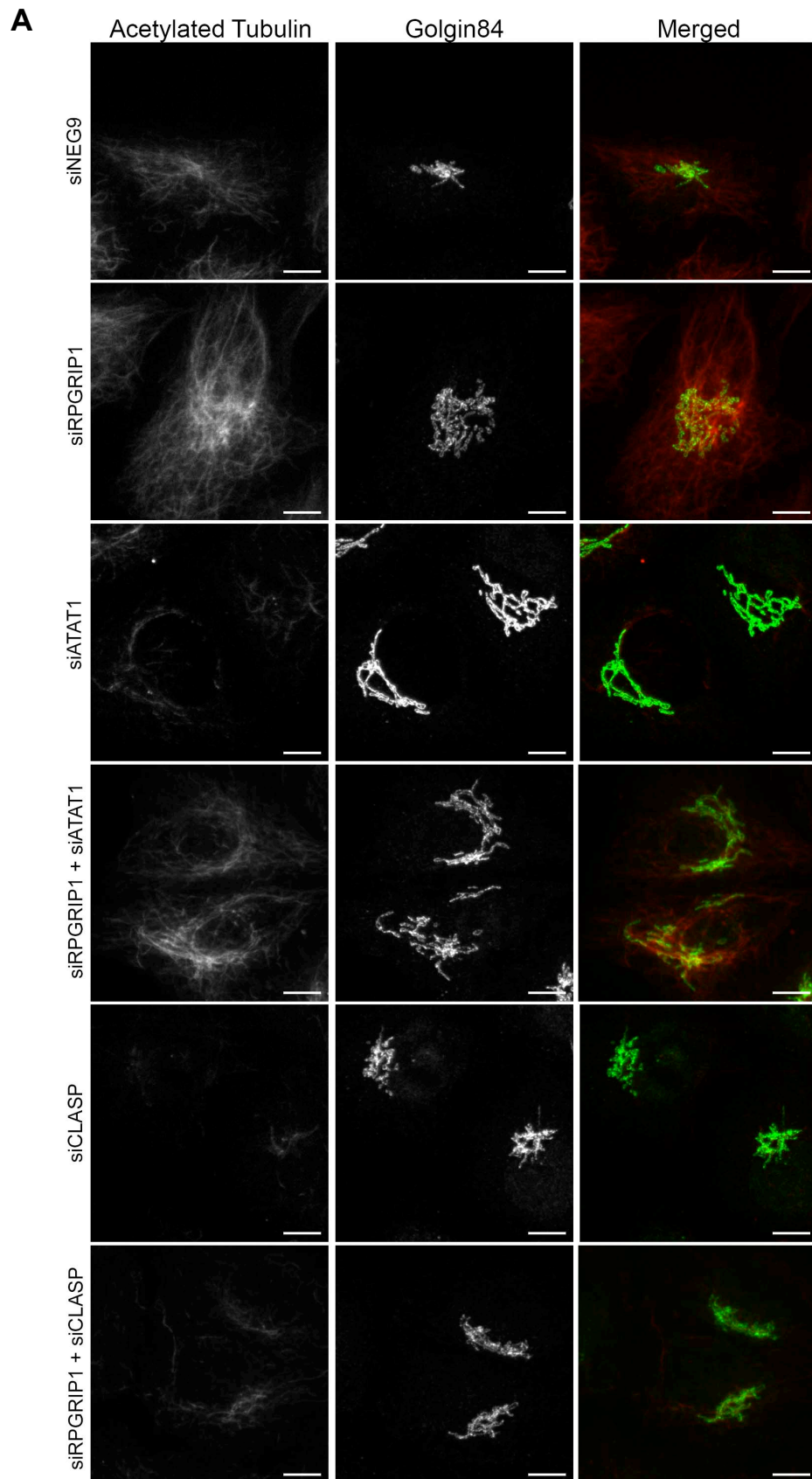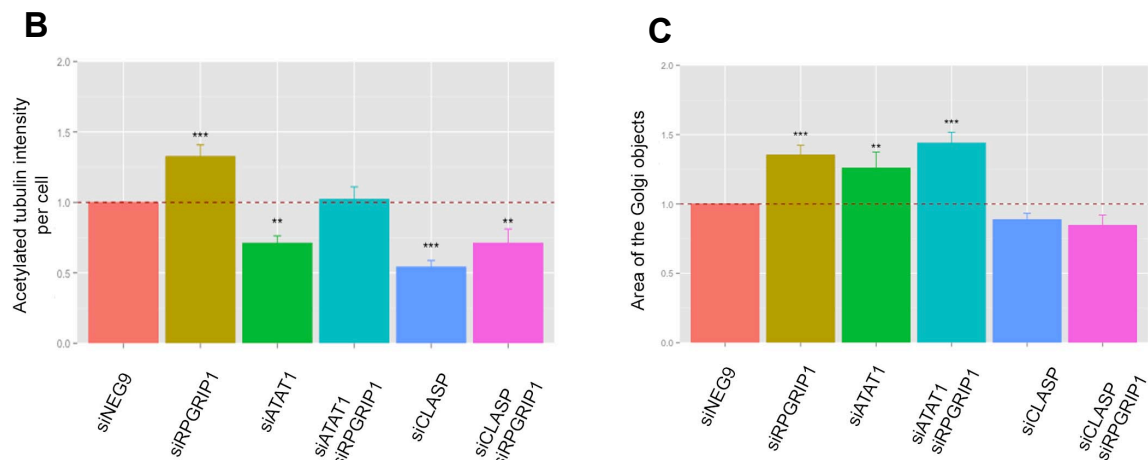
Figure 24: Effect of microtubule acetylation/stability regulators on Golgi organization.

A. Hela cells were stained for acetylated tubulin and Golgin84 upon siRPGRIP1, siATAT1, siCLASP single or upon siRPGRIP1 + siATAT1 and siRPGRIP1 + siCLASP double knockdowns. Scale bar - 5µm. **B.** Integrated intensity of acetylated tubulin per cell was measured after background thresholding. Intensities were then normalized against cell area (3-4 replicates). Both ATAT1 and CLASP depletion lead to significant decrease (t-test) as compared to control (siNEG9). Co-depletion of RPGRIP1 with ATAT1 rescued microtubule acetylation to control level, however co-depletion of RPGRIP1 and CLASP did not (t-test). Error bars represent standard error of the mean. **C.** Area of the Golgi objects are measured as described in Methods (see Quantification of 'BigGolgiBlob') and were normalized against Golgi area in control treatment (siNEG9). Single or co-depletion of RPGRIP1 and ATAT1 increased (t-test) the Golgi area. Depletion of CLASP alone or co-depletion with RPGRIP1 did not have any effect on Golgi area. The Golgi uncondensation occurred upon ATAT1 and RPGRIP1 single or double depletions even though they showed opposing phenotypes on microtubule acetylation level. Error bars represent standard error of the mean, '**' and '***' signs indicate 95% and 99% significance level, respectively.
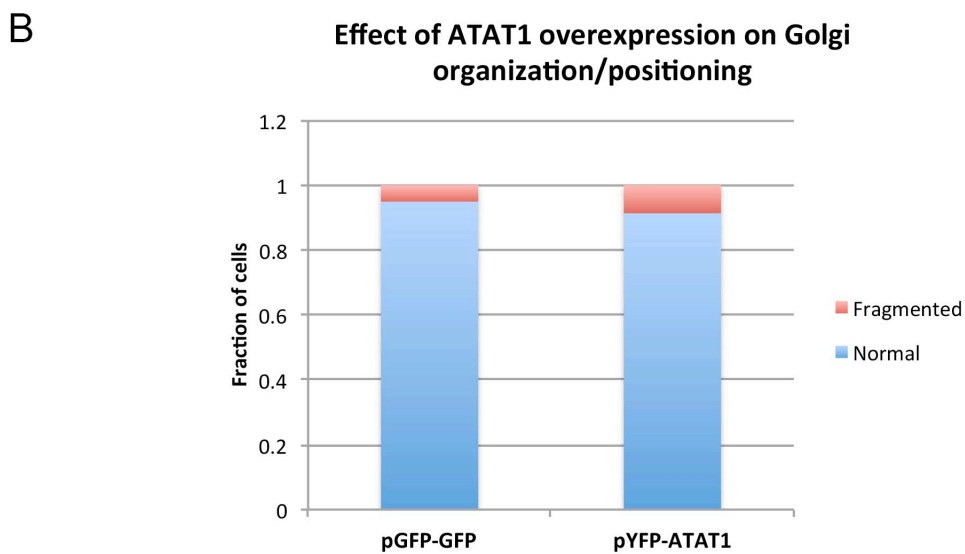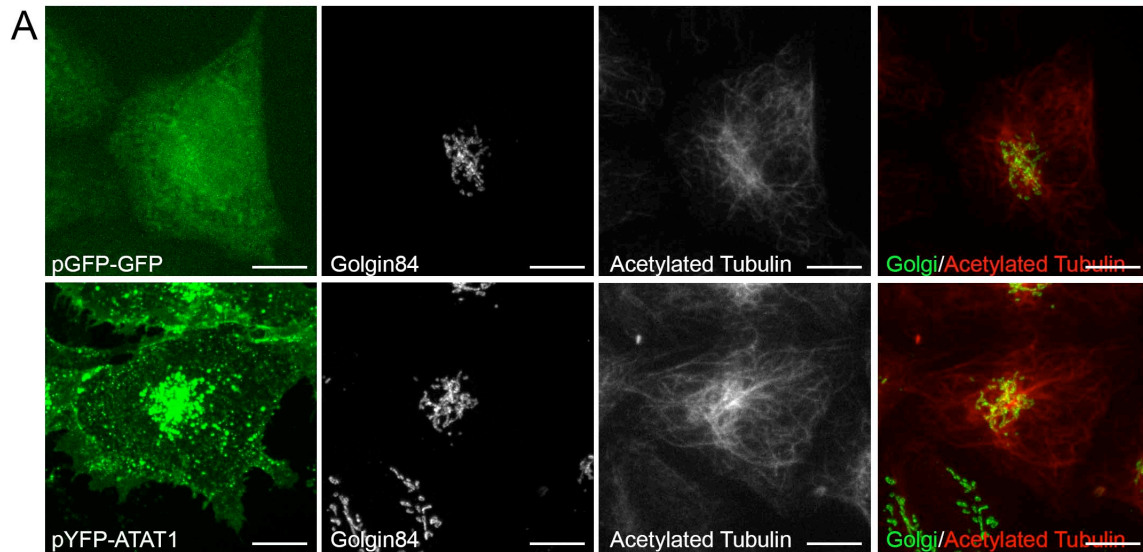
Figure 25: Effect of ATAT1 overexpression on Golgi organization in Hela cells.

A. YFP tagged ATAT1 construct is overexpressed in Hela cells and immunostained for acetylated tubulin and Golgin84. Scale bar - 10μm. **B.** Visual analysis of Golgi phenotypes revealed no significant change. 70-80 cells counted for each treatment (p-value > 0.5 with test for proportions).

siNEG9
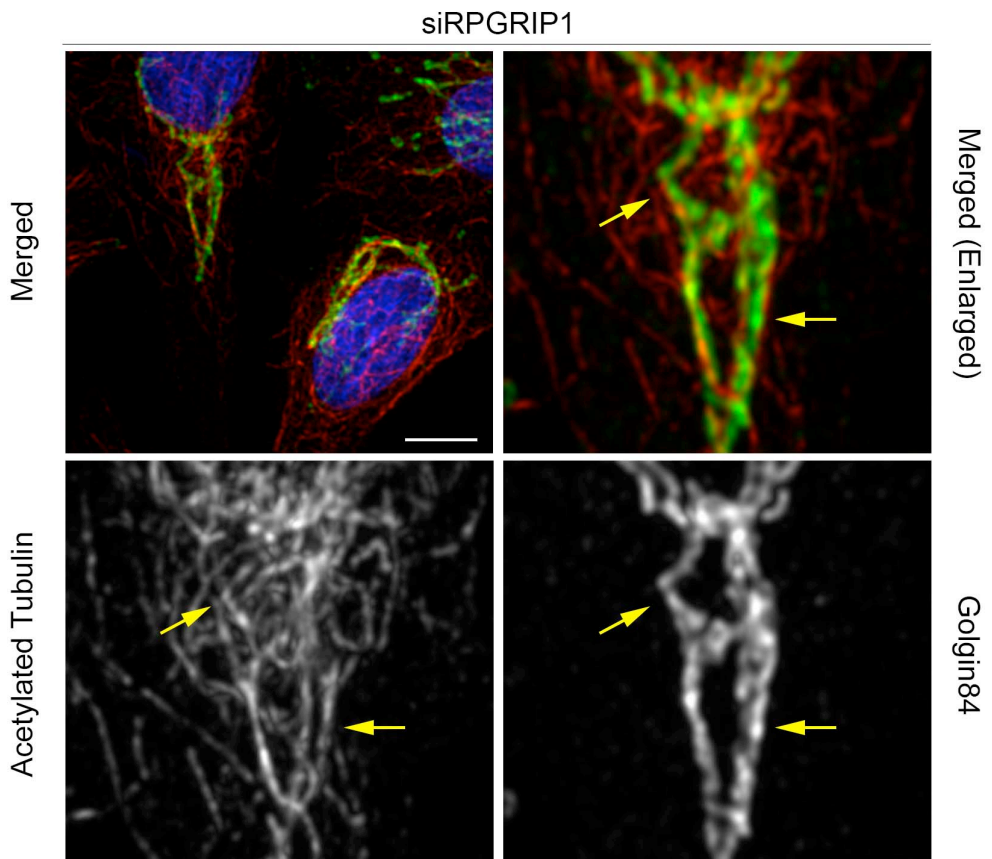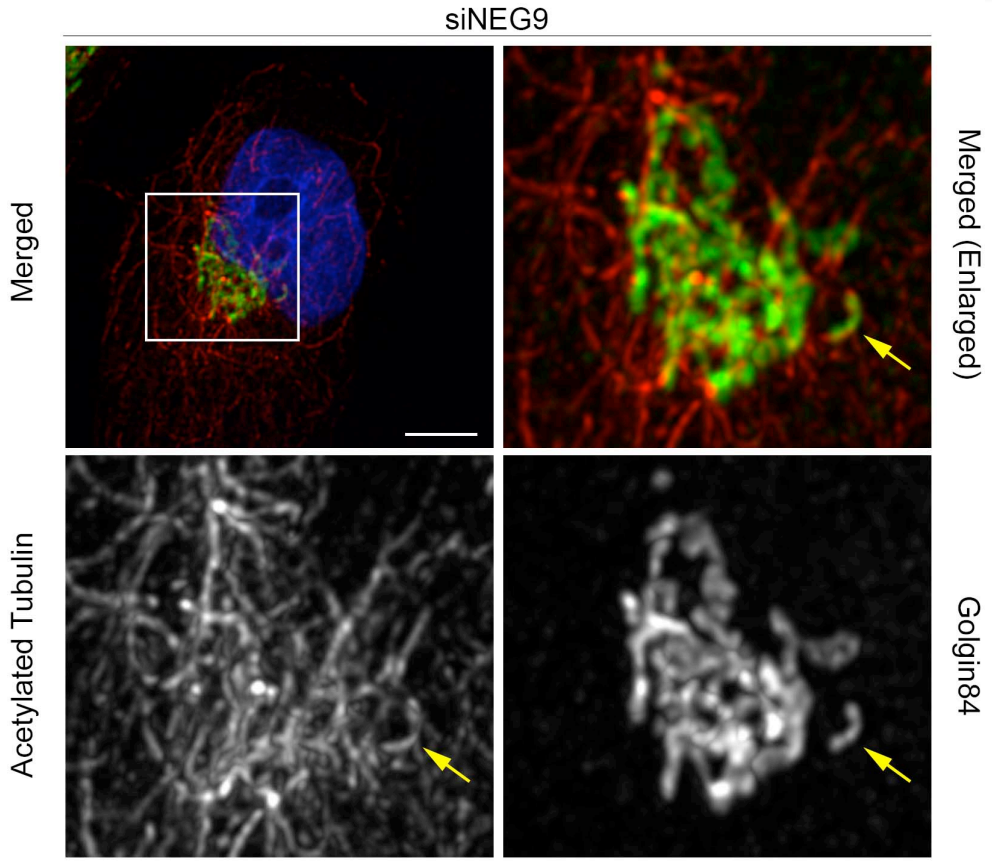
siRPGRIP1

Figure 26: Spatial association of stable microtubules and the Golgi ribbon.

Control and siRPGRIP1 treated Hela cells were immunostained against acetylated tubulin and the Golgin84. Cells were imaged on confocal high-resolution microscope and images were deconvolved. Part of merged image marked by white rectangle is enlarged in lower panels and right column. Images show extensive association (arrows) of acetylated microtubules and the Golgi. Scale bar – 5µm.

A

	Golgin84	Acetylated Tubulin	DAPI / Golgin84 / Acetylated Tubulin

siNEG9

siRPGRIP1

siGRASP65

siGRASP65 siRPGRIP1

siGM130
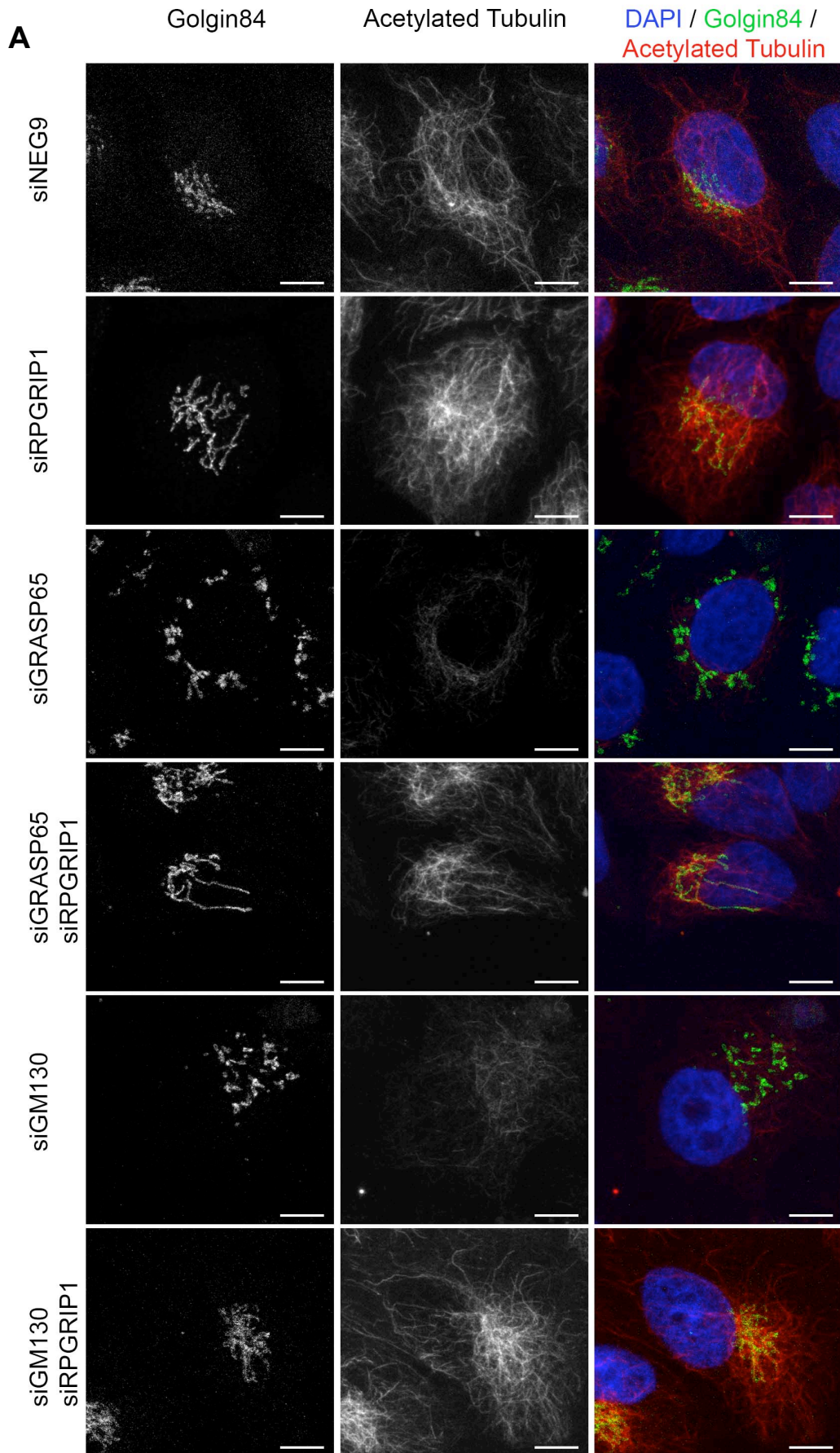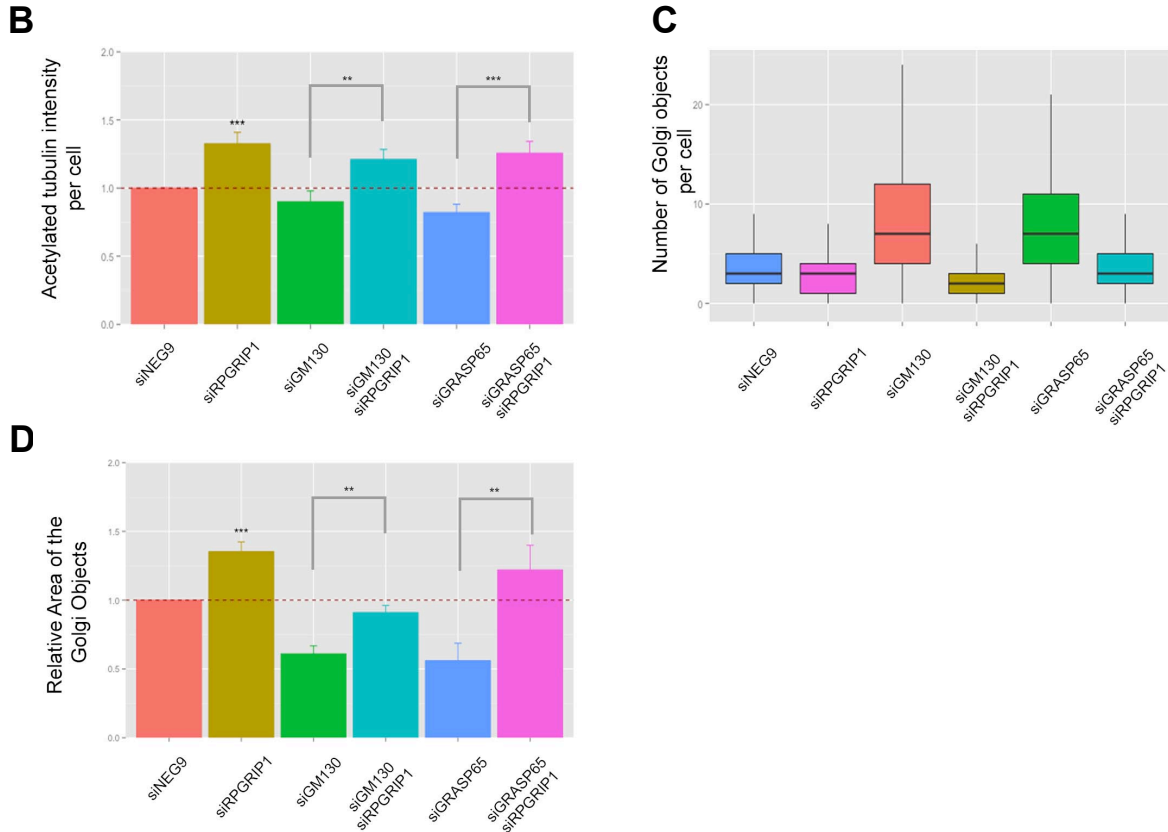
siGM130 siRPGRIP1

Figure 27: Effect of RPGRIP1 depletion on Golgi fragmentation.

A. Hela cells are treated with siGM130 and siGRASP65 alone or combined with siRPGRIP1. Cells were then immunostained for Golgin84 and acetylated tubulin (Scale bar, 5um) **B.** Integrated intensities of acetylated tubulin per cell are measured and normalized against cell area (3-4 replicates). Cell intensities are then normalized to mean of control treatment (siNEG9). Co-depletion of RPGRIP1 with GM130 or GRASP65 increased acetylated microtubule level as compared to single knock-downs of GM130 and GRASP65 (t-test). Error bars represent standard error of the mean. **C.** Number of Golgi objects per cell is quantified and pooled together form 3-4 replicates and shown in boxplots. Depletions of GM130 or GRASP65 alone lead to fragmentation of the Golgi ribbon. However, fragmentation was decreased when RPGRIP1 was co-depleted together with GM130 or GRASP65. **D.** Area of the Golgi objects is measured as described in Methods section (See quantification of 'BigGolgiBlob') and normalized against control treatment (3-4 replicates). Depletions of GM130 or GRASP65 alone lead to accumulation of small sized Golgi elements, whereas co-depletion of RGPRIP1 with GM130 or GRASP65 increased Golgi object areas (t-test). Error bars represent standard error of the mean. '**' and '***' signs indicate 95% and 99% significance levels respectively.
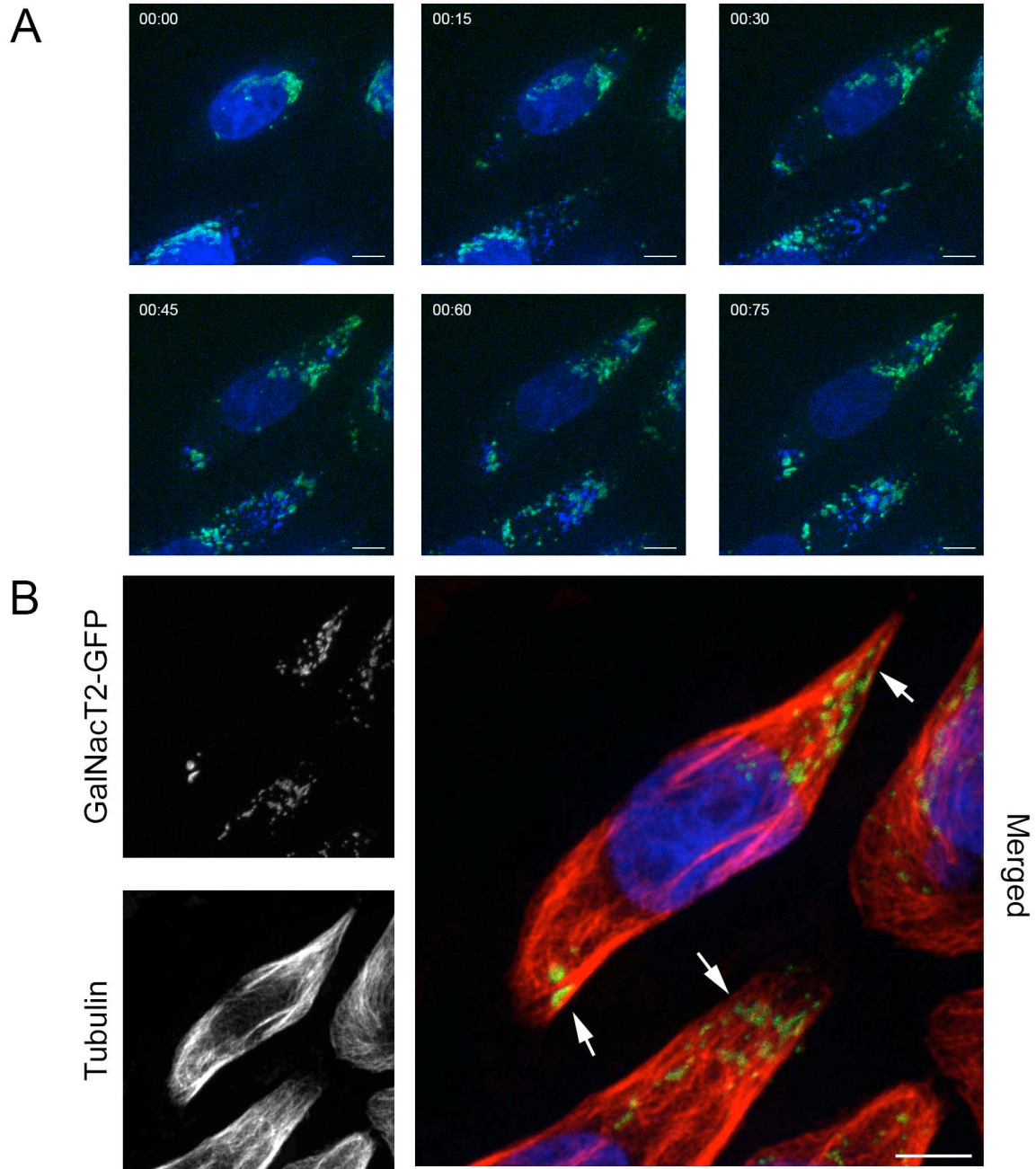
Figure 28: Golgi positioning upon microtubule stabilization.

A. Hela cells stably expressing GalNacT2-GFP are treated with 100nM Taxol and imaged every 15min for 75min. **B.** Cells were fixed at the end of live-imaging and immunostained for tubulin. The Golgi membranes re-position and accumulate at the cell periphery (arrows) upon microtubule stabilization. Scale bar - 5µm.

4   Discussion

4.1 RNAi screen and candidate hits

In this study we performed an RNAi screen to find new proteins that could provide new hints to understand and elucidate regulation and maintenance of Golgi organization and positioning. The screen targeted 680 peripheral genes that encode for membrane binding proteins. Visual quantification of the Golgi phenotypes in siRNA treated cells revealed 70 genes whose depletion lead to abnormal Golgi organization and positioning. Our literature analysis about candidate hits revealed that many of the genes were implicated in membrane trafficking, lipid signaling and in cell-to-cell and cell-to-matrix interactions. Candidate hits with already known functions in membrane trafficking underlined once more that the Golgi architecture is intimately associated to its function in vesicle trafficking. Consistently more than 15 of 60 known Rabs, which are regulators of the early secretory pathway and endosomal compartment, have been shown to localize to and function at the Golgi (Goud & Gleeson, 2010). The Golgi membranes are also distinguished by particular lipid composition and within the Golgi stack the lipid composition is also polarized from *cis* to *trans* cisternae (Holthuis et al., 2003; van Meer et al., 2008). For example, GOLPH3 is a phosphatidylinositol-4-phosphate (PI4P) effector and it localizes to the *trans*-Golgi by binding to PI4P. GOLPH3, by interacting with actin cytoskeleton and motor proteins, can stretch the Golgi cisternae and contribute to vesicle budding and trafficking (Dippold et al., 2009). In this screen we found other components of the phosphoinositide signaling pathway such as DGKD, DGKK, PIK3CG,

PIP5K3 and PLCG2 further supporting the importance of lipid homeostasis and dynamics on Golgi organization.

Our exploratory analysis about *a priori* functions of the candidates also revealed new pathways that might have a role in Golgi organization and vesicle trafficking. Increasing number of components of different signaling pathways are being implicated in organization of the Golgi, highlighting the critical function of regulating Golgi organization in the cell. Among the candidate hit list we also found a component of the nitric oxide signaling pathway nitric oxide synthase 1 (NOS1) whose depletion lead to fragmentation of the Golgi. Nitric oxide is a signaling molecule and plays a key role in cardiovascular homeostasis, pulmonary disease, and angiogenesis (Knowles & Moncada, 1994; Zhou & Zhu, 2009). Characterization of the effect of NOS1 on the Golgi organization might reveal new concepts on the regulation of the nitric oxide signaling pathway.

Depletion of two related proteins, PDLIM1 and PDLIM3 lead to an increased ER retention of the marker Golgi enzymes suggesting an inhibition of the early secretory pathway. PDLIM proteins are PDZ (at the N-terminus) and LIM (at the C-terminus) domain containing proteins and are thought to act as scaffold proteins and recruit different LIM domain interacting kinases to actin cytoskeleton (Zheng & Zhao, 2007). A recent report highlighted the role of PDLIM1 in breast cancer invasion pointing to a very interesting link between cancer cell migration and regulation of the early secretory pathway (Liu et al., 2014). As polarized and continuous secretion is required to maintain cell migration, identification and characterization of kinases that link early secretory pathway to PDLIM1 might provide new tools for cancer therapies.

4.2 Characterization of RPGRIP1

Among many Golgi phenotypes observed in the screen, RPGRIP1 depletion had a very interesting effect on the Golgi organization and positioning. Its depletion affected the Golgi in a particular way: the Golgi ribbon did not fragment but lost its compact organization and instead acquired a stretched and uncondensed architecture. We did not observe any difference in the distribution of Golgi markers upon RPGRIP1 depletion compared to control cells. This is consistent with the work by Simpson et al where RPGRIP1 depletion had no effect on VSVG transport (Simpson et al., 2012). This indicates that the observed RPGRIP1 depletion effect on the Golgi probably is not due to defects in membrane trafficking. Until now RPGRIP1 was thought to be a centrosomal protein and has been studied in the context of primary cilium organization and to our best knowledge, it has not been implicated in organization of the secretory pathway so far. As the understanding of the change in Golgi morphology occurring upon RPGRIP1 depletion will provide insight into the assembly and maintenance of the Golgi organization and positioning we decided to characterize in detail the function of RPGRIP1 outside of primary cilium context.

4.2.1 Isoform specific expression of RPGRIP1

The RPGRIP1 locus goes through extensive alternative splicing and isoforms display tissue-specific and species-specific expression and localization (Koenekoop, 2005; Lu & Ferreira, 2005; Shu et al., 2005). To understand how RPGRIP1 depletion is affecting the Golgi, we decided to first identify which isoform is expressed in Hela and RPE1 cells. Here in

this study we show that the 70kDa RGRIP1 isoform is expressed in RPE1 cells. There are several isoforms, both predicted (XM_006720209) and reported (AF265666, AF265667, AK301780, BC039089) with an approximate size of 70kDa. We observed a similar sized protein band using Hela cell lysates but no depletion was observed with three different siRNAs against RPGRIP1. We raised an antibody against RPGRIP1 where we saw several bands but none of them showed depletion upon anti-RPGRIP1 siRNAs. Shu et al. showed expression of RPGRIP1 in Hela cells with custom-made antibodies (Schu et al., 2005). So it still needs to be identified which isoform/isoforms is/are expressed in Hela cells. It is also possible that the 70kDa isoform is not the only isoform expressed in RPE1 cells.

4.2.2 Localization of C2 domains of RPGRIP1

As mentioned in the Introduction, some centrosomal proteins can bind to Golgi apparatus components and are thought to contribute to its pericentrosomal positioning. As RPGRIP1 was shown to have a C2 domain, a commonly found domain in peripheral proteins, we first hypothesized that it might bind to Golgi membranes, which are often localized close to the centrosome, and thus might be important for pericentrosomal retention of the Golgi membranes. But we didn't see any Golgi-like localization when we overexpressed full-length protein or C2 domain alone indicating Golgi uncondensation is not due to loss of a physical bridge between Golgi membranes and the centrosome.

4.2.3 Effect of RPGRIP1 on microtubule dynamics

We also did not observe any centrosomal organization defect upon RPGRIP1 depletion suggesting that it might not be involved in centrosome assembly. However, we noticed that the tubulin staining appeared reduced in RPGRIP1 knock-down cells compared to control stainings when we fixed cells with methanol, a procedure which extracts a large fraction of unpolymerized, free tubulin from cells (Lansbergen et al., 2006). Indeed our quantification of the respective microtubule stainings showed decreased density of polymerized tubulin in RPGRIP1 knock-down cells, which we speculate could probably be due to a decreased microtubule nucleation from the centrosome. We also show that these polymerized microtubules display increased acetylation levels and that this is not due altered enzymatic acetylation/deacetylation activities, but due to an increase in stabilization of microtubules, suggesting role of RPGRIP1 in microtubule dynamics. This is consistent with *in-vivo* studies where Rpgrip1 knock-out mice display increased levels of acetylated microtubules (Patil et al., 2012). In mass-spec studies RPGRIP1 was shown to interact with IQGAP1, Nek4 and many tubulin isoforms (Coene et al., 2011). RPGRIP1 was also found predominantly in the cytoskeletal fraction of bovine (Castagnet et al., 2003) and mouse (Patil et al., 2012) retinas of wild-type mice. Altogether, these observations are consistent with our observations and further strengthen the hypothesis of RPGRIP1 playing a role in microtubule dynamics.

In earlier studies, mutations in RPGRIP1 were discovered to lead to the autosomal recessive neuroretinopathy, Leber congenital amaurosis (LCA), in humans (Dryja et al., 2001; Gerber et al., 2001). LCA is the most severe form of all retinal dysplasias and with the earliest onset from birth (Castagnet et al., 2003). The molecular basis for the extreme severity of LCA caused by mutations in RPGRIP1 (and other genes) is so far not understood except that they lead to the degeneration of light sensitive,

modified primary cilium in rod and cones. In later studies RPGRIP1 was attributed a scaffolding role for the centrosome and the primary cilium of the ciliated cells and responsible for recruitment of NPHP4, SDCCAG8 and RPGR and to the cilium (Roepman et al., 2005). However, no isoform specific functions have been reported so far and it remains unclear if the RPGRIP1 scaffolding role is generalizable for all its isoforms as certain shorter isoforms do not a possess the C2 domain required for its interaction with NPHP4.

4.2.4 Localization of the different RPGRIP1 isoforms

Localization of the isoforms can provide important clues for isoform specific functions. Various localizations were shown for RPGRIP1 however no specific localization has been attributed to a particular isoform. In bovine and human retina, endogenous RPGRIP1 localized to outer-segments (Roepman et al., 2000) whereas in murine tissue it localized to the connecting cilium of photoreceptors (Hong et al., 2001). In addition localization of the isoforms differ from cell to cell. Various localizations were reported in cultured cells. In amacrine cells and the transformed murine photoreceptor line, 661W (Castagnet et al., 2003) RPGRIP1 localized to the nuclear envelope. In non-ciliated cell lines, such as Hela, HEK293, COS7, NIH3T3, and ARPE-19, RPGRIP1 localized to the centrosome and to the basal body in ciliated cells (Schu et al., 2005). However no centrosomal or basal body localization is reported so far with ectopic expression. In COS cells, a full-length overexpression construct localizes to the cytoplasm (Zhao et al., 2003). Overexpression of bovine RPGRIP1 (bRPGRIP1) and RPGRIP1b (bRPGRIP1b), the latter lacking the C2 domain, displayed either nuclear or cytoplasmic localization (Lu &

Ferreira, 2005). In some studies, overexpressed YFP-RPGRIP1alpha formed perinuclear aggregates (Patil et al., 2012). The fact that no centrosomal or ciliary localization was observed when ectopically expressed suggests that the epitope tags used might interfere with the centrosomal targeting sites of RPGRIP1. In this study we show centrosomal localization of full-length RPGRIP1 isoform in ARPE19, Hela and RPE1 cells, however, in the latter two cases the localization was not strong and it was only possible with small tags such as myc or flag and not all transfected cells showed centrosomal accumulation of RPGRIP1. For shorter isoforms, no centrosomal localization was detected with GFP tag, however they could still be tested with the smaller tags. Technical difficulties with overexpressed versions and their cell type dependency make it difficult to dissect isoform specific functions. Since this protein acts as a scaffold and interacts with many critical proteins its mis-localization, as seen with overexpression of tagged versions of the protein in this study, might deplete away its interacting partners causing unpredictable effects. This way, it will be impossible to see complementary effect when the construct is expressed in RPGRIP1 depleted cells to proof the specificity and attribute specific function to specific isoforms. For shorter isoforms, cytoplasmic and nuclear localizations were observed, nuclear localization being stronger shorter the isoform. As no specific localization was observed to any particular compartment, GFP-tag-based localizations remain uninformative to dissect isoform specific functions. As RPGRIP1 depletion increased microtubule stabilization, we overexpressed different isoforms and measured if any of the isoform could have complementary effects that might reveal isoform specific differences. Quantification of microtubule acetylation revealed no significant difference between cells transfected with the different RPGRIP1 isoforms tested in this work. However, we also noticed that ectopic expression of the isoforms caused

increased cell stress and subsequently cell death thus we failed to attribute any of the isoform to have a role in microtubule dynamics. This also hindered us to rule out role of RPGRIP1 in microtubule dynamics as possible off-target effect of RPGRIP1 siRNAs. However, we believe it's unlikely as we observed increased microtubule acetylation with two independent siRNAs. As listed above RPGRIP1 was already implicated in context of microtubule cytoskeleton before and a recent report from a study with Rpgrip1 deficient mouse showed increased microtubule acetylation in retinal tissue further strengthening specific role of RPGRIP1 in microtubule dynamics.

4.2.5. Novel function of RPGRIP1 in microtubule dynamics

In this study we propose for the first time a more general role of RPGRIP1 in microtubule dynamics in addition to a scaffolding role at the centrosome and primary cilium. There are several mechanisms known to achieve microtubule stabilization (Section 1.2.1). As the stable microtubules we observed do not form thick microtubule bundles around the nucleus, which is typically observed upon overexpression of microtubule bundling proteins such as Tau, we don't think microtubule stabilization upon RPGRIP1 depletion is induced by bundling. We also did not observe an increased accumulation of EB1 at microtubule plus ends, a common microtubule stabilization mechanism by plus end TIP network components (Akhmanova & Steinmetz, 2008). However, double knock down of RPGRIP1 and CLASP inhibited stabilization of the microtubules. CLASP (CLASP1 and CLASP2) proteins can localize to microtubule plus ends and lock the microtubules at a paused state and thus are a potent microtubule stabilizer (Mimori-Kiyosue et al., 2005; Sousa et al., 2007). We

speculate that RPGRIP1 might interfere with microtubule targeting of CLASP proteins however direct experiments need to be performed whether for example RPGRIP1 depletion leads to accumulation of CLASP at plus ends. The new role of RPGRIP1 in microtubule dynamics could also provide insight into the molecular mechanism of LCA. In LCA patients primary cilia, where microtubules are highly stabilized, rod and cones are rapidly lost and RPGRIP1 might function by locally coordinating the microtubule dynamics at the interface between the cytoplasm and lumen of primary cilium. Our results imply that RPGRIP1 functions to inhibit the microtubule stabilization as its depletion stabilizes microtubules. Interestingly, mild nocodazole treatment of cells, which destabilizes microtubules were shown to induce primary cilium growth (Sharma et al., 2011). It is possible that RPGRIP1 contributes to primary cilium growth and maintenance also by destabilizing microtubules.

4.3. The Golgi reorganization upon RPGRIP1 depletion

4.3.1 Effect of stable microtubules on the Golgi organization

As microtubules are heavily implicated in the regulating Golgi organization and positioning we suspected that the Golgi reorganization seen upon RPGRIP1 depletion is due to increased microtubule stabilization. We observed that after RPGRIP1 depletion in some cells, the increased pool of stable microtubules is highly polarized to one side of the cells and the Golgi is extended towards that direction. In addition CLASP is a known microtubule stabilizing protein and co-depletion of CLASP and RPGRIP1 did not lead to uncondensation of the Golgi, further pointing to an involvement of increased microtubule stabilization in Golgi

reorganization. Interestingly, high-resolution imaging revealed that the Golgi ribbon extends along the acetylated microtubules. This is observed not only in RPGRIP1 depleted cells but also in control cells when the Golgi is localized in the pericentrosomal region.

4.3.2 Interchangeable role of the Golgi matrix proteins and stable microtubules

GM130 and GRASP65 are well-known Golgi matrix proteins and result in Golgi fragmentation when depleted from cells (Barr et al., 1997; Puthenveedu et al., 2006; Wang et al., 2005). GM130 is also required for nucleation of the microtubules from the Golgi and these microtubules are thought to mediate homotypic fusion of ministacks to form a continuous Golgi ribbon (Nakamura et al., 1995; Puthenveedu et al., 2006). These Golgi derived microtubules then undergo stabilization in a CLASP dependent manner (Chabin-Brion et al., 2001). Our results do not support the idea that increased stabilization upon RPGRIP1 depletion is due to increased Golgi derived microtubule nucleation, as the co-depletion of GM130 and RPGRIP1 still results in increased microtubule stabilization. But interestingly, co-depletion of RPGRIP1 with GM130 and GRASP65 increased the microtubule acetylation level and concomitantly rescued integral Golgi ribbon organization and the Golgi ribbon is aligned along the convoluted acetylated microtubule protofilaments. This result further strengthens the role of acetylated microtubules as skeleton of the Golgi ribbon where in addition to act as skeleton, it might promote efficient assembly of the Golgi ministacks into a continuous ribbon.

4.3.3 Effect of microtubule post-translational modifications on the Golgi organization

Increased microtubule stabilization is often followed by increased acetylation. Treatments of cells with microtubule deacetylase inhibitors such as TSA and Tubacin lead to increased microtubule acetylation and the Golgi ribbon reorganization independent of microtubule stabilization (Koegler et al., 2010; Rivero et al., 2009; Ryan et al., 2012). This lead to a formulation of a model that features microtubule post-translational modification (PTM) based regulation of the Golgi ribbon organization and positioning. Recently, the major microtubule acetyltransferase, ATAT1 has been described in mammalians (Akella et al., 2010). In 2012 Kalebic et al reported that ATAT1 also destabilizes microtubules independent of its acetyltransferase activity and depletion of ATAT1 results in increased microtubule stabilization (Kalebic et al., 2013). Thus siRNAs targeting ATAT1 provide a great tool to uncouple increased microtubule stabilization from acetylation. Very interestingly, we observed a loss of perinuclear Golgi localization similar to RPGRIP1 depletion upon depletion of ATAT1 and the observed Golgi uncondensation phenotype was even potentiated when RPGRIP1 and ATAT1 depletion were combined. This result suggests that the Golgi reorganization observed here is not due to increased microtubule acetylation but due to increased microtubule stabilization. As both RPGRIP1 and ATAT1 depletion lead to increased microtubule stabilization and loss of Golgi compaction - with opposing outcomes on acetylated microtubules! – we conclude that the dynamics of the microtubules is the dominant factor in determining Golgi organization and positioning as opposed to PTMs.

4.4. Dynamic regulation of the Golgi organization and positioning

Our results favor stable microtubule mediated regulation of the Golgi positioning over centrosomal dictated Golgi positioning. Increase or loss of stable microtubules can lead to uncondensed or compact Golgi morphology, respectively. The fact that Golgi membranes do not form a ring around the centrosome and are not organized into radial conformation, as seen with microtubules that are anchored to the centrosome, indicates that the contribution of centrosome-Golgi linkers is not significant. This is consistent with the literature where laser ablation of the centrosome did not affect the Golgi organization and positioning (Vinogradova et al., 2012). One way how the centrosome might contribute to pericentrosomal accumulation is by generating a radial array of dynamic microtubules during early biogenesis of the Golgi. However, in Golgi biogenesis experiments where the Golgi and centrosome are removed by laser nano-surgery, the Golgi ribbon reformation preceded the reformation of the centrosome challenging the importance of centrosomal function in Golgi biogenesis even more in doubt (Tängemo et al., 2011). In differentiated epithelial cells, the centrosome and microtubules are detached form each other and the Golgi co-localizes with the microtubule cytoskeleton where they form parallel arrays at the cell cortex (Hehnly et al., 2010). Here we show for the first time with high-resolution imaging that the Golgi ribbon stretches are in fact aligned along the acetylated stable microtubule tracks and that they define the organization and positioning of the Golgi by acting as the skeleton of the ribbon.

Since the Golgi displays a high spatial correlation with stable microtubules, we hypothesized that the ectopic microtubule stabilization can displace the Golgi. Total stabilization of the microtubule cytoskeleton by Taxol lead to a concomitant repositioning of the Golgi. This result

provides an important clue on the dynamic regulation of the Golgi positioning during certain processes like cell migration where the Golgi is positioned towards the leading edge. During cell migration, the microtubule cytoskeleton is polarized in a way that microtubules at the leading edge are preferentially stabilized (Wittmann et al., 2003). Plus end TIPs facilitate cortical capture of the microtubule plus ends at the leading edge, which results in an increased number of stable microtubules directed towards the leading edge (Akhmanova & Hoogenraad, 2005). Even though the mechanisms of microtubule stabilization in leading edge are well described, the mechanism of polarization of the Golgi that facilitates increased trafficking of new proteins and lipids to the leading edge, is largely unknown. We can now propose a model for the regulation of the dynamic positioning of the Golgi ribbon. The Golgi membranes are actively targeted to the centrosomal area via dynamic microtubules in a dynein mediated manner in a 'search-and-capture' type mechanism (Vaughan, 2005). As the microtubule cytoskeleton is polarized, stable microtubules will not contribute to an active centripetal movement of the Golgi vesicles. In contrary, stable microtubules have much longer half-lives, they serve as much more stable substrates for plus-end directed kinesins (Reed et al., 2006), which also display higher affinity towards acetylated pool of microtubules. On the basis of our findings that the Golgi is bound and stretched along stable microtubules, the Golgi positioning might be regulated in a tug-of-war type of model. In this model dynamic microtubules actively position the Golgi membranes in pericentrosomal area in a dynein-mediated fashion, whereas the stable microtubules provide a stable substrate where the Golgi membranes can grip on and polymerize into the Golgi ribbon.

5   Outlook

In this study we identified many interesting proteins with a potential role in Golgi organization. In addition to morphological changes of the Golgi, the Golgi marker used in the screen (GalT or GalNAcT) also revealed factors that might have a role in early secretory pathway. Consequently, we found that two related proteins, PDLIM1 and PDLIM3, affect the trafficking of the Golgi markers from ER to Golgi suggesting a role in early secretory pathway. PDLIM1 and PDLIM3 proteins are thought to function at the plasma membrane and PDLIM1 was shown to have a role in cell migration. Characterization of effect of PDLIM1 and PDLIM3 proteins on secretion from ER might reveal interesting cross-regulatory network between late and early secretory compartments.

We further focused on characterization of RPGRIP1 and its effect on the Golgi morphology. Our experiments unfolded interesting role of RPGRIP1 in microtubule dynamics. However, RPGRIP1 locus in the genome undergoes extensive alternative splicing and at the moment we cannot attribute this function to any particular isoform. To resolve isoform specific functions, a mass-spec analysis can be performed to explore abundance of different isoforms and this can be combined with isoform specific siRNAs followed by quantification of microtubule stabilization. Another feasible approach is to develop isoform specific antibodies and study subcellular localization of different isoforms that can potentially provide clues about isoform specific function. Then once the isoform is identified with a role in microtubule dynamics the next challenge is tackle the detailed mechanism on how it regulates microtubule dynamics. Live imaging that allows measurement of microtubule dynamics and

quantification of different parameters of microtubule dynamics might shed light on detailed mechanism of microtubule stabilization upon RPGRIP1 isoform depletion or destabilization upon overexpression.

Characterization of effect of RPGRIP1 depletion on the Golgi morphology has revealed that the stable microtubule form the skeleton of the Golgi ribbon. However it would be interesting to find the molecular linkers of the Golgi ribbon and the stable microtubules. Small scale RNAi screen can be performed and look for candidates that lead to Golgi ribbon compaction. Once potential linkers have been identified, it would be interesting to see dynamics of the Golgi polarization in response to polarized microtubule stabilization. This can be tackled by inducing polarized microtubule stabilization. For instance photoactivatable Taxol has been used in some studies to induce polarized microtubule stabilization can serve as a great tool.

In earlier studies the Golgi is considered to be transient organelle and colocalizes with ER exit sites (ERES). In contrast, a recent publication from our group shows the existence of a positive feedback loop between the Golgi elements and the ERES such that a close spatial association between the Golgi element and ERES promotes activity of the ERES. As the Golgi and ERES display high colocalization in resting cells it's difficult to dissect the nature of positive feedback loop. However fast Golgi repositioning by artificially induced microtubule stabilization followed by localization and functional studies on ERES can provide better ideas about the nature of feedback loop between the Golgi and ERES.

6 Materials and Methods

6.1. Molecular Biology

6.1.1 Heat shock transformation

Competent DH5alpha cells are thawed on ice. 10-100ng of DNA is added to 50ul of competent cells and incubated on ice for 30min. Cells were exposed to heat shock for 45 seconds and incubated on ice for 2min. LB or SOC medium was added and incubated at 37°C for 1h on shaker. Finally cells are plated on agar plates with appropriate selection pressure.

6.1.2 Isolation and purification of plasmids

Bacterial stains are inoculated in 3ml LB medium with appropriate selection pressure O.N. at 37°C on a shaker. Next day bacterial culture is harvested by centrifugation at 12000 rpm for 1min. QIAGEN miniprep kit (Cat No: 27106) is used to isolate and purify DNA from harvested cells.

6.1.3 Subcloning of DNAs

All subcloning of constructs performed in this study including taggings are achieved by first amplifying the constructs with PCR using primers that generate >15bp of overlapping overhangs. Then amplicons are cleaned, checked by agarose gel for right size and recombined into final construct using Genscript CloneEZ PCR Cloning Kit (Cat. No: L00339). Then clones were verified by sequencing for absence of point mutations.

6.1.4 Handling of siRNAs

siRNAs were delivered either in lyophilized (Qiagen, Life Technologies) or in concentrated (Dharmacon) form. Lyophilized siRNAs were diluted in RNAase free water. All siRNAs are diluted and kept at 30uM solution stock at -20C.

6.2. Biochemistry

6.2.1 Sodium dodecyl sulfate polyacrylamide gel electrophoresis (SDS-PAGE)

Cell lysates were washed once with PBS and lysed in 5X SDS loading buffer and boiled at 95°C for 5min. After cooling to RT, Benzonase nuclease (Sigma, Cat. No: E1014-5KU) was added in 1:100 v/v ratios and incubated for 20-30 min. Then sodium dodecyl sulfate polyacrylamide gel electrophoresis (SDS-PAGE) was used to separate proteins by size. 5-15ul of sample was loaded on a precast 4% - 12% NuPage Electrophoresis. Gels run at 60V for 20 min and for another 90 min – 120 min in 3-(N-morpholino)propanesulfonic acid (MOPS) buffer.

6.2.2 Western Blotting

To quantify protein concentration in lysates proteins were first separated by SDS-PAGE as described above. Then proteins were transferred into nitrocellulose membrane using transfer buffer at 100V for 70min. Membranes were blocked for 2h at RT or ON at 4°C with PBS containing 0.1% Tween 20 (PBS-T) and 5% milk powder. Then primary antibody staining was done in PBS-T buffer for 60-120min or ON. Membranes were washed 3 times with PBS-T for 10 min. Secondary antibody staining was

done in PBS-T buffer for 60-120min. Membranes were washed 2 times with PBS-T for 10 min and final wash was done in PBS buffer for 10 min. Depending on the secondary antibody used, visualization of the bands was performed using Amersham^{TM} ECL^{TM} Western Blotting Detecting Reagents Kit or using LI-COR Odyssey^{R} fluorescence imager systems.

6.3. Cell Biology

6.3.1 Mammalian cell culture

6.3.1.1 Maintenance of cells

All cells were incubated at 37°C, 5% CO_2 and >95% humidity. Cells were split 1:5 or 1:10 dilution every 48 or 72h in 10cm (Nunc) dishes when they reached about 80% confluency. For passaging, cells were washed once with 2ml trypsing-EDTA and detached from the dishes by adding another 2ml of trypsin-EDTA for 5 min. Hela cells were maintained in DMEM 1g/l glucose (Cat. No: 11885) supplemented with 10% fetal calf serum (FCS) and 2mM glutamine whereas RPE1 and ARPE19 cells were maintained DMEM/F12 (Cat. No: 21331) supplemented with 10% FCS and 2mM glutamine. For experiments, cells between passage 3 – 20 were used. For RNAi experiments, confluent dishes were split 24h before at 1:2 dilution and seeded accordingly.

6.3.1.2 Freezing and thawing of cells

For freezing, confluent cells were seeded 24h before into 5-6 different 10cm dishes. One dish was kept for mycoplasma test. Rest of the cells were trypsinized as described above and precipitated at 300g for 5

min. Then cell were resuspended in freezing solution containing 20% FCS and 10% DMSO and transferred into cryotubes and kept at -80°C. Once mycoplasma test was negative, cryotubes were transferred to -160°C with liquid nitrogen tanks.

For thawing, cryotubes were first warmed up to 37°C. Then cells were precipitated at 300g for 5min. Freezing solution was removed away and cells were resuspended in growth medium and maintained as described above.

6.3.2 Transfection of mammalian cells

6.3.2.1 siRNA Transfections

All siRNA tranfections were performed using Oligofectamine acquired from Life Technologies (Cat. No: 12252-011). siRNAs and Oligofectamine were first diluted in Opti-MEM medium. Then two mixtures were mixed and incubated for 20 min at RT to allow complex formation. Final tranfection mix were added to pre-washed cells in appropriate growth medium with 0% FCS. After 4 hours 1/3 of the volume with 30% was added. siRNA concentrations were 3 nM for Life Technologies siRNA, 3 uM for Qiagen siRNAs.

6.3.2.2 cDNA Transfections

All cDNA tranfections were performed using Lipofectamine 2000 (Life Technologies, Cat. No: 11668-019). Plasmids and Lipofectamine were first diluted in Opti-MEM. Then two mixtures were mixed and incubated for another 10 min for transfection complexes to form. Transfection mix was then added to cells in appropriate growth medium.

Typically 2ug/ml of plasmids was used with 2.5ul/ml Lipofectamine solution.

6.3.2.3 Immunofluorescence and fluorescence microscopy

6.3.2.3.1 Immunostaining

Cells were either fixed with methanol or paraformaldehyde solution (PFA). For methanol fixation, cells were first washed with PBS and incubated in cold methanol for 4min at -20°C. Then cells were washed again in PBS and kept in PBS for immunostaining. For PFA fixation, cells were incubated in 4% PFA solution for 20min at RT. 30mM glycine solution was added to block the left over PFA subsequently and incubate for another 10min. Permeabilization of the cells was performed either in 0.02% Triton-X-100 or 0.2% Saponin solution for 10min.

Primary antibody staining was performed either in PBS for methanol fixed samples or in PBS containing permeabilization solution for PFA fixed samples. Antibodies were diluted in appropriate concentrations and incubated typically for 40min. Then cells were washed three times with PBS solution. All secondary antibody stainings were performed in PBS containing Hoechst solution (1:2000 dilution) and typically cells were incubated for 30-40min. Cells were then washed three times in PBS and mounted on glass slides in 5ul Mowiol.

6.3.2.3.2 Wide-field microscopy

Wide field microscopy was done on Olympus Scan^R system using CellR software. Depending on the experiment LUCPlanFLN 20x/0.45 Ph1, or LUCPlanFLN 40x/0.60 RC3 objectives were used.

6.3.2.3.3 Confocal microscopy

For confocal microscopy either PerkinElmer Ultraview ERS spinning disc or Leica TCS SP5 confocal microscopes were used. Depending on the experiment, typically ZEISS EC Plan-Neofluar 40x/1.30 Oil, ZEISS Plan-APOCHROMAT 63x/1.4 Oil DIC, or Leica PL APO HCX 63x / NA 1.40 – 0.60 objectives were used. For live-imaging experiments, microscope incubator was maintained at 5% CO_2, 37°C with ~60-70 humidity.

6.3.2.3.4 High-throughput microscopy

High-throughput microscopy was done on Olympus ScanR system using software developed at EMBL in collaboration with Olympus. Imaging was done using LUCPlanFLN 20x/0.45 Ph1 objective with autofocus.

6.3.2.3.5 Correlative Light –Electron Microscopy

Correlative light electron microscopy was done using Leica SP5 confocal system followed by Transmission Electron Microscope system at EMBL Electron Microscopy facility by Anna Steyer. GalNAcT2 cells were grown on a 3 cm culture dish with a coordinate system on the bottom (MatTek cooperation, P35G-2-14-CGRD). Cells were prefixed with 0.5% glutaraldehyde/4 % paraformaldehyde/ 0.05% malachite green in 0.1 M PHEM buffer (200 mM Pipes, 100 mM Hepes, 8 mM $MgCl_2$, 40 mM EGTA) in a microwave-assisted tissue processing (Ted Pella Inc.) with 100 W for 14 min at 20 °C. The cells were quenched with 150 mM glycine in 0.1 M PHEM buffer for 40 sec with 250 W at 20 °C in the microwave followed by rinsing with buffer and another round of quenching. Afterwards the cells were washed multiple times with buffer. The nuclei were stained with Hoechst, 1:1000 for 30 min. Later on confocal microscope, representative 3-4 cells were selected manually and stage coordinates were saved. Later

cells were imaged with HCX PL Apo 63x/1.4 oil Ph3 objective typically with 200 nm confocal slices. Once imaging was done, same coordinates were imaged again with HC PL Apo 10x/0.4 Ph1 air objective with transmission light to save coordinates of the cells on the grid. After confocal imaging, the cells were fixed again with 0.5% glutaraldehyde/4 % paraformaldehyde/ 0.05% malachite green in 0.1 M PHEM buffer in a microwave-assisted tissue processing with 100 W for 14 min at 20 °C. Followed by postfixation in 0.8% $K_3Fe(CN)_6$ / 1 % OsO_4 in 0.1 M PHEM for 14 min at 100 W at 20 °C. The cells were then stained with 1 % tannic acid for 7 min using 150 W followed by 1 % uranyl acetate for 7 min at 150 W at 20 °C. After dehydration in ethanol (7 steps from 25 %- 100 % ethanol, each 40 sec using 250 W) the cells were embedded in hard/very hard EPON. The EPON blocks were then either cut with a diamond knife (70 or 300 nm sections) and imaged with a Biotwin CM120 (Philips) or a TECNAI F30 (FEI) or imaged with a Auriga 060 (Zeiss).

6.3.2.4 Nocodazole assay

For measuring microtubule stability cells were incubated in 10 uM nocodazole containing medium. Cells were fixed with methanol as described above either after 8 min or after 20min.

6.3.2.5 Microtubule nucleation assay

For microtubule nucleation assay, cells were incubated on ice for 60min to depolymerize microtubules. Cells were then fixed with methanol as described above after 45, 90 or 150 seconds and processed further for immunostaining.

6.4. Computational Biology

6.4.1 ImageJ

ImageJ software (http://www.imagej.nih.gov/ij/) was used for visualization and pre-processing of the images. For pre-processing of the confocal images, following 'confocal_preprocessor_script' was used:

```
Confocal_preprocessor_script:
// Get root folder
var rootFolder  = getDirectory("Choose Source Directory");
// Traverse through the folders
traverseFolders(rootFolder, rootFolder);
function traverseFolders(currentFolder, rootFolder){
 // get all subfolders
 list = getFileList(currentFolder);
 for (i=0; i<list.length; i++) {
        showProgress(i, list.length);
        if (endsWith(list[i], "/")){
                traverseFolders("" + currentFolder + list[i], rootFolder);
        }
        else if (endsWith(list[i], ".ics")){
                // this is an image file, it should be processed
                processImage(currentFolder,  list[i]);
                //print(currentFolder + list[i]);
        }
 }
}
function processImage(folderPath, imageName){
        // sample image name
        // Pos001_S001_z00_ch00.ics
        delimiter1="_";
        parts1=split(imageName, delimiter1);
        var imageNumber = parts1[0];
        print("imageNo: " + imageNumber);
        // for debug
        print("Image number detected: " + imageNumber);
        //open DAPI image
        print("Reading image: " + imageName);
        run("Bio-Formats Importer", "open=[" + folderPath + "\\" + imageName + "] autoscale color_mode=Default
        split_channels view=[Standard ImageJ] stack_order=Default");
        // wait until image is read
        print("Number of open images: " + nImages);
        while (nImages != 4) {
                wait(100);
        }
        print("constructing image names..");
        getDimensions(width, height, channels, slices, frames);
        //construct stack image names
        var DAPI = imageName + " - C=0";
        var Golgin84 = imageName + " - C=1";
        var AceTub = imageName + " - C=2";
```

```
var Tubulin = imageName + " - C=3";
// get stack size
selectWindow(DAPI);
getDimensions(width, height, channels, slices, frames);
// run max and sum projections of all channels
selectWindow(DAPI);
run("Z Project...", "start=1 stop=" + slices+ " projection=[Max Intensity]");
selectWindow(AceTub);
run("Z Project...", "start=1 stop=" + slices+ " projection=[Max Intensity]");
selectWindow(Golgin84);
run("Z Project...", "start=1 stop=" + slices+ " projection=[Max Intensity]");
selectWindow(Tubulin);
run("Z Project...", "start=1 stop=" + slices+ " projection=[Max Intensity]");
selectWindow(AceTub);
run("Z Project...", "start=1 stop=" + slices+ " projection=[Sum Slices]");
selectWindow(Tubulin);
run("Z Project...", "start=1 stop=" + slices+ " projection=[Sum Slices]");
selectWindow(Golgin84);
run("Z Project...", "start=1 stop=" + slices+ " projection=[Sum Slices]");
while (nImages != 11) {
      wait(100); // wait until all projections are done
}
// construct max projected image names
// sample image name: MAX_XY point 1.ics - C=2
var max_DAPI = "MAX_" + DAPI;
var max_AceTub = "MAX_" + AceTub;
var max_Tubulin = "MAX_" + Tubulin;
var max_ Golgin84 = "MAX_" + Golgin84;
var sum_AceTub = "SUM_" + AceTub;
var sum_Tubulin = "SUM_" + Tubulin;
var sum_ Golgin84 = "SUM_" + Golgin84;

// setting brightness for DAPI channel
selectWindow(max_DAPI);
setMinAndMax(500, 5000);

// setting brightness for AceTub channel
selectWindow(max_AceTub);
setMinAndMax(600, 12000);

// setting brightness for Golgi channel
selectWindow(max_ Golgin84);
setMinAndMax(500, 8000);

// setting brightness for Tubulin channel
selectWindow(max_Tubulin);
setMinAndMax(500, 6000);

// save max projected images
selectWindow(max_DAPI);
saveAs("Tiff", folderPath + "/" + imageNumber + "_MAX_DAPI");
selectWindow(max_AceTub);
saveAs("Tiff", folderPath + "/" + imageNumber + "_MAX_AceTub");
selectWindow(max_Tubulin);
saveAs("Tiff", folderPath + "/" + imageNumber + "_MAX_Tubulin");
selectWindow(max_Golgin84);
saveAs("Tiff", folderPath + "/" + imageNumber + "_MAX_Golgin84");
```

```
// save sum projected images
selectWindow(sum_AceTub);
saveAs("Tiff", folderPath + "/" + imageNumber + "_SUM_AceTub");
selectWindow(sum_Tubulin);
saveAs("Tiff", folderPath + "/" + imageNumber + "_SUM_Tubulin");
selectWindow(sum_Golgin84);
saveAs("Tiff", folderPath + "/" + imageNumber + "_SUM_Golgin84");

// close all images
while (nImages>0) {
    selectImage(nImages);
    close();
}
}
```

Preprocessing of confocal slices for quantification of the polymerized tubulin following procedure was followed:

1. *Enhance for tubular structures each slice of image with Tubulin staining using 'Tubeness' plugin*
2. *Determine best threshold value to separate free tubulin signal from polymerized tubulin signal and apply this threshold for all images.*
3. *Sum slices and quantify integrated intensity of Tubulin per cell*

6.4.2 Cell Profiler

Cell Profiler software (http://www.cellprofiler.org/) was used for quantification of effect of RPGRIP1 on centrosome organization, EB1 comet shape distribution and Golgi organization.

6.4.2.1 Quantification of centrosome organization

Acquired confocal images were first pre-processed using confocal_preprocessore_script as described above as Cell Profile version does not yet support 3D stacks. Then following Cell Profiler pipeline was

used to quantify intensities of gamma tubulin and pericentrin at the centrosome and number of pericentrin dots per cell:

Module Name	Parameters
Input Modules	
Images	*Image path*
Metadata	*Necessary metadata to identify images is already mentioned in file name or path. Following metadata are extracted:* • *Date of the experiment* • *Treatment* • *ImageID* • *Channel*
NamesAndTypes	*Following images were loaded: MAX_DAPI, MAX_TUBG, MAX_Pericentrin, SUM_TUBG, SUM_Pericentrin, IlluminationCorrectionFunction*
Analysis Modules	
RescaleIntensity	*MAX_DAPI, Stretch each image to use the full intensity range*
RescaleIntensity	*MAX_TUBG, Stretch each image to use the full intensity range*
RescaleIntensity	*MAX_Pericentrin, Stretch each image to use the full intensity range*
RescaleIntensity	*SUM_TUBG, Stretch each image to use the full intensity range*
RescaleIntensity	*SUM_Pericentrin, Stretch each image to use the full intensity range*
CorrectIlluminationApply	For PerkinElmer Ultraview ERS spinning disc images following illumination correction was applied:
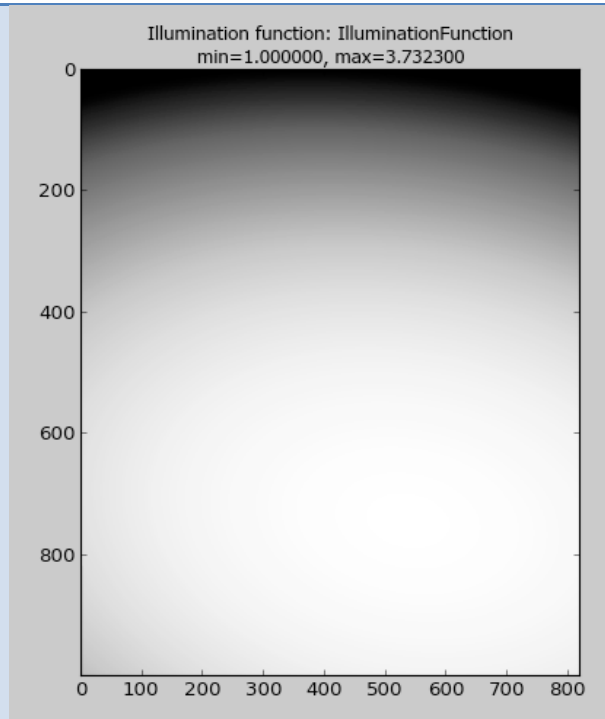
Illumination function: IlluminationFunction
min=1.000000, max=3.732300
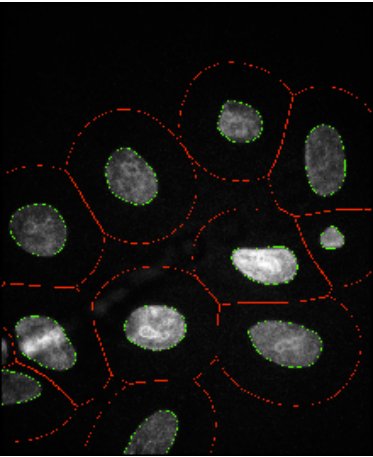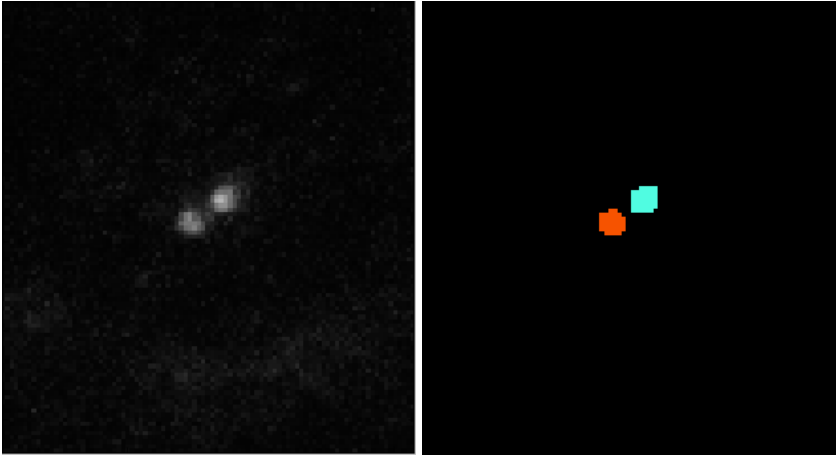
Morph	*MAX_DAPI; Operation 1 = 'Open'; Kernel = 'Disc' kernel; Scale = 3; ; Operation 2 = 'Close'; Kernel = 'Disc' kernel; Scale =10;* ** First operation is required to separate nuclei touching each other, while second operation is required to fill holes and make nuclei intensity uniform*
IdentifyPrimaryObjects	*'Otsu' algorithm was used for segmentation of nuclei:* ** Segmented nuclei are color coded*
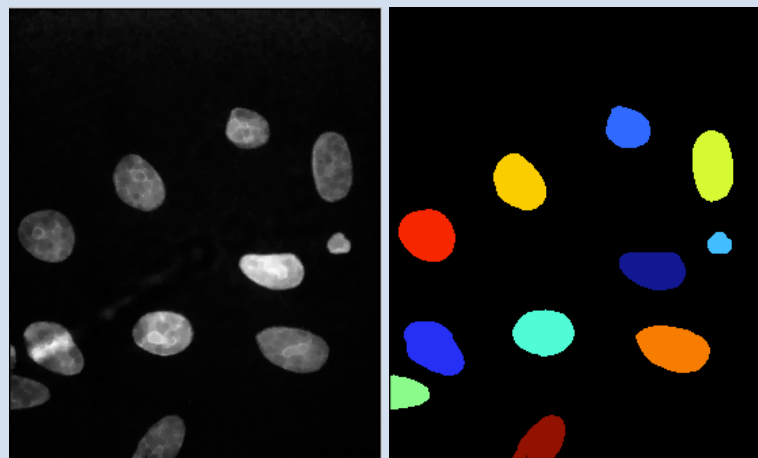
IdentifySecondaryObjects	*Cells borders were estimated by expanding the nuclei:* ** Estimated cell borders is shown with red lines*
Crop	*Crop out part of MAX_Pericentin image not covered by 'Cells'*
IdentifyPrimaryObjects	*'Otsu' algorithm was used to segment pericentrin:* ** Segmented pericentrin objects are color coded* ** Image not scaled same as before*
IdentifySecondaryObjects	*Pericentrin object areas are enlarged for 7 pixels and named as 'Pericentrin_area'. Pericentrin segmentation sometimes only segments brightest spot but this can be solved by enlarging their area*
RelateObjects	*Assign 'nuclei' objects to 'cells' obejcts as child. This allows access for per-cell measurements and counts.*
RelateObjects	*Assign 'pericentrin' objects to 'cells' objects as child.*
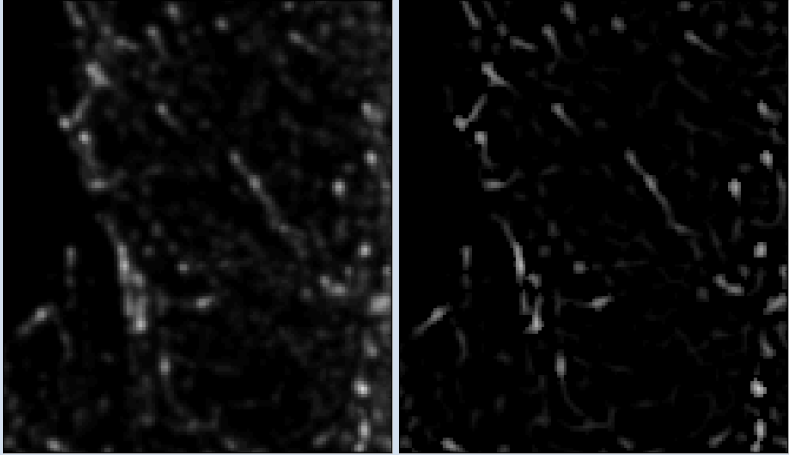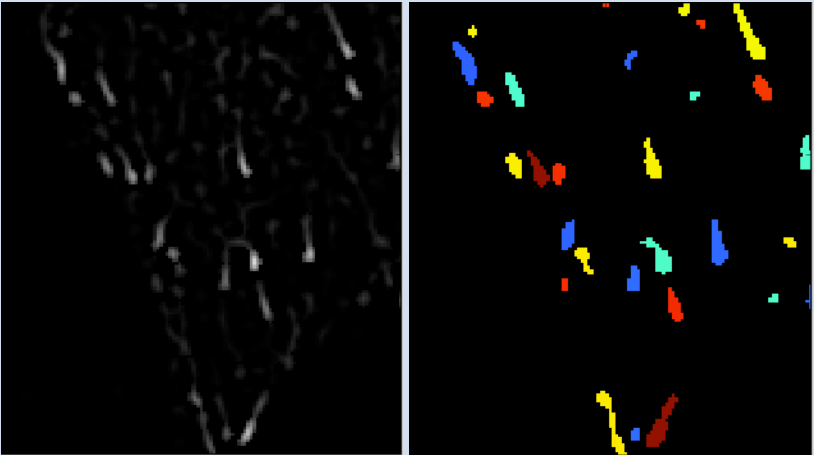
Module Name	Parameters
RelateObjects	*Assign 'Pericentrin_area' objects to 'cells' objects as child.*
MeasureObjectsIntensity	*Intensities of 'Pericentrin' and 'Pericentrin_area' objects are measured in SUM_Pericentrin, SUM_TUBG, MAX_Pericentrin, MAX_TUBG images.*
MeasureObjectsSizeShape	*Sizes and shapes of 'Pericentrin' and 'Pericentrin_area' obejcts are measured.*
OverlayOutlines	*This is done to later verify quality of Pericentrin segmentation.*
ExportToSpreadsheet	*Export all the measurements*

Once analysis was done, either Microsoft Excel or R software was used for visualization and quantification.

6.4.2.2 Quantification of the EB1 comet shape

Acquired confocal images were first pre-processed using confocal_preprocessore_script as described above. Later following Cell Profiler pipeline was used to quantify EB1 comet shapes:

Module Name	Parameters
<mark>Input modules</mark>	
Images	*Image path*
Metadata	*Necessary metadata to identify images is already mentioned in file name or path. Following metadata are extracted:* • *Date of the experiment* • *Treatment* • *ImageID* • *Channel*
NamesAndTypes	*Following images are loaded: MAX_TUBG, SUM_TUBG, IlluminationCorrectionFunction*
<mark>Analysis module</mark>	

RescaleIntensity	*MAX_TUBG, Stretch each image to use the full intensity range*
RescaleIntensity	*SUM_TUBG, Stretch each image to use the full intensity range*
CorrectIlluminationApply	*As described in first pipeline.*
EnhanceOrSuppressFeatures	*Image='MAX_TUBG'; Operation='Enhance'; Type='Neurites'; Methods='Tubeness'; Scale = 1.1;* ** Images before(left) and after(right)*
EnhanceOrSuppressFeatures	*Image='SUM_TUBG'; Operation='Enhance'; Type='Neurites'; Methods='Tubeness'; Scale = 1.1;*
IdentifyPrimaryObjects	*'Otsu' algorithm was used for comet segmentation:* ** Segmented comets are color coded*
MeasureObjectSizeShape	*Measure intensities of all comets detected.*
ExportToSpreadsheet	*Export all measurements*
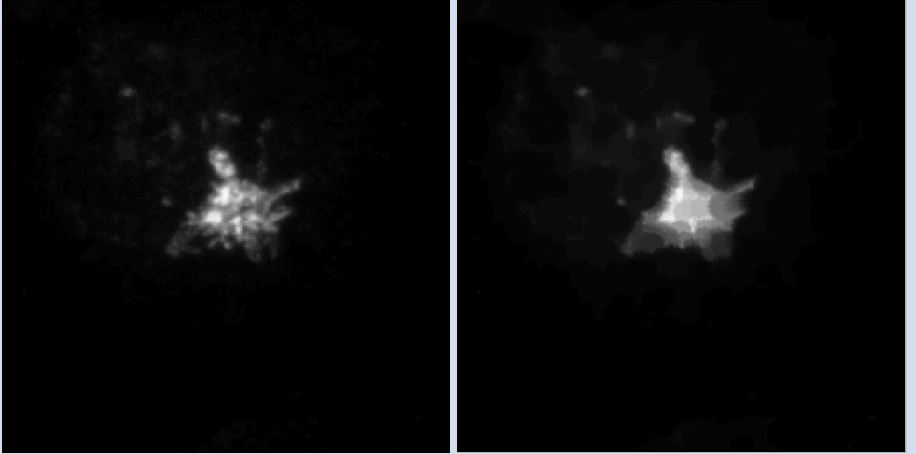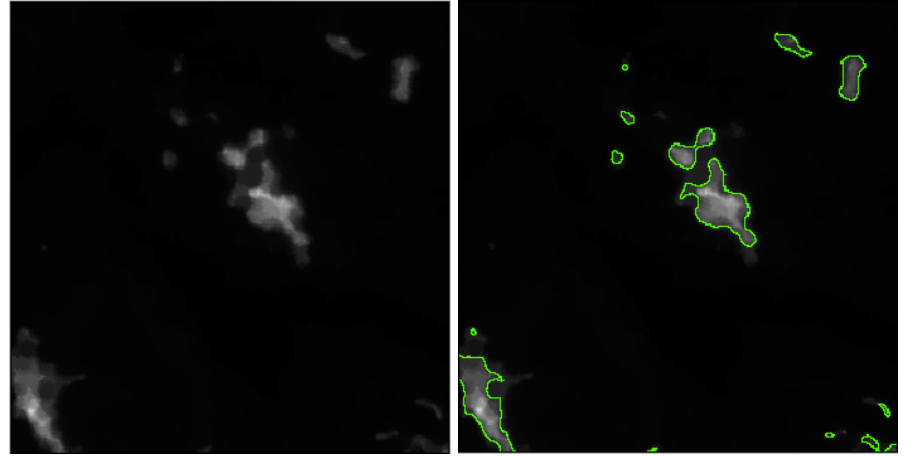
After analysis is done, measurement results using R software environment. EB1 comets major axis and minor axis measurement from different experiments are combined into two single data frames, first for control and second for siRPGRIP1 measurements. Then in each comet data frames were further classified into 3 subgroups: non-growing (if MajorAxisLength/MinorAxisLength < 1.5), intermediate (if 1.5 < MajorAxisLength/MinorAxisLength < 4.5), growing (if MajorAxisLength/MinorAxisLength > 4.5). Finally, test for proportion (prop.test) was used to check whether the difference observed between non-growing fraction in control and siRPGRIP1 treated cells is significant.
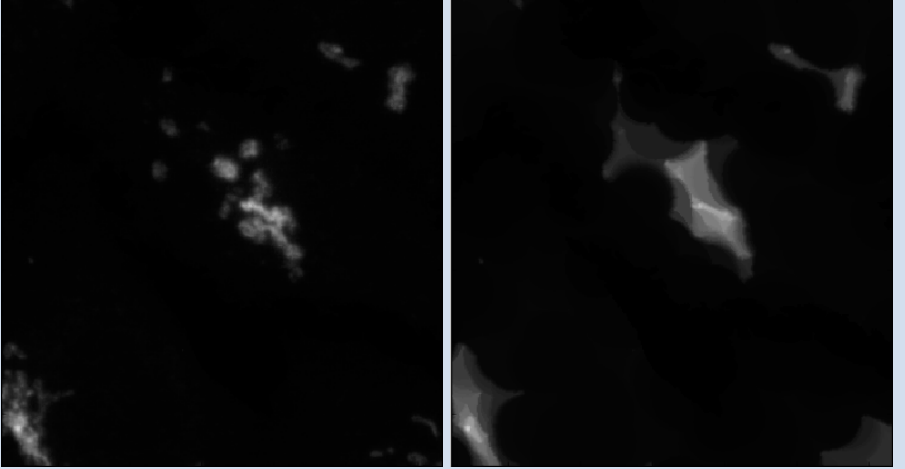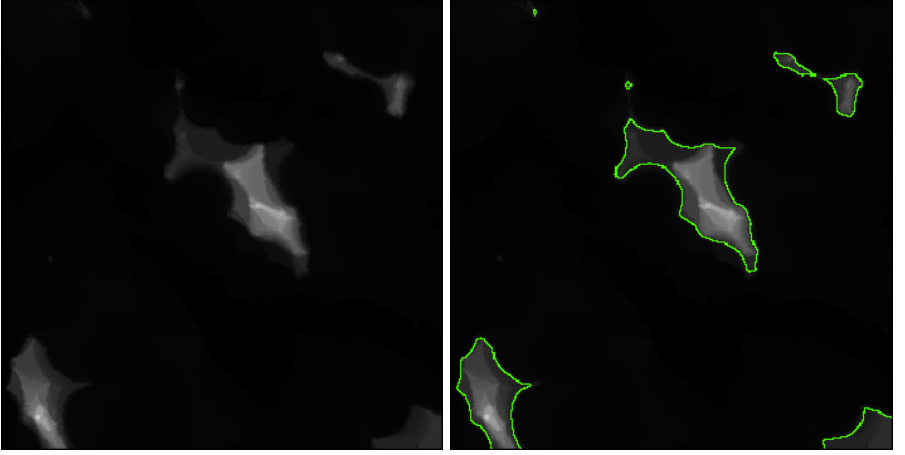
6.4.2.3 Quantification of Golgi phenotype
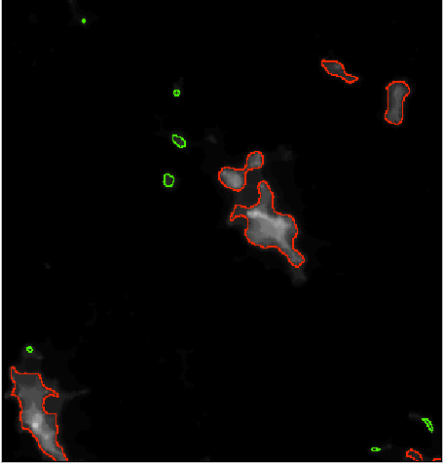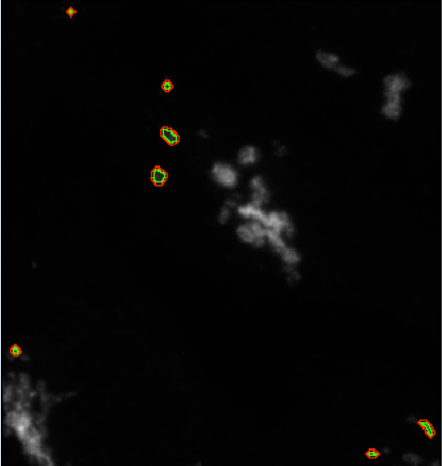
Acquired confocal images were first pre-processed using confocal_preprocessore_script as described above. Later following Cell Profiler pipeline was used to quantify Golgi phenotypes and acetylated tubulin intensity:
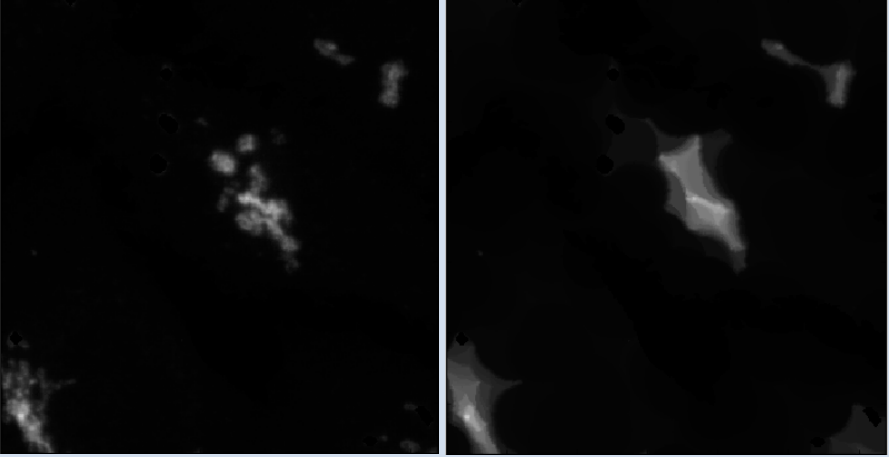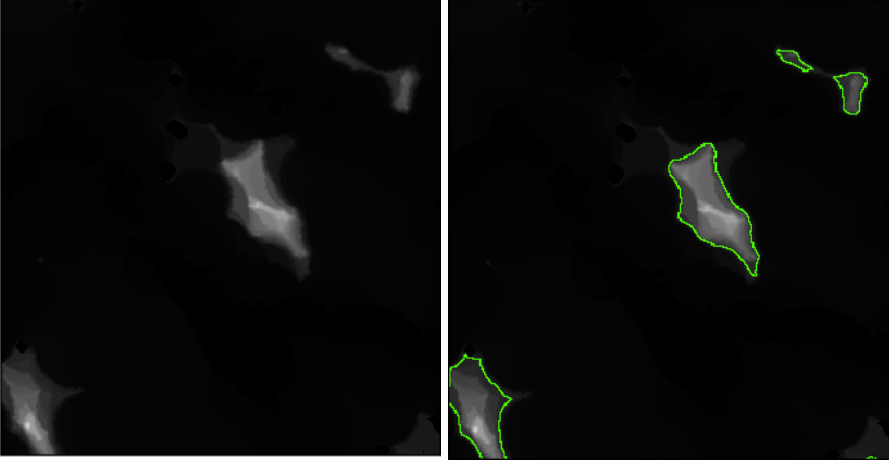
Input modules	
Images	*Image path*
Metadata	*Necessary metadata to identify images is already mentioned in file name or path. Following metadata are extracted:* • *Date of the experiment* • *Treatment* • *ImageID* • *Channel*
NamesAndTypes	*Following images were loaded: MAX_DAPI, SUM_AcetylatedTubulin,*

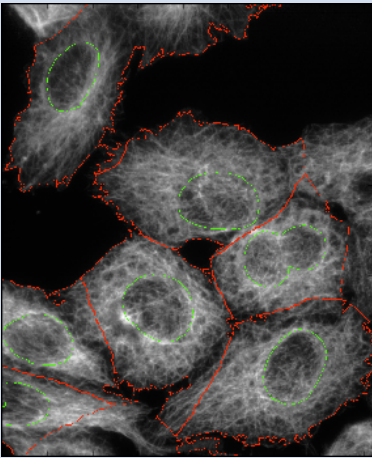|	
	SUM_Tubulin, SUM_Golgin84
<mark>**Analysis modules**</mark>	
RescaleIntensity	*MAX_DAPI, Stretch each image to use the full intensity range*
RescaleIntensity	*SUM_AcetylatedTubulin, Stretch each image to use the full intensity range*
RescaleIntensity	*SUM_Tubulin, Stretch each image to use the full intensity range*
RescaleIntensity	*SUM_Golgin84, Stretch each image to use the full intensity range*
Morph	*MAX_DAPI; Operation 1 = 'Open'; Kernel = 'Disc' kernel; Scale = 3; ; Operation 2 = 'Close'; Kernel = 'Disc' kernel; Scale =10;* ** First operation is required to separate nuclei touching each other, while second operation is required to fill holes and make nuclei intensity uniform*
CorrectIlluminationApply	*As described in first pipeline.*
IdentifyPrimaryObjects	*As described in first pipeline.*
IdentifySecondaryObjects	*Cell segmentation was performed using SUM_Tubulin channel:* ** Estimated cell borders are shown in red, nuclei borders in green*
Crop	*Parts of SUM_Golgin84 image not covered by 'Cells' were cropped out.*
Morph	*SUM_Golgin84; Operation='Close'; Scale='10'* *This operation fills the holes inside the Golgi and it is required for proper segmentation of the Golgi object:*

	 Images before(left) and after(right)
IdentifyPrimaryObjects	*The Golgi elements were segmented using 'RobustBackground' algorithm. Identified objects were named as 'Golgi' objects.* *Segmented Golgi objects is encircled with green line* *Segmented Golgi elements were used for quantification of number of Golgi elements per cell*
Morph	*'Close' operation performed on Golgi images where holes inside the Golgi are filled*

* Image before(left) and after(right) processing

IdentifyPrimaryObjects	*'Otsu' algorithm was used for segmentation of the Golgi elements. Segmented Golgi obejcts were named 'AllGolgiBlob'.* ** Segmented Golgi objects are encircled with green line*
MeasureObjectSizeShape	*Size and shapes of the 'Golgi' objects are measured.*
FilterObjects	*The Golgi objects with area of smaller than 150 (pixel to pixel) were selected. Objects selected were named as 'SmallGolgiElements'*

	  * The Golgi objects matching the parameters shown in green, rest in red
IdentifySecondaryObjects	*SmallGolgiElements were enlarged by 2px to capture and named is SmallGolgiElements_area. This is required to solve incomplete segmentation.* ** Enlarged areas are encircled with red line*
MaskImage	*The Golgi objects within the SmallGolgiElements_area were removed away by masking.*
Morph	*'Close' operation was performed in Golgi images where small dots are filtered out.*

	 Image before(left) and after(right) processing
IdentifyPrimaryObjects	'Otsu' algorithm was used for segmentation of Golgi objects. Segmented objects were named as 'BigGolgiBlob': *Segmented objects are encircled with green line.*
ApplyThreshold	SUM_AcetylatedTubulin images were thresholded. Threshold values were first determined by 'Automatic'. Then this value were used for all images in 'Manual' mode.
RelateObjects	Assign 'Golgi' objects to 'Cells' obejcts as child. This allows access for per-cell measurements and counts.
RelateObjects	Assign 'AllGolgiBlob' objects to 'Cells' obejcts as child.
RelateObjects	Assign 'BigGolgiBlob' objects to 'Cells' obejcts as child.
MeasureObjectIntensity	Intensities of 'Golgi', 'AllGolgiBlob' and 'BigGolgiBlob' objects were measured.

MeasureObjectSizeShape	*Sizes and shapes of 'Golgi', 'AllGolgiBlob' and 'BigGolgiBlob' objects were measured.*
OverlayOutlines	*Outlines of 'Golgi', 'AllGolgiBlob' and 'BigGolgiBlob' objects were overlayed on top of SUM_Golgin84 image.*
SaveImages	*Overlayed images were saved for verification of the parameters for segmentation.*
ExportToSpreadsheet	*All measurements were exported*

Once analysis was done, Microsoft Excel or R software was used to quantify number of Golgi objects per cell, area of AllGolgiBlob and BigGolgiBlob, intengrated intensity of acetylated tubulin staining per cell for control and treated cells.

6.4.3 Western Blot

Quantification of the western blot bands was done using ImageStudiLite software (http://www.licor.com/bio/products/software/image_studio_lite/) provided by LI-COR. First bands to be quantified were selected manually by assigning rectangular shapes around the bands. Then shapes were further enlared vertically for another 10% and median of the of this enlarged was used for estimated of the background. Later this median value was used a threshold value and subtracted out from every pixel in corresponding rectangles. Then total intensity of each rectangle was recorded as an amount of protein.

6.5. Reagents

6.5.1 Antibodies and Dyes

Details of all antibodies in this study is depicted in the following table:

Target	Concentration	Vendor	Catalog number
Alpha-Tubulin	MeOH/PFA IF: 1:500 WB 1:10 000	Neomarkers	MS581
Beta-Tubulin	1:100 MeOH, 1:3000 WB	Abcam	ab6046
Acetylated tubulin	MeOH 1:2000	Sigma	T7451
EB1	MeOH 1:300	BD Bioscience	610534
Gamma-tubulin	MeOH 1:750	Sigma	T6557
Pericentrin	PFA 1:4000	Abcam	ab4448
RPGRIP1 (abRPGRIP1)	WB 1:1000	Proteintech	13214-1-AP
RPGRIP1 (gs-abRPGRIP1)	1:1000	Custom	NA
Golgin84	1:500	Martin Lowe	NA
GM130	MeOH/ PFA 1:500	BD Bioscience	610822
Giantin	PFA, 1:2000	abcam	ab24586
GRASP65	1:3000 MeOH/ PFA	Martin Lowe	NA
Hoechst			

6.5.2 siRNAs

All siRNAs used in this study (siRNAs used in the screen are not included)

Target	Vendor	Catalog Number
RPGRIP1	QIAGEN	SI00125902
RPGRIP1	QIAGEN	SI00125923
RPGRIP1	QIAGEN	SI03035480
RPGRIP1L	QIAGEN	SI04319763
RPGRIP1L	QIAGEN	SI04329710
RPGR	Life Technologies	s12124
RPGR	Life Technologies	s12125
ATAT1	Dharmacon	L-014510-02
CLASP1	Life Technologies	s23581
CLASP1	Life Technologies	s23582
CLASP2	Life Technologies	s223572
CLASP2	Life Technologies	s223573
GM130	Life Technologies	s5942
GRASP65	Life Technologies	s34819

6.5.3 Plasmids

Details of all plasmids used in this study are listed in the following table:

Plasmid Name	Insert	Source
pGFP-RPGRIP1	NM_020366.3 isoform of RPGRIP1	Origene (Cat. No: SC304750)
pAF_265666	AF_265666 isoform of RPGRIP1	This study
pXM_006720208	XM_006720208 isoform of RPGRIP1	This study
pXM_006720209	XM_006720209 isoform of RPGRIP1	This study
pXM_006720210	XM_006720210 isoform of RPGRIP1	This study
pXM_005267881	XM_005267881 isoform of RPGRIP1	This study
pGFP-RPGRIP1L	RPGRIP1	Kazusa cDNA Collection
pYFP-ATAT1	ATAT1	Kindly provided by Dr. Kalebic, Heppenstall group

7   Appendix

Supplementary Table 1: *RNAi screening candidate hits*

Symbol (ID)	Golgi Phenotype	Localization	Function	Source
AHNAK (ENSG00000124942)	Fragmented	Localizes to desmosomes in polarized cells. Plasma membrane and cytoplasmic (Protein Atlas).	Regulates cell membrane cytoarchitecture	Sussman, Joshua, et al. "Protein kinase B phosphorylates AHNAK and regulates its subcellular localization." *The Journal of cell biology* 154.5 (2001): 1019-1030.
ANLN (ENSG00000011426)	Stretched, mislocalized, cytokinesis defect	Nuclear in interphase and peripheral in prometaphase, and then accumulate at furrow sites	Links together different components of cytokinetic machinery	D'Avino, Pier Paolo, et al. "Interaction between Anillin and RacGAP50C connects the actomyosin contractile ring with spindle microtubules at the cell division site." *Journal of cell science* 121.8 (2008): 1151-1158.
AP2M1 (ENSG00000161203)	Mild fragmentation	Punctate structures at the plasma membrane	Links Clathrin lattice to the underlying membrane	Gaidarov, Ibragim, and James H. Keen. "Phosphoinositide–AP-2 interactions required for targeting to plasma membrane clathrin-coated pits." *The Journal of cell biology* 146.4 (1999): 755-764.
BRPF1 (ENSG00000156983)	Fragmented	Cytoplasmic but can be translocated to nucleus upon activation. Plasma membrane and cytoplasmic (Protein Atlas)	Activator of Moz/Morf transcription factors	Ullah, Mukta, et al. "Molecular architecture of quartet MOZ/MORF histone acetyltransferase complexes." *Molecular and cellular biology* 28.22 (2008): 6828-6843.
CC2D1A (ENSG00000132024)	Mild fragmentation	Nuclear. Cytoplasmic (Protein Atlas)	Transcriptional regulator of serotonin receptor 5HT1A	Rogaeva, Anastasia, and Paul R. Albert. "The mental retardation gene CC2D1A/Freud-1 encodes a long isoform that binds conserved DNA elements to repress gene transcription." *European Journal of Neuroscience* 26.4 (2007): 965-974.
CNKSR1 (ENSG00000142675)	Mild Fragmentation	Plasma membrane localization. Cytoplasmic (Protein Atlas)	The CNK1 scaffold binds cytohesins and promotes insulin pathway signaling	Lim, Junghwa, et al. "The CNK1 scaffold binds cytohesins and promotes insulin pathway signaling." *Genes & development* 24.14 (2010): 1496-1506.
CPNE7 (ENSG00000178773)	Fragmented	Nuclear but translocates to plasma membrane upon Ca++ stimulation	Regulation of plasma membrane lipid and protein content	Perestenko, Pavel V., et al. "Copines-1,2,-3,-6 and-7 show different calcium-dependent intracellular membrane translocation and targeting." *FEBS Journal* 277.24 (2010): 5174-5189.

Gene (ENSG ID)	Morphology	Localization	Function	Reference
DFNB31 (ENSG00000095397)	Mild Fragmentation	Cytoplasm		van Wijk, Erwin, et al. "The DFNB31 gene product whirlin connects to the Usher protein network in the cochlea and retina by direct association with USH2A and VLGR1." *Human molecular genetics* 15.5 (2006): 751-765.
DGKD (ENSG00000077044)	Fragmented	Cytoplasmic, translocates to plasma membrane when stimulated by TPA	Lipid signalling by producing DAG and PA	Sakane, Fumio, et al. "Alternative splicing of the human diacylglycerol kinase δ gene generates two isoforms differing in their expression patterns and in regulatory functions." *Journal of Biological Chemistry* 277.45 (2002): 43519-43526.
DGKK (ENSG00000068366)	Mild Fragmentation	Plasma membrane	Attenuates DAG mediated signalling.	Imai, Shin-ichi, et al. "Identification and characterization of a novel human type II diacylglycerol kinase, DGKκ." *Journal of Biological Chemistry* 280.48 (2005): 39870-39881.
DKFZP586P0123 (ENSG00000168014)	Fragmented	Centrioles. Cytoplasmic (Protein Atlas)	Mediates Ca++ dependent vesicular transport during cilia biogenesis	Hoover, Amber N., et al. "C2cd3 is required for cilia formation and Hedgehog signaling in mouse." *Development* 135.24 (2008): 4049-4058.
DKFZP686M0199 (ENSG00000226259)	Fragmented	NA	NA	NA
DLG3 (ENSG00000082458)	Fragmented	Nucleus and Cytoplasm. Nucleus and nucleoli (Protein Atlas)	Regulate cell adhesion and plasticity at cell junctions	García-Mata, Rafael, et al. "The nuclear RhoA exchange factor Net1 interacts with proteins of the Dlg family, affects their localization, and influences their tumor suppressor activity." *Molecular and cellular biology* 27.24 (2007): 8683-8697.
DNM2 (ENSG00000079805)	Fragmented	Centrosomes and Cytoplasm	Mediate vesicle formation in endocytosis esp. budding of clathrin coated vesicles	Bitoun, Marc, et al. "Mutations in dynamin 2 cause dominant centronuclear myopathy." *Nature genetics* 37.11 (2005): 1207-1209.
DPF2 (ENSG00000133884)	Stretched, Fragmented	Nuclear and Cytoplasmic. Nucleus, Vesicles, Cytoplasm and Centrioles (Protein Atlas)	Represses transcription of estrogen related receptor alpha target genes	Matsuyama, Reiko, et al. "Double PHD Fingers Protein DPF2 Recognizes Acetylated Histones and Suppresses the Function of Estrogen-related Receptor α through Histone Deacetylase 1." *Journal of Biological Chemistry* 285.24 (2010): 18166-18176.
DVL1 (ENSG00000107404)	Fragmented	Intracellular vesicles and plasma membrane.	Binds to AP2, clathrin coats and inhibits	Shafer, Beth, et al. "Vangl2 promotes Wnt/planar cell polarity-like signaling by antagonizing Dvl1-mediated

Gene	Fragmentation	Localization	Function	Reference
		Cytoplasmic (Protein Atlas).	Frizzled4 receptor internalization	feedback inhibition in growth cone guidance."*Developmental cell* 20.2 (2011): 177-191.
FAM62C (ENSG00000158220)	Mild Fragmentation	Plasma membrane. Golgi, COPI (Bergeron)	also called Esyt3	Min, Sang-Won, Wen-Pin Chang, and Thomas C. Südhof. "E-Syts, a family of membranous Ca2+-sensor proteins with multiple C2 domains." *Proceedings of the National Academy of Sciences* 104.10 (2007): 3823-3828.
FGD4 (ENSG00000139132)	Fragmented	Cytoplasmic and colocalizes with f-actin and induces their polymerization. Cytoplasm and membranes (Protein Atlas)	Induces filopodium like microspike formation	Ono, Yuichi, et al. "Two actions of frabin: direct activation of Cdc42 and indirect activation of Rac." *Oncogene* 19.27 (2000): 3050-3058.
FRMPD4 (ENSG00000169933)	Fragmented	Cytoplasmic	It functions as a positive regulator of dendritic spine morphogenesis and density, and is required for the maintenance of excitatory synaptic transmission	Lee, Hyun Woo, et al. "Preso, a novel PSD-95-interacting FERM and PDZ domain protein that regulates dendritic spine morphogenesis." *The Journal of Neuroscience* 28.53 (2008): 14546-14556.
GRASP (ENSG00000161835)	Fragmented	Plasma membrane	This gene encodes a protein that functions as a molecular scaffold, linking receptors, including group 1 metabotropic glutamate receptors, to neuronal proteins	Lai, Chun-Liang, et al. "Molecular mechanism of membrane binding of the GRP1 PH domain." *Journal of molecular biology* 425.17 (2013): 3073-3090.
GRIP1 (ENSG00000155974)	Mild Fragmentation	Plasma membrane. Membranes and cytoplasmic (Protein Atlas)	Bind to Kinesin motor protein and causes dendrite targeting of kinesin cargo	Setou, Mitsutoshi, et al. "Glutamate-receptor-interacting protein GRIP1 directly steers kinesin to dendrites." *Nature* 417.6884 (2002): 83-87.
GTF2H2 (ENSG00000145736)	Fragmented	Nuclear	Transcription and DNA repair	Bürglen, L., et al. "The gene encoding p44, a subunit of the transcription factor TFIIH, is involved in large-scale deletions associated with Werdnig-Hoffmann disease." *American journal of human genetics* 60.1 (1997): 72.

Gene	Phenotype	Localization	Function	Reference
ING2 (ENSG00000168556)	Increased ER intensity, Fragmentation	Nuclear. Nucleus but not nucleoli (Protein Atlas)	Nuclear PtdIns receptor	Gozani, Or, et al. "The PHD finger of the chromatin-associated protein ING2 functions as a nuclear phosphoinositide receptor." Cell 114.1 (2003): 99-111.
KALRN (ENSG00000160145)	Mild Fragmentation	Golgi. Nucleus but not nucleoli, vesicles (Protein Atlas)	Induces lamellipodia formation in Pak dependent manner	Mains, Richard E., et al. "Kalirin, a multifunctional PAM COOH-terminal domain interactor protein, affects cytoskeletal organization and ACTH secretion from AtT-20 cells." Journal of Biological Chemistry 274.5 (1999): 2929-2937.
KIF1A (ENSG00000130294)	Increased ER intensity, Fragmented	Cytoplasmic. Cytoplasmic (Protein Atlas)	anterograde motor protein that transports membranous organelles along axonal microtubules	Lee, Jae-Ran, et al. "Characterization of the movement of the kinesin motor KIF1A in living cultured neurons." Journal of Biological Chemistry 278.4 (2003): 2624-2629.
LIN7B (ENSG00000104863)	Mild Fragmentation	Plasma membrane, Tight junctions	Plays a role in establishing and maintaining the asymmetric distribution of channels and receptors at the plasma membrane of polarized cells	Perego, C., et al. "Mammalian LIN-7 PDZ proteins associate with β-catenin at the cell-cell junctions of epithelia and neurons." The EMBO journal 19.15 (2000): 3978-3989.
LIN7C (ENSG00000148943)	Mild Fragmentation	Plasma membrane, Tight junctions	Required to localize Kir2 channels, GABA transporter (SLC6A12) and EGFR/ERBB1, ERBB2, ERBB3 and ERBB4 to the basolateral membrane of epithelial cells	Perego, C., et al. "Mammalian LIN-7 PDZ proteins associate with β-catenin at the cell-cell junctions of epithelia and neurons." The EMBO journal 19.15 (2000): 3978-3989.
LNX1 (ENSG00000072201)	Fragmented	Cytoplasmic. Mainly nuclear and punctuate cytoplasmic (Protein Atlas).	Functions as scaffold to organize cell adhesion junctions, facilitates endocytosis of JAM4	Weiss, Andreas, et al. "c-Src is a PDZ interaction partner and substrate of the E3 ubiquitin ligase Ligand-of-Numb protein X1." FEBS letters 581.26 (2007): 5131-5136.
MAGI-3 (ENSG00000081026)	Mild Fragmentation	Cell to cell contact sites. Cytoplasmic (Protein Atlas)	Involved in formation of planar cell polarity	Yao, Ryoji, Yasuko Natsume, and Tetsuo Noda. "MAGI-3 is involved in the regulation of the JNK signaling pathway as a scaffold protein for frizzled and Ltap." Oncogene 23.36 (2004): 6023-6030.
MLL5 (ENSG00000005483)	Mild Fragmentation	Nuclear	Overexpression induces cell cycle inhibition	Deng, Lih-Wen, Isaac Chiu, and Jack L. Strominger. "MLL 5 protein forms intranuclear foci, and overexpression inhibits cell cycle

Gene	Phenotype	Localization	Description	Reference
				progression." *Proceedings of the National Academy of Sciences of the United States of America* 101.3 (2004): 757-762.
MLLT4 (ENSG00000130396)	Fragmented	Cell-cell adherens and tight junctions. Nucleus but not nucleoli, plasma membrane, cell junctions (Protein Atlas)	Interacts with JAM-A, and decreased Afadin results in decreased beta-integrin and reduced cell migration	Severson, Eric A., et al. "Junctional adhesion molecule A interacts with Afadin and PDZ-GEF2 to activate Rap1A, regulate β1 integrin levels, and enhance cell migration." *Molecular biology of the cell* 20.7 (2009): 1916-1925.
MTMR4 (ENSG00000108389)	Mild Fragmentation	Localizes at the interface between early and recycling endosomes	PI3 phosphatase, involved in receptor sorting at endosomes	Naughtin, Monica J., et al. "The myotubularin phosphatase MTMR4 regulates sorting from early endosomes." *Journal of cell science* 123.18 (2010): 3071-3083.
MYO9B (ENSG00000099331)	Stretched, Partial Fragmentation	Localized to the leading edge of polarized cells.	Key signalling molecule in membrane protrusion and retraction	Hanley, Peter J., et al. "Motorized RhoGAP myosin IXb (Myo9b) controls cell shape and motility." *Proceedings of the National Academy of Sciences* 107.27 (2010): 12145-12150.
NOS1 (ENSG00000089250)	Fragmented	Endoplasmic Reticulum. Cytoplasmic (Protein Atlas)	Nos1 knock down leads to decreased Ca++ uptake by ER	Wang, Honglan, et al. "Neuronal nitric oxide synthase signaling within cardiac myocytes targets phospholamban." *American Journal of Physiology-Cell Physiology* 294.6 (2008): C1566-C1575.
OSBPL5 (ENSG00000021762)	Stretched	Golgi Apparatus. Cytoplasmic (Protein Atlas)	Golgi localized protein that regulates cholesterol and sphingomyelin production	Nbek, Sokha, et al. "Regulation of Oxysterol-binding Protein Golgi Localization through Protein Kinase D-mediated Phosphorylation." *Molecular biology of the cell* 21.13 (2010): 2327-2337.
PARD3B (ENSG00000116117)	Fragmented	Tight junctions. Cytoplasmic, low amount on membranes (Protein Atlas)	Localize to tight junctions and regulate cell polarity	Kohjima, Motoyuki, et al. "PAR3β, a novel homologue of the cell polarity protein PAR3, localizes to tight junctions." *Biochemical and biophysical research communications* 299.4 (2002): 641-646.
PDLIM1 (ENSG00000107438)	Increased ER intensity	Cytoplasm and also colocalizes with a-actin. Nucleus, plasma membranes (Protein Atlas)	Involved in formation of stress fibers and focal adhesions	Vallenius, Tea, and Tomi P. Mäkelä. "Clik1: a novel kinase targeted to actin stress fibers by the CLP-36 PDZ-LIM protein." *Journal of cell science* 115.10 (2002): 2067-2073.

Gene	Phenotype	Localization	Function	Reference
PDLIM3 (ENSG00000154553)	Increased ER intensity, Mild Fragmentation	Cytoplasm and colocalizes with a-actin. Cytoplasmic (Protein Atlas)	Involved in targeting intracellular kinases because they can bind both cytoskeleton and kinases	Gillette, Jennifer M., and Sheila M. Nielsen-Preiss. "The role of annexin 2 in osteoblastic mineralization." *Journal of cell science* 117.3 (2004): 441-449.
PDLIM5 (ENSG00000163110)	Mild Fragmentation	Cytoplasmic and also colocalizes with synaptic vesicles. Plasma membrane (Protein Atlas)	Involved in targeting intracellular kinases because they can bind both cytoskeleton and kinases	Nakagawa, Norikazu, et al. "ENH, containing PDZ and LIM domains, heart/skeletal muscle-specific protein, associates with cytoskeletal proteins through the PDZ domain." *Biochemical and biophysical research communications* 272.2 (2000): 505-512.
PDZD4 (ENSG00000067840)	Mild Fragmentation	Plasma membrane. Cytoplasmic (Protein Atlas)		Nagayama, Satoshi, et al. "Identification of PDZK4, a novel human gene with PDZ domains, that is upregulated in synovial sarcomas." *Oncogene* 23.32 (2004): 5551-5557.
PHF12 (ENSG00000109118)	Stretched, Mild Fragmentation	Nuclear. Nucleus but not nucleoli (Protein Atlas)	Transcriptional corepressor protein	Yochum, Gregory S., and Donald E. Ayer. "Pf1, a novel PHD zinc finger protein that links the TLE corepressor to the mSin3A-histone deacetylase complex." *Molecular and cellular biology* 21.13 (2001): 4110-4118.
PIK3C2B (ENSG00000133056)	Mild Fragmentation	Endosomes and plasma membrane. But upon EGF stimulation localizes to nuclei. Intermediate filaments (Protein Atlas)	Produce 3-PtdIns	Banfic, Hrvoje, et al. "Epidermal growth factor stimulates translocation of the class II phosphoinositide 3-kinase PI3K-C2beta to the nucleus." *Biochem. J* 422 (2009): 53-60.
PIK3CG (ENSG00000105851)	Fragmented	Predominantly cytoplasmic, but recruited to plasma membrane upon activation. Cytoplasmic (Protein Atlas)	Produce 3-PtdIns and an important modulator of extracellular signals, including those elicited by E-cadherin-mediated cell-cell adhesion, which plays an important role in maintenance of the structural and functional integrity of epithelia.	Xie, Yan, et al. "Identification of upregulated phosphoinositide 3-kinase γ as a target to suppress breast cancer cell migration and invasion." *Biochemical pharmacology* 85.10 (2013): 1454-1462.
PIP5K3 (ENSG00000115020)	Mild Fragmentation	TGN	Role in biogenesis of endosome carrier vesicles	Shisheva, Assia, et al. "Localization and insulin-regulated relocation of phosphoinositide 5-kinase

Gene (ENSG)	Phenotype	Localization	Function	Reference
			from early endosomes	PIKfyve in 3T3-L1 adipocytes." *Journal of Biological Chemistry* 276.15 (2001): 11859-11869.
PLCG2 (ENSG00000197943)	Fragmented	Predominantly cytoplasmic, but recruited to plasma membrane upon activation. Nucleus but not nucleoli, Mitochondria (Protein Atlas)	Catalyzes PtdIns-P2(4,5) to produce InsP3 and DAG	Piechulek, Thomas, et al. "Isozyme-specific stimulation of phospholipase C-γ2 by Rac GTPases." *Journal of Biological Chemistry* 280.47 (2005): 38923-38931.
PLCL1 (ENSG00000115896)	Mild Fragmentation	Cell surface. Cytoplasmic (Protein Atlas)	Roles in receptor assembly at the plasma membrane	Kanematsu, Takashi, et al. "Modulation of GABAA receptor phosphorylation and membrane trafficking by phospholipase C-related inactive protein/protein phosphatase 1 and 2A signaling complex underlying brain-derived neurotrophic factor-dependent regulation of GABAergic inhibition." *Journal of Biological Chemistry* 281.31 (2006): 22180-22189.
PLCZ1 (ENSG00000139151)	Mild Fragmentation	Predominantly nuclear, but also present in cytoplasm	Causes Ca++ flux from ER oscillations in mammalian eggs	Ito, Masahiko, et al. "Difference in Ca2+ oscillation-inducing activity and nuclear translocation ability of PLCZ1, an egg-activating sperm factor candidate, between mouse, rat, human, and medaka fish." *Biology of reproduction* 78.6 (2008): 1081-1090.
PLEKHC1 (ENSG00000073712)	Mild Fragmentation	Focal adhesion points. Cytoplasmic (Protein Atlas)	Activator of Integrin/Maturation of focal adhesions	Ma, Yan-Qing, et al. "Kindlin-2 (Mig-2): a co-activator of β3 integrins." *The Journal of cell biology* 181.3 (2008): 439-446.
PLEKHO1 (ENSG00000023902)	Fragmented	Plasma membrane	Regulation of action cytoskeleton and cell morphology	Canton, David A., et al. "The pleckstrin homology domain-containing protein CKIP-1 is involved in regulation of cell morphology and the actin cytoskeleton and interaction with actin capping protein." *Molecular and cellular biology* 25.9 (2005): 3519-3534.
PRX (ENSG00000105227)	Mild Fragmentation	Periaxonal membranes of Schwann cells. Golgi apparatus (Protein Atlas)		Gillespie, C. Stewart, et al. "Periaxin, a novel protein of myelinating Schwann cells with a possible role in axonal ensheathment." *Neuron* 12.3 (1994): 497-508.
PSD (ENSG00000059915)	Stretched	Cytosol		Brumell, John H., et al. "Expression of the protein kinase C substrate pleckstrin in macrophages:

Gene (ENSG)	Morphology	Localization	Function	Reference
PSD3 (ENSG00000156011)	Stretched	Nuclear		association with phagosomal membranes." *The Journal of Immunology* 163.6 (1999): 3388-3395. Suzuki, Ryoji, et al. "Localization of EFA6A, a guanine nucleotide exchange factor for ARF6, in spermatogenic cells of testes of adult mice." *Journal of molecular histology* 40.1 (2009): 77-80.
RAPGEF6 (ENSG00000158987)	Mild Fragmentation	Cell-to-cell contact sites. Cytoplasmic (Protein Atlas)	Role in membrane barrier and cell migration by forming complex with Jam-A and MLLT4	Severson, Eric A., et al. "Junctional adhesion molecule A interacts with Afadin and PDZ-GEF2 to activate Rap1A, regulate β1 integrin levels, and enhance cell migration." *Molecular biology of the cell* 20.7 (2009): 1916-1925.
RASGRP3 (ENSG00000152689)	Mild Fragmentation	Cytoplasm and perinuclear staining	Activates H-Ras, R-Ras and Rap1(integrin protein)	Okamura, Sara M., Carolyn E. Oki-Idouchi, and Patricia S. Lorenzo. "The exchange factor and diacylglycerol receptor RasGRP3 interacts with dynein light chain 1 through its C-terminal domain." *Journal of Biological Chemistry* 281.47 (2006): 36132-36139.
RIMS3 (ENSG00000117016)	Mild Fragmentation	Actin Filaments (Protein Atlas)	Induces Ca++ evoked exocytosis/ Effector of Rab3A	Uriu, Yoshitsugu, et al. "Rab3-interacting molecule γ isoforms lacking the Rab3-binding domain induce long lasting currents but block neurotransmitter vesicle anchoring in voltage-dependent P/Q-type Ca2+ channels." *Journal of Biological Chemistry* 285.28 (2010): 21750-21767.
RPGRIP1 (ENSG00000092200)	Stretched	Centrioles	Could function as a core component of centrioles and basal bodies	Shu, X., et al. "RPGR ORF15 isoform co-localizes with RPGRIP1 at centrioles and basal bodies and interacts with nucleophosmin." *Human molecular genetics* 14.9 (2005): 1183-1197.
RUFY2 (ENSG00000204130)	Mislocalized, cytokinesis defect	Endosomes. Nuclear (Protein Atlas)	Regulation of endocytosis	Yang, Jianbo, et al. "Interaction between Tyrosine Kinase Etk and a RUN Domain-and FYVE Domain-containing Protein RUFY1 A POSSIBLE ROLE OF ETK IN REGULATION OF VESICLE TRAFFICKING." *Journal of Biological Chemistry* 277.33 (2002): 30219-30226.
SCRIB (ENSG00000180900)	Fragmented	Cell junctions.	Involved in cell adhesion, cell shape, plarity	Petit, Marleen MR, et al. "The tumor suppressor Scrib interacts with the zyxin-related protein LPP, which

Gene (ID)	Fragmentation	Localization	Function	Reference
SDCBP (ENSG00000137575)	Mild Fragmentation	Membrane junctions and nucleus. Nucleus but not nucleoli, Cytoplasm (Protein Atlas)	involved in cell adhesion and polarity	shuttles between cell adhesion sites and the nucleus." *BMC cell biology* 6.1 (2005): 1. Sulka, Béatrice, et al. "Tyrosine dephosphorylation of the syndecan-1 PDZ binding domain regulates syntenin-1 recruitment." *Journal of Biological Chemistry* 284.16 (2009): 10659-10671.
SH2B1 (ENSG00000178188)	Mild Fragmentation	Plasma membrane and cytosol	In response to GF stimulation, localizes to actin ruffles of leading edge	Herrington, James, et al. "SH2-B is required for growth hormone-induced actin reorganization." *Journal of Biological Chemistry* 275.17 (2000): 13126-13133.
SIPA1 (ENSG00000213445)	Mild Fragmentation	Cortical area of the cell OR perinuclear localization. Nuclear and cytoplasmic (Protein Atlas)	Inhibitor of Rap1 and leads to reduced cell adhesion	Tsukamoto, Noriyuki, et al. "Rap1 GTPase-activating protein SPA-1 negatively regulates cell adhesion." *Journal of Biological Chemistry* 274.26 (1999): 18463-18469.
SNTB2 (ENSG00000168807)	Fragmented	Cytosolic predominantly, but can translocate to membrane upon activation	Integral component of cytoskeleton at the neuro muscular junctions. Links vesicles to cytoskeleton	Iwata, Yuko, et al. "Syntrophin is an actin-binding protein the cellular localization of which is regulated through cytoskeletal reorganization in skeletal muscle cells." *European journal of cell biology* 83.10 (2004): 555-565.
SNX14 (ENSG00000135317)	Mild Fragmentation	Cytoplasm (Protein Atlas)	Membrane trafficking and protein sorting at the endosomes	Worby, Carolyn A., and Jack E. Dixon. "Sorting out the cellular functions of sorting nexins." *Nature reviews Molecular cell biology* 3.12 (2002): 919-931.
SNX24 (ENSG00000064652)	Mild Fragmentation		Probably sorting role at the endosomes	Worby, Carolyn A., and Jack E. Dixon. "Sorting out the cellular functions of sorting nexins." *Nature reviews Molecular cell biology* 3.12 (2002): 919-931.
SPTBN1 (ENSG00000115306)	Mild Fragmentation	GOLGI_ER (Bergeron) Cytoplasmic (Protein Atlas)	Required for E-Cadherin accumulation at the lateral membranes in epithelial cells	Abdi, Khadar M., and Vann Bennett. "Adducin promotes micrometer-scale organization of β2-spectrin in lateral membranes of bronchial epithelial cells." *Molecular biology of the cell* 19.2 (2008): 536-545.
SPTBN5 (ENSG00000137877)	Fragmented	Cytoplasmic and apical membranes depending on tissue type	Confined to apical membranes and together with cadherins contributes to the maintenance od adherence junctions	Stabach, Paul R., and Jon S. Morrow. "Identification and Characterization of βV Spectrin, a Mammalian Ortholog of Drosophila βHSpectrin." *Journal of Biological Chemistry* 275.28 (2000): 21385-21395.

Gene		Localization	Function	Reference
UNC13A (ENSG00000130477)	Fragmented	Presynaptic transmitter release sites	Regulate synaptic functions. Localize to presynaptic release site (polarity?)	Betz, Andrea, et al. "Munc13-1 is a presynaptic phorbol ester receptor that enhances neurotransmitter release." Neuron 21.1 (1998): 123-136.
WDFY1 (ENSG00000085449)	Fragmented	Early endosomes		Ridley, S. H., et al. "FENS-1 and DFCP1 are FYVE domain-containing proteins with distinct functions in the endosomal and Golgi compartments." Journal of cell science 114.22 (2001): 3991-4000.
ZFYVE19 (ENSG00000166140)	Fragmented	Midbody. Cytoplasmic,mildly membranous (Protein Atlas)	Abscission checkpoint during cytokinesis.	Thoresen, Sigrid B., et al. "ANCHR mediates Aurora-B-dependent abscission checkpoint control through retention of VPS4." Nature cell biology (2014).
ZFYVE28 (ENSG00000159733)	Fragmented	Endosomal localization. Membranous and Cytoplasmic (Protein Atlas)	Localizes to endosomes and promotes degradative sorting of activated EGFRs	Mosesson, Yaron, et al. "Monoubiquitinylation regulates endosomal localization of Lst2, a negative regulator of EGF receptor signaling." Developmental cell16.5 (2009): 687-698.

8   References

Akella, J. S., Wloga, D., Kim, J., Starostina, N. G., Lyons-Abbott, S., Morrissette, N. S., … Gaertig, J. (2010). MEC-17 is an alpha-tubulin acetyltransferase. *Nature*, *467*(7312), 218–22.

Akhmanova, A., & Hoogenraad, C. C. (2005). Microtubule plus-end-tracking proteins: mechanisms and functions. *Current opinion in cell biology*, *17*(1), 47–54.

Akhmanova, A., & Steinmetz, M. O. (2008). Tracking the ends: a dynamic protein network controls the fate of microtubule tips. *Nature reviews. Molecular cell biology*, *9*(4), 309–22.

Arts, H. H., Doherty, D., van Beersum, S. E., Parisi, M. A., Letteboer, S. J., Gorden, N. T., … Roepman, R. (2007). Mutations in the gene encoding the basal body protein RPGRIP1L, a nephrocystin-4 interactor, cause Joubert syndrome. *Nature genetics*, *39*(7), 882–8.

De Anda, F. C., Pollarolo, G., Da Silva, J. S., Camoletto, P. G., Feiguin, F., & Dotti, C. G. (2005). Centrosome localization determines neuronal polarity. *Nature*, *436*(7051), 704–8.

Babiá, T., Ayala, I., Valderrama, F., Mato, E., Bosch, M., Santarén, J. F., Renau-Piqueras, J., et al. (1999). N-Ras induces alterations in Golgi complex architecture and in constitutive protein transport. *Journal of cell science*, *112 (Pt 4)*, 477–89.

Balch, W. E., Dunphy, W. G., Braell, W. A., & Rothman, J. E. (1984). Reconstitution of the transport of protein between successive compartments of the Golgi measured by the coupled incorporation of N-acetylglucosamine. *Cell*, *39*(2 Pt 1), 405–16.

Bard, F., & Malhotra, V. (2006). The formation of TGN-to-plasma-membrane transport carriers. *Annual review of cell and developmental biology*, *22*, 439–55.

Barr, F. A. (1999). A novel Rab6-interacting domain defines a family of Golgi-targeted coiled-coil proteins. *Current biology : CB*, *9*(7), 381–4.

Barr, F. A., Nakamura, N., & Warren, G. (1998). Mapping the interaction between GRASP65 and GM130, components of a protein complex involved in the stacking of Golgi cisternae. *The EMBO journal*, *17*(12), 3258–68.

Barr, F. A., Puype, M., Vandekerckhove, J., & Warren, G. (1997). GRASP65, a protein involved in the stacking of Golgi cisternae. *Cell*, *91*(2), 253–62.

Bascom, R. A., Srinivasan, S., & Nussbaum, R. L. (1999). Identification and characterization of golgin-84, a novel Golgi integral membrane protein with a cytoplasmic coiled-coil domain. *The Journal of biological chemistry*, *274*(5), 2953–62.

Beck, K. A. (2005). Spectrins and the Golgi. *Biochimica et biophysica acta*, *1744*(3), 374–82.

Bennett, V., & Chen, L. (2001). Ankyrins and cellular targeting of diverse membrane proteins to physiological sites. *Current opinion in cell biology*, *13*(1), 61–7.

Bevis, B. J., Hammond, A. T., Reinke, C. A., & Glick, B. S. (2002). De novo formation of transitional ER sites and Golgi structures in Pichia pastoris. *Nature cell biology*, *4*(10), 750–6.

Bieling, P., Laan, L., Schek, H., Munteanu, E. L., Sandblad, L., Dogterom, M., … Surrey, T. (2007). Reconstitution of a microtubule plus-end tracking system in vitro. *Nature*, *450*(7172), 1100–5.

Bisel, B., Wang, Y., Wei, J.-H. H., Xiang, Y., Tang, D., Miron-Mendoza, M., Yoshimura, S., et al. (2008). ERK regulates Golgi and centrosome orientation towards the leading edge through GRASP65. *The Journal of cell biology*, *182*(5), 837–43.

Buey, R. M., Díaz, J. F., & Andreu, J. M. (2006). The nucleotide switch of tubulin and microtubule assembly: a polymerization-driven structural change. *Biochemistry*, *45*(19), 5933–8.

Bulinski, J. C., & Gundersen, G. G. (1991). Stabilization of post-translational modification of microtubules during cellular morphogenesis. *BioEssays : news and reviews in molecular, cellular and developmental biology*, *13*(6), 285–93.

Cao, X., Ballew, N., & Barlowe, C. (1998). Initial docking of ER-derived vesicles requires Uso1p and Ypt1p but is independent of SNARE proteins. *The EMBO journal*, *17*(8), 2156–65.

Castagnet, P., Mavlyutov, T., Cai, Y., Zhong, F., & Ferreira, P. (2003). RPGRIP1s with distinct neuronal localization and biochemical properties associate selectively with RanBP2 in amacrine neurons. *Human molecular genetics*, *12*(15), 1847–63.

Chabin-Brion, K., Marceiller, J., Perez, F., Settegrana, C., Drechou, A., Durand, G., & Poüs, C. (2001). The Golgi complex is a microtubule-organizing organelle. *Molecular biology of the cell*, *12*(7), 2047–60.

Coene, K. L., Mans, D. A., Boldt, K., Gloeckner, C. J., van Reeuwijk, J., Bolat, E., … Roepman, R. (2011). The ciliopathy-associated protein homologs RPGRIP1 and RPGRIP1L are linked to cilium integrity through interaction with Nek4 serine/threonine kinase. *Human molecular genetics*, *20*(18), 3592–605.

Colón-Franco, J. M., Gomez, T. S., & Billadeau, D. D. (2011). Dynamic remodeling of the actin cytoskeleton by FMNL1γ is required for structural maintenance of the Golgi complex. *Journal of cell science*, *124*(Pt 18), 3118–26.

Dehmelt, L., & Halpain, S. (2004). Actin and microtubules in neurite initiation: are MAPs the missing link? *Journal of neurobiology*, *58*(1), 18–33.

Dippold, H. C., Ng, M. M., Farber-Katz, S. E., Lee, S.-K. K., Kerr, M. L., Peterman, M. C., Sim, R., et al. (2009). GOLPH3 bridges phosphatidylinositol-4- phosphate and actomyosin to stretch and shape the Golgi to promote budding. *Cell*, *139*(2), 337–51.

Dogterom, M., Kerssemakers, J. W., Romet-Lemonne, G., & Janson, M. E. (2005). Force generation by dynamic microtubules. *Current opinion in cell biology*, *17*(1), 67–74.

Drabek, K., van Ham, M., Stepanova, T., Draegestein, K., van Horssen, R., Sayas, C. L., Akhmanova, A., et al. (2006). Role of CLASP2 in microtubule stabilization and the regulation of persistent motility. *Current biology : CB*, *16*(22), 2259–64.

Drubin, D. G., & Kirschner, M. W. (1986). Tau protein function in living cells. *The Journal of cell biology*, *103*(6 Pt 2), 2739–46.

Drubin, D., Kobayashi, S., & Kirschner, M. (1986). Association of tau protein with microtubules in living cells. *Annals of the New York Academy of Sciences*, *466*, 257–68.

Dryja, T. P., Adams, S. M., Grimsby, J. L., McGee, T. L., Hong, D. H., Li, T., … Berson, E. L. (2001). Null RPGRIP1 alleles in patients with Leber congenital amaurosis. *American journal of human genetics*, *68*(5), 1295–8.

Dunphy, W. G., & Rothman, J. E. (1985). Compartmental organization of the Golgi stack. *Cell*, *42*(1), 13–21.

Echeverri, C. J., Paschal, B. M., Vaughan, K. T., & Vallee, R. B. (1996). Molecular characterization of the 50-kD subunit of dynactin reveals function for the complex in chromosome alignment and spindle organization during mitosis. *The Journal of cell biology*, *132*(4), 617–33.

Efimov, A., Kharitonov, A., Efimova, N., Loncarek, J., Miller, P. M., Andreyeva, N., Gleeson, P., et al. (2007). Asymmetric CLASP-dependent nucleation of noncentrosomal microtubules at the trans-Golgi network. *Developmental cell*, *12*(6), 917–30.

Egea, G., Lázaro-Diéguez, F., & Vilella, M. (2006). Actin dynamics at the Golgi complex in mammalian cells. *Current opinion in cell biology*, *18*(2), 168–78.

Farquhar, M. G. (1985). Progress in unraveling pathways of Golgi traffic. *Annual review of cell biology*, *1*, 447–88.

Galjart, N. (2005). CLIPs and CLASPs and cellular dynamics. *Nature reviews. Molecular cell biology*, *6*(6), 487–98.

Gao, Y., & Sztul, E. (2001). A novel interaction of the Golgi complex with the vimentin intermediate filament cytoskeleton. *The Journal of cell biology*, *152*(5), 877–94.

Gao, Y.-S. S., Vrielink, A., MacKenzie, R., & Sztul, E. (2002). A novel type of regulation of the vimentin intermediate filament cytoskeleton by a Golgi protein. *European journal of cell biology*, *81*(7), 391–401.

Gee, M. A., Heuser, J. E., & Vallee, R. B. (1997). An extended microtubule-binding structure within the dynein motor domain. *Nature*, *390*(6660), 636–9.

Gerber, S., Perrault, I., Hanein, S., Barbet, F., Ducroq, D., Ghazi, I., … Rozet, J. M. (2001). Complete exon-intron structure of the RPGR-interacting protein (RPGRIP1) gene allows the identification of mutations underlying Leber congenital amaurosis. *European journal of human genetics : EJHG*, *9*(8), 561–71.

Gillingham, A. K., & Munro, S. (2003). Long coiled-coil proteins and membrane traffic. *Biochimica et biophysica acta*, *1641*(2-3), 71–85.

Gillingham, A. K., Pfeifer, A. C., & Munro, S. (2002). CASP, the alternatively spliced product of the gene encoding the CCAAT-displacement protein transcription factor, is a Golgi membrane protein related to giantin. *Molecular biology of the cell*, *13*(11), 3761–74.

Glick, B. S., & Malhotra, V. (1998). The curious status of the Golgi apparatus. *Cell*, *95*(7), 883–9.

Gonçalves, J., Nolasco, S., Nascimento, R., Lopez Fanarraga, M., Zabala, J. C., & Soares, H. (2010). TBCCD1, a new centrosomal protein, is required for centrosome and Golgi apparatus positioning. *EMBO reports*, *11*(3), 194–200.

Goud, B., & Gleeson, P. A. (2010). TGN golgins, Rabs and cytoskeleton: regulating the Golgi trafficking highways. *Trends in cell biology*, *20*(6), 329–36.

Gough, L. L., Fan, J., Chu, S., Winnick, S., & Beck, K. A. (2003). Golgi localization of Syne-1. *Molecular biology of the cell*, *14*(6), 2410–24.

Harada, A., Takei, Y., Kanai, Y., Tanaka, Y., Nonaka, S., & Hirokawa, N. (1998). Golgi vesiculation and lysosome dispersion in cells lacking cytoplasmic dynein. *The Journal of cell biology*, *141*(1), 51–9.

Hayes, G. L., Brown, F. C., Haas, A. K., Nottingham, R. M., Barr, F. A., & Pfeffer, S. R. (2009). Multiple Rab GTPase binding sites in GCC185 suggest a model for vesicle tethering at the trans-Golgi. *Molecular biology of the cell*, *20*(1), 209–17.

Hehnly, H., Xu, W., Chen, J.-L. L., & Stamnes, M. (2010). Cdc42 regulates microtubule-dependent Golgi positioning. *Traffic (Copenhagen, Denmark)*, *11*(8), 1067–78.

Holleran, E. A., Ligon, L. A., Tokito, M., Stankewich, M. C., Morrow, J. S., & Holzbaur, E. L. (2001). beta III spectrin binds to the Arp1 subunit of dynactin. *The Journal of biological chemistry*, *276*(39), 36598–605.

Holthuis, J. C., van Meer, G., & Huitema, K. (2003). Lipid microdomains, lipid translocation and the organization of intracellular membrane transport (Review). *Molecular membrane biology*, *20*(3), 231–41.

Hong, D. H., Yue, G., Adamian, M., & Li, T. (2001). Retinitis pigmentosa GTPase regulator (RPGRr)-interacting protein is stably associated with the photoreceptor ciliary axoneme and anchors RPGR to the connecting cilium. *The Journal of biological chemistry*, *276*(15), 12091–9. doi:10.1074/jbc.M009351200

Hoppeler-Lebel, A., Celati, C., Bellett, G., Mogensen, M. M., Klein-Hitpass, L., Bornens, M., & Tassin, A.-M. M. (2007). Centrosomal CAP350 protein stabilises microtubules associated with the Golgi complex. *Journal of cell science*, *120*(Pt 18), 3299–308.

Hubbert, C., Guardiola, A., Shao, R., Kawaguchi, Y., Ito, A., Nixon, A., … Yao, T.-P. P. (2002). HDAC6 is a microtubule-associated deacetylase. *Nature*, *417*(6887), 455–8. doi:10.1038/417455a

Hurtado, L., Caballero, C., Gavilan, M. P., Cardenas, J., Bornens, M., & Rios, R. M. (2011). Disconnecting the Golgi ribbon from the centrosome prevents directional cell migration and ciliogenesis. *The Journal of cell biology*, *193*(5), 917–33.

Ikonen, E., de Almeid, J. B., Fath, K. R., Burgess, D. R., Ashman, K., Simons, K., & Stow, J. L. (1997). Myosin II is associated with Golgi membranes: identification of p200 as nonmuscle myosin II on Golgi-derived vesicles. *Journal of cell science*, *110 (Pt 18)*, 2155–64.

Infante, C., Ramos-Morales, F., Fedriani, C., Bornens, M., & Rios, R. M. (1999). GMAP-210, A cis-Golgi network-associated protein, is a minus end microtubule-binding protein. *The Journal of cell biology*, *145*(1), 83–98.

Kalebic, N., Martinez, C., Perlas, E., Hublitz, P., Bilbao-Cortes, D., Fiedorczuk, K., … Heppenstall, P. A. (2013). Tubulin acetyltransferase αTAT1 destabilizes microtubules independently of its acetylation activity. *Molecular and cellular biology*, *33*(6), 1114–23.

Kanai, Y., Takemura, R., Oshima, T., Mori, H., Ihara, Y., Yanagisawa, M., Masaki, T., et al.

(1989). Expression of multiple tau isoforms and microtubule bundle formation in fibroblasts transfected with a single tau cDNA. *The Journal of cell biology*, *109*(3), 1173–84.

Kjer-Nielsen, L., Teasdale, R. D., van Vliet, C., & Gleeson, P. A. (1999). A novel Golgi-localisation domain shared by a class of coiled-coil peripheral membrane proteins. *Current biology : CB*, *9*(7), 385–8.

Knowles, R. G., & Moncada, S. (1994). Nitric oxide synthases in mammals. *The Biochemical journal*, *298 (Pt 2)*, 249–58.

Kodani, A., & Sütterlin, C. (2008). The Golgi protein GM130 regulates centrosome morphology and function. *Molecular biology of the cell*, *19*(2), 745–53. doi:10.1091/mbc.E07-08-0847

Koegler, E., Bonnon, C., Waldmeier, L., Mitrovic, S., Halbeisen, R., & Hauri, H.-P. P. (2010). p28, a novel ERGIC/cis Golgi protein, required for Golgi ribbon formation. *Traffic (Copenhagen, Denmark)*, *11*(1), 70–89.

Koenekoop, R. K. (2005). RPGRIP1 is mutated in Leber congenital amaurosis: a mini-review. *Ophthalmic genetics*, *26*(4), 175–9. doi:10.1080/13816810500374441

Komarova, Y. A., Akhmanova, A. S., Kojima, S.-I., Galjart, N., & Borisy, G. G. (2002). Cytoplasmic linker proteins promote microtubule rescue in vivo. *The Journal of cell biology*, *159*(4), 589–99.

Kondylis, V., Spoorendonk, K. M., & Rabouille, C. (2005). dGRASP localization and function in the early exocytic pathway in Drosophila S2 cells. *Molecular biology of the cell*, *16*(9), 4061–72.

Kreis, T. E. (1987). Microtubules containing detyrosinated tubulin are less dynamic. *The EMBO journal*, *6*(9), 2597–606.

Ladinsky, M. S., Mastronarde, D. N., McIntosh, J. R., Howell, K. E., & Staehelin, L. A. (1999). Golgi structure in three dimensions: functional insights from the normal rat kidney cell. *The Journal of cell biology*, *144*(6), 1135–49.

Lansbergen, G., & Akhmanova, A. (2006). Microtubule plus end: a hub of cellular activities. *Traffic (Copenhagen, Denmark)*, *7*(5), 499–507.

Lansbergen, G., Grigoriev, I., Mimori-Kiyosue, Y., Ohtsuka, T., Higa, S., Kitajima, I., Demmers, J., et al. (2006). CLASPs attach microtubule plus ends to the cell cortex through a complex with LL5beta. *Developmental cell*, *11*(1), 21–32.

Lansbergen, G., Komarova, Y., Modesti, M., Wyman, C., Hoogenraad, C. C., Goodson, H. V., Lemaitre, R. P., et al. (2004). Conformational changes in CLIP-170 regulate its binding to microtubules and dynactin localization. *The Journal of cell biology*, *166*(7), 1003–14.

Lanzetti, L. (2007). Actin in membrane trafficking. *Current opinion in cell biology*, *19*(4), 453–8.

Lee, I., Tiwari, N., Dunlop, M. H., Graham, M., Liu, X., & Rothman, J. E. (2014). Membrane adhesion dictates Golgi stacking and cisternal morphology. *Proceedings of the National Academy of Sciences of the United States of America*, *111*(5), 1849–54.

Liu, Z., Zhan, Y., Tu, Y., Chen, K., Liu, Z., & Wu, C. (2014). PDZ and LIM domain protein 1(PDLIM1)/CLP36 promotes breast cancer cell migration, invasion and metastasis through interaction with α-actinin. *Oncogene*, *0*. doi:10.1038/onc.2014.64

Lu, Z., Joseph, D., Bugnard, E., Zaal, K. J., & Ralston, E. (2001). Golgi complex reorganization

during muscle differentiation: visualization in living cells and mechanism. *Molecular biology of the cell*, *12*(4), 795–808.

Lu, X., & Ferreira, P. A. (2005). Identification of novel murine- and human-specific RPGRIP1 splice variants with distinct expression profiles and subcellular localization. *Investigative ophthalmology & visual science*, *46*(6), 1882–90. doi:10.1167/iovs.04-1286

Marsh, B. J., Volkmann, N., McIntosh, J. R., & Howell, K. E. (2004). Direct continuities between cisternae at different levels of the Golgi complex in glucose-stimulated mouse islet beta cells. *Proceedings of the National Academy of Sciences of the United States of America*, *101*(15), 5565–70.

De Matteis, M. A., & Luini, A. (2008). Exiting the Golgi complex. *Nature reviews. Molecular cell biology*, *9*(4), 273–84.

McNally, F. J., Okawa, K., Iwamatsu, A., & Vale, R. D. (1996). Katanin, the microtubule-severing ATPase, is concentrated at centrosomes. *Journal of cell science*, *109 (Pt 3)*, 561–7.

Mellman, I., & Simons, K. (1992). The Golgi complex: in vitro veritas? *Cell*, *68*(5), 829–40.

Miles, S., McManus, H., Forsten, K. E., & Storrie, B. (2001). Evidence that the entire Golgi apparatus cycles in interphase HeLa cells: sensitivity of Golgi matrix proteins to an ER exit block. *The Journal of cell biology*, *155*(4), 543–55.

Miller, P. M., Folkmann, A. W., Maia, A. R. R., Efimova, N., Efimov, A., & Kaverina, I. (2009). Golgi-derived CLASP-dependent microtubules control Golgi organization and polarized trafficking in motile cells. *Nature cell biology*, *11*(9), 1069–80.

Mimori-Kiyosue, Y., Grigoriev, I., Lansbergen, G., Sasaki, H., Matsui, C., Severin, F., Galjart, N., et al. (2005). CLASP1 and CLASP2 bind to EB1 and regulate microtubule plus-end dynamics at the cell cortex. *The Journal of cell biology*, *168*(1), 141–53.

Mitchison, T., & Kirschner, M. (1984). Dynamic instability of microtubule growth. *Nature*, *312*(5991), 237–42.

Mollenhauer, H. H., & Morré, D. J. (1991). Perspectives on Golgi apparatus form and function. *Journal of electron microscopy technique*, *17*(1), 2–14.

Montes de Oca, G., Lezama, R. A., Mondragón, R., Castillo, A. M., & Meza, I. (1997). Myosin I interactions with actin filaments and trans-Golgi-derived vesicles in MDCK cell monolayers. *Archives of medical research*, *28*(3), 321–8.

Munro, S. (2011). The golgin coiled-coil proteins of the Golgi apparatus. *Cold Spring Harbor perspectives in biology*, *3*(6).

Munro, S., & Nichols, B. J. (1999). The GRIP domain - a novel Golgi-targeting domain found in several coiled-coil proteins. *Current biology : CB*, *9*(7), 377–80.

Nakamura, N., Lowe, M., Levine, T. P., Rabouille, C., & Warren, G. (1997). The vesicle docking protein p115 binds GM130, a cis-Golgi matrix protein, in a mitotically regulated manner. *Cell*, *89*(3), 445–55.

Nakamura, N., Rabouille, C., Watson, R., Nilsson, T., Hui, N., Slusarewicz, P., … Warren, G. (1995). Characterization of a cis-Golgi matrix protein, GM130. *The Journal of cell biology*, *131*(6 Pt 2), 1715–26.

Nogales, E., & Wang, H.-W. W. (2006). Structural intermediates in microtubule assembly and disassembly: how and why? *Current opinion in cell biology*, *18*(2), 179–84.

Nogales, E., Wolf, S. G., & Downing, K. H. (1998). Structure of the alpha beta tubulin dimer by electron crystallography. *Nature*, *391*(6663), 199–203.

Oddoux, S., Zaal, K. J., Tate, V., Kenea, A., Nandkeolyar, S. A., Reid, E., Liu, W., et al. (2013). Microtubules that form the stationary lattice of muscle fibers are dynamic and nucleated at Golgi elements. *The Journal of cell biology*, *203*(2), 205–13.

Orci, L., Glick, B. S., & Rothman, J. E. (1986). A new type of coated vesicular carrier that appears not to contain clathrin: its possible role in protein transport within the Golgi stack. *Cell*, *46*(2), 171–84.

Patil, H., Tserentsoodol, N., Saha, A., Hao, Y., Webb, M., & Ferreira, P. A. (2012). Selective loss of RPGRIP1-dependent ciliary targeting of NPHP4, RPGR and SDCCAG8 underlies the degeneration of photoreceptor neurons. *Cell death & disease*, *3*, e355.

Pavelka, M., & Ellinger, A. (1983). Effect of colchicine on the Golgi complex of rat pancreatic acinar cells. *The Journal of cell biology*, *97*(3), 737–48.

Pelham, H. R. (1998). Getting through the Golgi complex. *Trends in cell biology*, *8*(1), 45–9.

Pelletier, L., Stern, C. A., Pypaert, M., Sheff, D., Ngô, H. M., Roper, N., He, C. Y., et al. (2002). Golgi biogenesis in Toxoplasma gondii. *Nature*, *418*(6897), 548–52.
Piperno, G., LeDizet, M., & Chang, X. J. (1987). Microtubules containing acetylated alpha-tubulin in mammalian cells in culture. *The Journal of cell biology*, *104*(2), 289–302. doi:10.2307/1612244

Presley, J. F., Cole, N. B., Schroer, T. A., Hirschberg, K., Zaal, K. J., & Lippincott-Schwartz, J. (1997). ER-to-Golgi transport visualized in living cells. *Nature*, *389*(6646), 81–5.

Preuss, D., Mulholland, J., Franzusoff, A., Segev, N., & Botstein, D. (1992). Characterization of the Saccharomyces Golgi complex through the cell cycle by immunoelectron microscopy. *Molecular biology of the cell*, *3*(7), 789–803.

Puthenveedu, M. A., Bachert, C., Puri, S., Lanni, F., & Linstedt, A. D. (2006). GM130 and GRASP65-dependent lateral cisternal fusion allows uniform Golgi-enzyme distribution. *Nature cell biology*, *8*(3), 238–48.

Rambourg, A., & Clermont, Y. (1990). Three-dimensional electron microscopy: structure of the Golgi apparatus. *European journal of cell biology*, *51*(2), 189–200.

Rambourg, A., Clermont, Y., Nicaud, J. M., Gaillardin, C., & Kepes, F. (1996). Transformations of membrane-bound organelles in sec 14 mutants of the yeasts Saccharomyces cerevisiae and Yarrowia lipolytica. *The Anatomical record*, *245*(3), 447–58.

Ramirez, I. B., & Lowe, M. (2009). Golgins and GRASPs: holding the Golgi together. *Seminars in cell & developmental biology*, *20*(7), 770–9.

Reed, N. A., Cai, D., Blasius, T. L., Jih, G. T., Meyhofer, E., Gaertig, J., & Verhey, K. J. (2006). Microtubule acetylation promotes kinesin-1 binding and transport. *Current biology : CB*, *16*(21), 2166–72.

Renna, L., Hanton, S. L., Stefano, G., Bortolotti, L., Misra, V., & Brandizzi, F. (2005). Identification

and characterization of AtCASP, a plant transmembrane Golgi matrix protein. *Plant molecular biology*, *58*(1), 109–22.

Rios, R. M., & Bornens, M. (2003). The Golgi apparatus at the cell centre. *Current opinion in cell biology*, *15*(1), 60–6.

Ríos, R. M., Sanchís, A., Tassin, A. M., Fedriani, C., & Bornens, M. (2004). GMAP-210 recruits gamma-tubulin complexes to cis-Golgi membranes and is required for Golgi ribbon formation. *Cell*, *118*(3), 323–35.

Rios, R. M., Tassin, A. M., Celati, C., Antony, C., Boissier, M. C., Homberg, J. C., & Bornens, M. (1994). A peripheral protein associated with the cis-Golgi network redistributes in the intermediate compartment upon brefeldin A treatment. *The Journal of cell biology*, *125*(5), 997–1013.

Rivero, S., Cardenas, J., Bornens, M., & Rios, R. M. (2009). Microtubule nucleation at the cis-side of the Golgi apparatus requires AKAP450 and GM130. *The EMBO journal*, *28*(8), 1016–28.

Roepman, R., Bernoud-Hubac, N., Schick, D., Maugeri, A., Berger, W., Ropers, H.-H., … Ferreira, P. (2000). The retinitis pigmentosa GTPase regulator (RPGR) interacts with novel transport-like proteins in the outer segments of rod photoreceptors. *Human Molecular Genetics*, *9*(14), 2095–2105.

Roepman, R., Letteboer, S. J., Arts, H. H., van Beersum, S. E., Lu, X., Krieger, E., … Cremers, F. P. (2005). Interaction of nephrocystin-4 and RPGRIP1 is disrupted by nephronophthisis or Leber congenital amaurosis-associated mutations. *Proceedings of the National Academy of Sciences of the United States of America*, *102*(51), 18520–5.

Rogalski, A. A., & Singer, S. J. (1984). Associations of elements of the Golgi apparatus with microtubules. *The Journal of cell biology*, *99*(3), 1092–100.

Roghi, C., & Allan, V. J. (1999). Dynamic association of cytoplasmic dynein heavy chain 1a with the Golgi apparatus and intermediate compartment. *Journal of cell science*, *112 (Pt 24)*, 4673–85.

Rothman, J. E., & Wieland, F. T. (1996). Protein sorting by transport vesicles. *Science (New York, N.Y.)*, *272*(5259), 227–34.

Ryan, S. D., Bhanot, K., Ferrier, A., De Repentigny, Y., Chu, A., Blais, A., & Kothary, R. (2012). Microtubule stability, Golgi organization, and transport flux require dystonin-a2-MAP1B interaction. *The Journal of cell biology*, *196*(6), 727–42.

Sandoval, I. V., Bonifacino, J. S., Klausner, R. D., Henkart, M., & Wehland, J. (1984). Role of microtubules in the organization and localization of the Golgi apparatus. *The Journal of cell biology*, *99*(1 Pt 2), 113s–118s.

Satoh, A., & Warren, G. (2008). In situ cleavage of the acidic domain from the p115 tether inhibits exocytic transport. *Traffic (Copenhagen, Denmark)*, *9*(9), 1522–9.

Schulze, E., Asai, D. J., Bulinski, J. C., & Kirschner, M. (1987). Posttranslational modification and microtubule stability. *The Journal of cell biology*, *105*(5), 2167–77.

Schuyler, S. C., & Pellman, D. (2001). Microtubule "plus-end-tracking proteins": The end is just the beginning. *Cell*, *105*(4), 421–4.

Shanks, R. A., Larocca, M. C., Berryman, M., Edwards, J. C., Urushidani, T., Navarre, J., & Goldenring, J. R. (2002). AKAP350 at the Golgi apparatus. II. Association of AKAP350 with a

novel chloride intracellular channel (CLIC) family member. *The Journal of biological chemistry*, *277*(43), 40973–80.

Shanks, R. A., Steadman, B. T., Schmidt, P. H., & Goldenring, J. R. (2002). AKAP350 at the Golgi apparatus. I. Identification of a distinct Golgi apparatus targeting motif in AKAP350. *The Journal of biological chemistry*, *277*(43), 40967–72.

Sharma, N., Kosan, Z. A., Stallworth, J. E., Berbari, N. F., & Yoder, B. K. (2011). Soluble levels of cytosolic tubulin regulate ciliary length control. *Molecular biology of the cell*, *22*(6), 806–16.

Short, B., Haas, A., & Barr, F. A. (2005). Golgins and GTPases, giving identity and structure to the Golgi apparatus. *Biochimica et biophysica acta*, *1744*(3), 383–95.

Short, B., Preisinger, C., Körner, R., Kopajtich, R., Byron, O., & Barr, F. A. (2001). A GRASP55-rab2 effector complex linking Golgi structure to membrane traffic. *The Journal of cell biology*, *155*(6), 877–83.

Shorter, J., & Warren, G. (1999). A role for the vesicle tethering protein, p115, in the post-mitotic stacking of reassembling Golgi cisternae in a cell-free system. *The Journal of cell biology*, *146*(1), 57–70.

Shorter, J., & Warren, G. (2002). Golgi architecture and inheritance. *Annual review of cell and developmental biology*, *18*, 379–420.

Shu, X., Fry, A. M., Tulloch, B., Manson, F. D., Crabb, J. W., Khanna, H., … Wright, A. F. (2005). RPGR ORF15 isoform co-localizes with RPGRIP1 at centrioles and basal bodies and interacts with nucleophosmin. *Human molecular genetics*, *14*(9), 1183–97.

Simpson, J. C., Joggerst, B., Laketa, V., Verissimo, F., Cetin, C., Erfle, H., … Pepperkok, R. (2012). Genome-wide RNAi screening identifies human proteins with a regulatory function in the early secretory pathway. *Nature cell biology*, *14*(7), 764–74.

Sinka, R., Gillingham, A. K., Kondylis, V., & Munro, S. (2008). Golgi coiled-coil proteins contain multiple binding sites for Rab family G proteins. *The Journal of cell biology*, *183*(4), 607–15.

Skoufias, D. A., Burgess, T. L., & Wilson, L. (1990). Spatial and temporal colocalization of the Golgi apparatus and microtubules rich in detyrosinated tubulin. *The Journal of cell biology*, *111*(5 Pt 1), 1929–37.

Slusarewicz, P., Nilsson, T., Hui, N., Watson, R., & Warren, G. (1994). Isolation of a matrix that binds medial Golgi enzymes. *The Journal of cell biology*, *124*(4), 405–13.

Sousa, A., Reis, R., Sampaio, P., & Sunkel, C. E. (2007). The Drosophila CLASP homologue, Mast/Orbit regulates the dynamic behaviour of interphase microtubules by promoting the pause state. *Cell motility and the cytoskeleton*, *64*(8), 605–20. doi:10.1002/cm.20208

Striegl, H., Andrade-Navarro, M. A., & Heinemann, U. (2010). Armadillo motifs involved in vesicular transport. *PloS one*, *5*(2), e8991.

Sütterlin, C., & Colanzi, A. (2010). The Golgi and the centrosome: building a functional partnership. *The Journal of cell biology*, *188*(5), 621–8.

Tängemo, C., Ronchi, P., Colombelli, J., Haselmann, U., Simpson, J. C., Antony, C., … Reynaud, E. G. (2011). A novel laser nanosurgery approach supports de novo Golgi biogenesis in mammalian cells. *Journal of cell science*, *124*(Pt 6), 978–87. doi:10.1242/jcs.079640

Thyberg, J., & Moskalewski, S. (1985). Microtubules and the organization of the Golgi complex. *Experimental cell research*, *159*(1), 1–16.

Thyberg, J., & Moskalewski, S. (1989). Subpopulations of microtubules with differential sensitivity to nocodazole: role in the structural organization of the Golgi complex and the lysosomal system. *Journal of submicroscopic cytology and pathology*, *21*(2), 259–74.

Toivola, D. M., Tao, G.-Z. Z., Habtezion, A., Liao, J., & Omary, M. B. (2005). Cellular integrity plus: organelle-related and protein-targeting functions of intermediate filaments. *Trends in cell biology*, *15*(11), 608–17.

Turner, J. R., & Tartakoff, A. M. (1989). The response of the Golgi complex to microtubule alterations: the roles of metabolic energy and membrane traffic in Golgi complex organization. *The Journal of cell biology*, *109*(5), 2081–8.

Vaisberg, E. A., Grissom, P. M., & McIntosh, J. R. (1996). Mammalian cells express three distinct dynein heavy chains that are localized to different cytoplasmic organelles. *The Journal of cell biology*, *133*(4), 831–42.

Valderrama, F., Babià, T., Ayala, I., Kok, J. W., Renau-Piqueras, J., & Egea, G. (1998). Actin microfilaments are essential for the cytological positioning and morphology of the Golgi complex. *European journal of cell biology*, *76*(1), 9–17.

Valderrama, F., Durán, J. M., Babià, T., Barth, H., Renau-Piqueras, J., & Egea, G. (2001). Actin microfilaments facilitate the retrograde transport from the Golgi complex to the endoplasmic reticulum in mammalian cells. *Traffic (Copenhagen, Denmark)*, *2*(10), 717–26.

Van Meer, G., Voelker, D. R., & Feigenson, G. W. (2008). Membrane lipids: where they are and how they behave. *Nature reviews. Molecular cell biology*, *9*(2), 112–24. doi:10.1038/nrm2330

Vaughan, K. T. (2005). Microtubule plus ends, motors, and traffic of Golgi membranes. *Biochimica et biophysica acta*, *1744*(3), 316–24. doi:10.1016/j.bbamcr.2005.05.001

Vinogradova, T., Paul, R., Grimaldi, A. D., Loncarek, J., Miller, P. M., Yampolsky, D., Magidson, V., et al. (2012). Concerted effort of centrosomal and Golgi-derived microtubules is required for proper Golgi complex assembly but not for maintenance. *Molecular biology of the cell*, *23*(5), 820–33.

Walenta, J. H., Didier, A. J., Liu, X., & Krämer, H. (2001). The Golgi-associated hook3 protein is a member of a novel family of microtubule-binding proteins. *The Journal of cell biology*, *152*(5), 923–34.

Wang, H.-W. W., & Nogales, E. (2005). Nucleotide-dependent bending flexibility of tubulin regulates microtubule assembly. *Nature*, *435*(7044), 911–5.

Wang, Y., Satoh, A., & Warren, G. (2005). Mapping the functional domains of the Golgi stacking factor GRASP65. *The Journal of biological chemistry*, *280*(6), 4921–8. doi:10.1074/jbc.M412407200

Ward, T. H., Polishchuk, R. S., Caplan, S., Hirschberg, K., & Lippincott-Schwartz, J. (2001). Maintenance of Golgi structure and function depends on the integrity of ER export. *The Journal of cell biology*, *155*(4), 557–70.

Webster, D. R., & Borisy, G. G. (1989). Microtubules are acetylated in domains that turn over slowly. *Journal of cell science*, *92 (Pt 1)*, 57–65.

Wen, Y., Eng, C. H., Schmoranzer, J., Cabrera-Poch, N., Morris, E. J., Chen, M., Wallar, B. J., et al. (2004). EB1 and APC bind to mDia to stabilize microtubules downstream of Rho and promote cell migration. *Nature cell biology*, *6*(9), 820–30.

Westermann, S., & Weber, K. (2003). Post-translational modifications regulate microtubule function. *Nature reviews. Molecular cell biology*, *4*(12), 938–47.

Wittmann, T., Bokoch, G. M., & Waterman-Storer, C. M. (2003). Regulation of leading edge microtubule and actin dynamics downstream of Rac1. *The Journal of cell biology*, *161*(5), 845–51. doi:10.1083/jcb.200303082

Wu, X., Kodama, A., & Fuchs, E. (2008). ACF7 regulates cytoskeletal-focal adhesion dynamics and migration and has ATPase activity. *Cell*, *135*(1), 137–48.

Xu, D., & Esko, J. D. (2009). A Golgi-on-a-chip for glycan synthesis. *Nature chemical biology*, *5*(9), 612–3.

Yadav, S., Puri, S., & Linstedt, A. D. (2009). A primary role for Golgi positioning in directed secretion, cell polarity, and wound healing. *Molecular biology of the cell*, *20*(6), 1728–36.

Zaal, K. J., Smith, C. L., Polishchuk, R. S., Altan, N., Cole, N. B., Ellenberg, J., Hirschberg, K., et al. (1999). Golgi membranes are absorbed into and reemerge from the ER during mitosis. *Cell*, *99*(6), 589–601.

Zhao, Y., Hong, D.-H. H., Pawlyk, B., Yue, G., Adamian, M., Grynberg, M., … Li, T. (2003). The retinitis pigmentosa GTPase regulator (RPGR)- interacting protein: subserving RPGR function and participating in disk morphogenesis. *Proceedings of the National Academy of Sciences of the United States of America*, *100*(7), 3965–70.

Zheng, Q., & Zhao, Y. (2007). The diverse biofunctions of LIM domain proteins: determined by subcellular localization and protein-protein interaction. *Biology of the cell / under the auspices of the European Cell Biology Organization*, *99*(9), 489–502. doi:10.1042/BC20060126

Zhou, L., & Zhu, D.-Y. Y. (2009). Neuronal nitric oxide synthase: structure, subcellular localization, regulation, and clinical implications. *Nitric oxide : biology and chemistry / official journal of the Nitric Oxide Society*, *20*(4), 223–30. doi:10.1016/j.niox.2009.03.001

Zilberman, Y., Alieva, N. O., Miserey-Lenkei, S., Lichtenstein, A., Kam, Z., Sabanay, H., & Bershadsky, A. (2011). Involvement of the Rho-mDia1 pathway in the regulation of Golgi complex architecture and dynamics. *Molecular biology of the cell*, *22*(16), 2900–11.

Zilberman, Y., Ballestrem, C., Carramusa, L., Mazitschek, R., Khochbin, S., & Bershadsky, A. (2009). Regulation of microtubule dynamics by inhibition of the tubulin deacetylase HDAC6. *Journal of cell science*, *122*(Pt 19), 3531–41. doi:10.1242/jcs.046813

Zmuda, J. F., & Rivas, R. J. (1998). The Golgi apparatus and the centrosome are localized to the sites of newly emerging axons in cerebellar granule neurons in vitro. *Cell motility and the cytoskeleton*, *41*(1), 18–38.